Implications of discrete flavor symmetries on neutrino mixing

A thesis submitted for the award of the degree of
Doctor of Philosophy in Physics

BY
Sruthilaya M
12PHPH28

Under the guidance of
Prof. Rukmani Mohanta

School of Physics
University of Hyderabad
Hyderabad-500 046
India

December, 2017

Declaration

I hereby declare that, this thesis titled **Implications of discrete flavor symmetries on neutrino mixing** submitted by me, under the guidance and supervision of Prof. Rukmani Mohanta, is a bonafide research work and is free from plagiarism. I also declare that it has not been submitted previously, in part or in full to this University or any other University or Institution, for the award of any degree or diploma. I hereby agree that my thesis can be deposited in Shodhganga/INFLIBNET.

A report on plagiarism statistics from the University Librarian is enclosed.

Place: Hyderabad
Date:

Sruthilaya M
Reg. No. 12PHPH28

Certificate

This is to certify that the thesis titled **Implications of discrete flavor symmetries on neutrino mixing** submitted by Sruthilaya M (Reg. No. 12PHPH28), in partial fulfillment of the requirements for award of Doctor of Philosophy in Physics, is a bonafide work carried out by her under my supervision and guidance.

This thesis is free from plagiarism and has not been submitted previously, in part or in full to this or any other University or Institution, for an award of any degree or diploma. Further, the student has the following publications before the submission of the thesis for adjudication.

1) Sruthilaya M., Soumya C., K. N. Deepthi and R. Mohanta, New J. Phys. **17** 083028 (2015), (ISSN No: 1367-2630 (online)), chapter 3.

2) Sruthilaya M and R. Mohanta, Eur. Phys. C **77**: 140 (2017), (ISSN No: 1434-6052 (online)), chapter 4.

3) Sruthilaya M., Rukmani Mohanta, and Sudhanwa Patra, [arXiv:1709.01737(hep-ph)], chapter 5.

Further, the student has passed the following courses towards fulfillment of coursework requirement for Ph.D:

Course Code	Name of the Course	Credits	Pass/Fail
PY801	Advanced Quantum Mechanics	4	Pass
PY803	Advanced Statistical Mechanics	4	Pass
PY804	Advanced Electromagnetic Theory	4	Pass
PY821	Research Methodology	4	Pass

Prof. Rukmani Mohanta
Thesis Advisor,
School of Physics,
University of Hyderabad

Prof. Bindu A. Bambah
Dean,
School of Physics,
University of Hyderabad

Date:

Acknowledgement

This thesis becomes a reality with the kind of support and help from many individuals. I would like to extend my sincere thanks to all of them.

Foremost I would like to take this opportunity to express my gratitude to my supervisor Prof. Rukmani Mohanta. I am extremely grateful and indebted to her for her guidance and encouragement extended to me. I would also thank my doctoral committee members Prof. E. Harikumar and Dr. Soma Sanyal for their valuable suggestions to improve the quality of my work. I thank my teachers Prof. A. K. Kapoor, Prof. P. K. Suresh and Prof. K. P. N Murthy from whom I learned various aspects of physics. I would like to thank my collaborator Dr. Sudhanwa Patra for teaching me various aspects of neutrino physics. I take this opportunity to thank the present Dean Prof. Bindu A. Bambah and former Deans: Prof. S. Chaturvedi, and Prof. R. Singh for providing all the academic facilities. I am very thankful to the office staffs of School of Physics, especially Mr.Abraham and Ms. Deepika for their help in administrative activities. I express my gratitude to UGC for the financial support during my research.

I would like to extend my heartfelt thanks to my friend Soumya for helping out in all my difficulties and for being with me in my good and bad times. I thank Anjana, Zuhair, Anoop and Masroor for the nice group discussions and the pleasant atmosphere created by them. I also thank my friend Jilna Mohan for her encouragement and constant support. I thank my teachers Dr. K. V Devadasan, Mrs. Sandhya C. V and G Harikrishnan for the efforts they had taken to teach me and for introducing University of Hyderabad and many good institutes to me. Without them it would not be possible for me to study in University of Hyderabad. I wish to express my thanks to my family for sharing all my worries and tensions during my Ph.D. I feel extremely grateful for the love and care I received from my family.

Sruthilaya M

To

My family

Abstract

The discovery of neutrino oscillation confirmed that neutrinos are massive and flavor eigenstates are mixture of mass eigenstates. Thus, many experiments focused on determining neutrino mass and mixing. As a result most of the oscillation parameters are measured precisely and it is confirmed that atleast two of active neutrinos are massive but the masses are very small demanding a different origin for neutrino mass from other fermion masses. Various seesaw mechanisms explain tiny neutrino mass but not the mixing. If it is only the SM symmetry that governs particle interactions then all the parameters in active neutrino mass matrix are independent from each other. But if there exists flavor symmetry, one which relates fermions of different generations then the number of free parameters in neutrino mass matrix reduces. As a result the neutrino mixing matrix takes some special forms such as tribimaximal mixing, bimaximal mixing, golden ratio A, golden ratio B, hexagonal mixing etc. All these forms of neutrino mixing matrix predict mixing angles other than θ_{13} close to the experimental values but have vanishing θ_{13} while oscillation experiments measure moderately large θ_{13}. Hence, we consider the effect of perturbations to these mixing matrices and find that the above mentioned mixing matrices with suitable perturbations can accommodate non-zero θ_{13}. Then we consider a model based on A_4 symmetry which gives co-bimaximal form for neutrino mixing matrix at leading order while correction in neutrino sector from effective dimensional five operators modify the mixing matrix. We also study the implications of the model in lepton flavor violation decay $\mu \to e\gamma$. We then study A_4 realization of linear seesaw where SM symmetry is extended with $A_4 \times Z_4 \times Z_3$ and a global symmetry $U(1)_X$ which is broken explicitly in Higgs potential. We found that for chosen representations of fields under symmetry groups of the model the mixing parameters obtained are inline with experimental observations. Moreover, we discuss the scope of this model to explain the baryon asymmetry of the universe through Leptogenesis and the possibility of probing the non-unitarity effect in this scenario.

Contents

1 Introduction **1**

1.1 Standard Model of particle physics . . . 3

1.1.1 Higgs mechanism . . . 9

1.1.2 Weinberg Salam model . . . 12

1.2 Neutrino oscillations . . . 16

1.3 Outline of thesis . . . 19

2 Neutrino mass and mixing in beyond standard model **21**

2.1 Type-I seesaw . . . 21

2.1.1 Type-II seesaw . . . 24

2.2 Type-III seesaw . . . 26

2.3 Linear and Inverse seesaw . . . 26

2.4 Neutrinoless double beta decay . . . 28

2.5 Neutrino mixing patterns . . . 29

2.5.1 Tri-Bimaximal mixing . . . 31

2.5.2 Bimaximal mixing . . . 31

2.5.3 Golden ratio A and Golden ratio B . . . 31

2.5.4 Hexagonal mixing . . . 31

3 Predicting Leptonic CP phase by considering deviations in charged lepton and neutrino sectors **33**

3.1 Introduction . . . 33

3.2 Framework . . . 35

3.3 Deviation in Neutrino sector . . . 36

3.3.1 Deviation due to (23) rotation . . . 36

3.3.2 Simulation details . . . 39

3.3.3 Deviation due to (13) rotation . . . 42

3.4 Deviation in the charged lepton sector . . . 44

3.4.1 Deviation due to rotation in (12) and (13) sectors 45
3.5 Summary and Conclusions 48

4 Non-zero θ_{13} and leptonic CP phase with A_4 Symmetry 51
4.1 Introduction 51
4.2 The Model 53
4.3 Perturbation in neutrino sector 57
4.4 Vacuum alignment 59
4.5 Effect of additional Higgs doublets on lepton flavor violating decay $\mu \to e\gamma$ . . 62
4.6 Summary and Conclusions 63

5 A_4 realization of Linear Seesaw and Neutrino Phenomenology 65
5.1 Introduction 65
5.2 The model framework for linear seesaw 67
5.3 An A_4 realization of linear seesaw 68
5.4 Neutrino Masses and Mixing 70
5.5 Numerical results 73
5.5.1 Correlation between model parameters with $\tan\psi = 0$ 75
5.5.2 Correlation between model parameters with $\tan\psi \neq 0$. 76
5.6 Leptogenesis 79
5.7 Summary and Conclusions 84

6 Summary and Conclusions 87

Chapter 1

Introduction

Neutrinos are the lightest fermions belonging to the lepton family of elementary particles. Being colourless and electrically neutral, they are sensitive only to weak interactions, hence interact very rarely, which made them hidden from rest of the universe for a very long time until some conscious efforts were made to observe them as the existence of neutrino was predicted by theory to explain beta decay. There exists three flavors of neutrinos: electron (ν_e), muon (ν_μ) and tau (ν_τ) neutrinos corresponding to their charged lepton partners electron (e), muon (μ) and tau (τ). Electron anti-neutrino was first detected in a reactor neutrino experiment by Reins and Cowan in 1956 [1, 2], for which Reins received Nobel prize in 1995. Later in 1962 Lederman, Schwartz and Steinberger discovered muon neutrino [3] and won Nobel prize in 1988 while tau neutrino was discovered in 2000 by DONUT collaboration [4]. Pauli proposed the existence of neutrinos in order to show that beta decay does not violate any of the conservation laws, such as energy-momentum conservation and angular momentum conservation. Prior to it, beta decay was thought to be a two body process where a neutron inside a nucleus is converted into a proton by emitting an electron. Being a two body problem and the daughter nuclei is almost at rest, the energy-momentum conservation suggests energy spectrum of emitted electron to be discrete with energy close to the binding energy of the nucleus and recoiling of the nucleus to be opposite to the direction of emission of electron. But energy spectrum of beta decay was found to be continuous [5] and the recoiling of nucleus was not exactly opposite to the direction of emission of electron. Other than this, beta decay as a two body problem seems to violate angular momentum conservation as a spin-half particle decays into two spin-half particles. To explain this spectacular result, Pauli suggested that in beta decay along with electron a neutral spin-half particle is also emitted and the binding energy is distributed among them. These particles later named as neutrino meaning 'little neutral one' by Fermi. In β-decay, the maximum energy of electrons is close to the binding energy of nucleus suggesting neutrinos are almost massless. Being light and

not yet observed suggest that neutrinos are rarely interacting. The maximum energy electron can have depends upon the mass of neutrino. Hence, the β-decay spectrum is sensitive to neutrino mass and the effect of neutrino mass on β-decay spectrum is well visualized by Kurie plot, which is shown in Fig. 1.1.

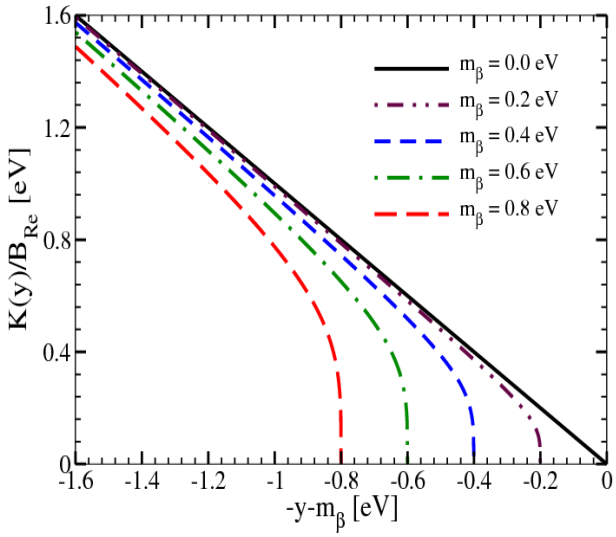

Figure 1.1: Kurie plot taken from [6]. The plot shows the variation in the endpoint energy of emitted electrons with non-zero neutrino mass

The beta decay experiments could only set an upper bound on neutrino mass till date [7], as the mass of neutrinos are well below the experimental sensitivity. Hence, many beta decay experiments are designed with improved sensitivity for direct measurement of neutrino mass [8, 9].

Incorporating Pauli's idea and inspired by electromagnetic interaction, Fermi put forward four-fermion interaction as the mechanism behind β decay [10]. Fermi proposed electrons and neutrinos are created during the transition of neutron to proton like photons are created during the emission by an atom. Hence, beta decay rate is proportional to transition probability. Fermi also gave a formula to calculate transition probability, which is named as Fermi's golden rule. Thus, Fermi's theory allowed to calculate beta decay life-time, also gives a quantitative description of beta decay emission spectrum. Fermi's four-fermion interaction with suitable amendments in response to experimental discoveries [11, 12, 13] evolved to the present form of weak interaction which serves a major part of the well established theory, the Standard Model (SM) of particle physics.

Even though SM explains most of the phenomenon in the universe and its predictions are verified with great accuracy, there are some problems, such as the existence of dark matter [14, 15], matter-antimatter asymmetry [16], etc which are beyond the scope of SM hence,

hint towards Physics beyond SM. Among all the elementary particles, neutrino is the only particle which behaves differently from SM predictions. Right-handed neutrinos are absent in the standard model as they were neither observed [17] nor needed for the completeness of SM. In standard model all fermions that interact with Higgs get their mass due to its non-zero vacuum expectation value. Higgs interacts with a left-handed and a right-handed fermion hence, does not interact with neutrinos keeping neutrinos massless in SM. But they are found to be massive falsifying the SM prediction. Neutrinos are proved to be massive by the experimental confirmation of neutrino oscillation [18, 19, 20, 21], a phenomenon in which neutrino changes its flavor as it propagates [22, 23]. Neutrino oscillation demands neutrino flavor states different from mass states [24], hence, atleast one of the mass states should be non-degenerate i.e., atleast one among the three neutrinos is massive [25, 26].
Neutrino oscillation experiments probe neutrino mixing and mass squared differences, hence, the structure of neutrino mass matrix which in turn gives an idea about the symmetry across the generations and perhaps an explanation for existence of three generations of fermions for which SM has no answer. And beta decay [27], neutrinoless double beta decay ($0\nu\beta\beta$) [28] and cosmological bound on sum of neutrino mass give the idea about the absolute scale of neutrino mass. Hence these experiments collectively uncover neutrino mass sector making neutrino a good place to look for the nature of new physics beyond SM. No standard model particles can account for the dark matter also matter-antimatter asymmetry requires CP violation [29]. The only source of CP violation in the SM is from the complex elements in CKM matrix that relate flavor and mass states of down type quarks which is not enough to account for the observed asymmetry. Mass models for neutrino require extension of SM in terms of particle content, the new particles can be dark matter candidates [30, 31, 32, 33, 34, 35, 36] and complex elements in neutrino mass matrix can add up the CP violation hence, give rise to correct matter-antimatter asymmetry [37, 38, 39]. A right model for neutrino mass may solve the mystery of dark matter and matter-antimatter asymmetry. Hence, building a model to explain neutrino mass is a step towards finding a theory which explains all these mysteries.

1.1 Standard Model of particle physics

SM includes all the elementary particles discovered till now and describes the fundamental interactions strong, electromagnetic, and weak based on the gauge groups $SU(3)_C \times SU(2)_L \times U(1)_Y$ [40]. $SU(3)_C$ describes the strong interaction [41] while $SU(2)_L \times U(1)_Y$ describes the electroweak interaction which unifies electromagnetic and weak interactions [42]. The elementary particles belong to different representations of SM symmetry group as shown in

Table 1.1.

Fields	$SU(3)_C$	$SU(2)_L$	$U(1)_Y$
$\begin{pmatrix} \nu_e \\ e \end{pmatrix}_L, \begin{pmatrix} \nu_\mu \\ \mu \end{pmatrix}_L, \begin{pmatrix} \nu_\tau \\ \tau \end{pmatrix}_L$	1	2	-1
e_R, μ_R, τ_R	1	1	-2
$\begin{pmatrix} u \\ d \end{pmatrix}_L, \begin{pmatrix} c \\ s \end{pmatrix}_L, \begin{pmatrix} t \\ b \end{pmatrix}_L$	3	2	$\frac{1}{3}$
u_R, c_R, t_R	3	1	$\frac{4}{3}$
d_R, s_R, b_R	3	1	$-\frac{2}{3}$
H	1	2	1

Table 1.1: Fermion and scalar contents of SM model along with their $SU(3)_C \times SU(2)_L$ representations and hypercharge.

SM classifies the elementary particles based on their properties into different categories: fermions and bosons. Fermions are again classified into two groups quarks and leptons while bosons are of two types, gauge bosons with spin one (vector bosons) and Higgs boson with spin zero (scalar boson). Quarks and leptons are two classes of fermions, the one which is sensitive to strong interaction falls into quarks category while the one which is not into leptons. Quarks belong to triplet representation of $SU(3)_C$ hence, there are three equivalent states of each quark species which differ from each other by color, the charge of strong interaction. Fermions are put into three generations and the stability of fermions decreases as going from first to third. Gauge bosons are spin 1 particles that mediate interactions and Higgs, the only spin-0 boson in SM gives masses to all elementary particles. Strong interactions are mediated by eight types of gluons, W and Z bosons mediate weak interactions while electromagnetic interactions are mediated by photons.

Strong interaction: The strong interaction is dictated by $SU(3)$ local symmetry, which is a non-abelian symmetry. $SU(3)_C$ symmetry requires the physics to be invariant under the local $SU(3)$ transformation in color space, where a triplet, $\psi(x)^T = (\psi^1(x), \psi^2(x), \psi^3(x))$ transforms as

$$\psi(x) = e^{i\alpha_a(x)T_a}\psi(x) \ , \tag{1.1}$$

$\alpha_a,\ a = 1, ..., 8$ are group parameters and T_a are generators of $SU(3)$ symmetry and obey the commutation relation

$$[T_a, T_b] = i f_{abc} T_c \ , \tag{1.2}$$

where f_{abc} are real constants known as structure constants of the group. Hence, the Lagrangian of a color triplet is given by

$$\mathcal{L} = \bar{\psi}(x) \left(i\gamma^\mu \partial_\mu - m\right) \psi(x) - g_s \left(\bar{\psi}(x)\gamma^\mu T_a \psi(x)\right) G^a_\mu - \frac{1}{4} G^a_{\mu\nu} G^{\mu\nu}_a \ , \tag{1.3}$$

where

$$G^a_{\mu\nu} = \partial_\mu G^a_\nu - \partial_\nu G^a_\mu - g_s f_{abc} G^b_\mu G^c_\nu \ . \tag{1.4}$$

G^a_μ are the gauge boson (gluon) fields and transform under $SU(3)$ as

$$G^a_\mu \to G^a_\mu - \frac{1}{g_s} \partial_\mu \alpha_a - f_{abc} \alpha_b G^c_\mu \ , \tag{1.5}$$

introduced to ensure $SU(3)$ local symmetry. The first term in the Lagrangian (1.3) is the kinetic and mass term of the field ψ, second term is the interaction between the field ψ and gluons and the last term is the kinetic energy and self-interaction of gluons. Mass terms for gluons, $G^a_\mu G^\mu_a$ are absent in the Lagrangian, as such terms spoil the $SU(3)$ symmetry. Hence, $SU(3)$ symmetry results in eight massless gluons. Equation (1.3) is the interaction Lagrangian describing a color triplet and eight massless gluons which tells that any particle which has color interacts with gluons with a coupling g_s. Hence, strong interaction between particles are mediated by eight types of self-interacting massless gluons. Quarks are triplet under $SU(3)_C$ while leptons are singlets, hence, the above Lagrangian describes the interactions of quarks with gluons.

Electroweak interaction: Electroweak interaction is governed by $SU(2)_L \times U(1)_Y$ symmetry [43]. The subscript L on $SU(2)$ indicates only left-chiral fields have non trivial representation under $SU(2)$, in other words only left-chiral fields transform under $SU(2)_L$ [44]. The transformation property of particle under $SU(2)_L$ is defined by its Isospin (I) while that under $U(1)_Y$ by hypercharge (Y) which are related to electric charge (Q) of particle as

$$Q = I_3 + \frac{Y}{2} \ , \tag{1.6}$$

where I_3 is the third component of Isospin which changes from I to $-I$ in steps of one from top to bottom within $SU(2)_L$ multiplet. A particle with Isospin I belongs to a multiplet of dimension $2I + 1$, for example particle with Isospin $\frac{1}{2}$ belongs to a doublet. Fermion content

of SM belongs to different representation of $SU(2)_L \times U(1)_Y$ as shown in Table 1.1. The left chiral projections of fermions belong to $SU(2)_L$ doublet while right chiral projections are singlet. Both left and right chiral fields have nonzero hypercharge. For example, left chiral projection of electron along with electron neutrino form an isospin doublet having hyperchage -1, while right chiral projection of electron is an isospin singlet with hypercharge -2 and right handed neutrinos are absent in SM. Hence, under $SU(2)_L \times U(1)_Y$ the left and right chiral projections of fermions transform as

$$\begin{aligned} \chi_L &= e^{i\boldsymbol{\alpha}(x).\boldsymbol{\tau}} e^{i\beta(x)Y_L} \chi_L \,, \\ \psi_R &= e^{i\beta(x)Y_R} \psi_R \,, \end{aligned} \tag{1.7}$$

where $\tau_i = \frac{1}{2}\sigma_i$, σ_i's are Pauli matrices given by

$$\sigma_1 = \begin{pmatrix} 0 & 1 \\ 1 & 0 \end{pmatrix}, \quad \sigma_2 = \begin{pmatrix} 0 & -i \\ i & 0 \end{pmatrix}, \quad \sigma_3 = \begin{pmatrix} 1 & 0 \\ 0 & -1 \end{pmatrix}. \tag{1.8}$$

Y_L and Y_R are hypercharge of χ_L and ψ_R respectively, χ_L is isospin doublet and ψ_R is isospin singlet. The left and right chiral projections of fermion field ψ is given by

$$\psi_R = \frac{1}{2}\left(1 + \gamma^5\right)\psi \,, \tag{1.9}$$

$$\psi_L = \frac{1}{2}\left(1 - \gamma^5\right)\psi \,, \tag{1.10}$$

where $P_{R,L} = \frac{1}{2}\left(1 \pm \gamma^5\right)$ are the projection operators. The $SU(2)_L \times U(1)_Y$ invariant Lagrangian describing χ_L and ψ_R is given by

$$\begin{aligned} \mathcal{L} &= \bar{\chi}_L \gamma^\mu \left(i\partial_\mu - g\boldsymbol{\tau}.\boldsymbol{W_\mu} - g'\frac{Y_L}{2}B_\mu\right)\chi_L \\ &+ \bar{\psi}_R \gamma^\mu \left(i\partial_\mu - g'\frac{Y_R}{2}B_\mu\right)\psi_R - \frac{1}{4}\boldsymbol{W_{\mu\nu}}\boldsymbol{W^{\mu\nu}} - \frac{1}{4}B_{\mu\nu}B^{\mu\nu} \,, \end{aligned} \tag{1.11}$$

where $\boldsymbol{W_{\mu\nu}}$ and $B_{\mu\nu}$ are given by

$$\begin{aligned} \boldsymbol{W_{\mu\nu}} &= \partial_\mu \boldsymbol{W_\nu} - \partial_\nu \boldsymbol{W_\mu} - g\boldsymbol{W_\mu} \times \boldsymbol{W_\nu} \,, \\ B_{\mu\nu} &= \partial_\mu B_\nu - \partial_\nu B_\mu \,. \end{aligned} \tag{1.12}$$

The gauge fields $\boldsymbol{W_\mu} = \{W_\mu^1, W_\mu^2, W_\mu^3\}$, transform under $SU(2)_L$ as

$$\boldsymbol{W_\mu} \to \boldsymbol{W_\mu} - \frac{1}{g}\partial_\mu \boldsymbol{\alpha}(x) - \boldsymbol{\alpha}(x) \times \boldsymbol{W_\mu} \,, \tag{1.13}$$

while B_μ transforms under $U(1)_Y$ as

$$B_\mu \to B_\mu - \frac{1}{g'}\partial_\mu \beta(x). \tag{1.14}$$

The left-handed chiral field χ_L in (1.11) represents all isospin doublets of elementary fermions and ψ_R represents all right handed fermions of SM. For example, for

$$\chi_L = \begin{pmatrix} \nu_{eL} \\ e_L \end{pmatrix}, \qquad \psi_R = e_R, \tag{1.15}$$

the Lagrangian (1.11) describes electron and electron-type neutrino. Substituting (1.15) in Eq. (1.11), we obtain

$$\begin{aligned} \mathcal{L} &= (\bar{\nu}_{eL}\bar{e}_L)\,\gamma^\mu \begin{pmatrix} i\partial_\mu & 0 \\ 0 & i\partial_\mu \end{pmatrix} \begin{pmatrix} \nu_{eL} \\ e_L \end{pmatrix} \\ &- \frac{1}{2}(\bar{\nu}_{eL}\bar{e}_L)\,\gamma^\mu \begin{pmatrix} gW_\mu^3 + g'Y_L B_\mu & g\left(W_\mu^1 - iW_\mu^2\right) \\ g\left(W_\mu^1 + iW_\mu^2\right) & -gW_\mu^3 + g'Y_L B_\mu \end{pmatrix} \begin{pmatrix} \nu_{eL} \\ e_L \end{pmatrix} \\ &+ \bar{e}_R\gamma^\mu\left(i\partial_\mu - \frac{1}{2}g'Y_R B_\mu\right) e_R\,, \end{aligned} \tag{1.16}$$

with $Y_L = -1$ and $Y_R = -2$. From Eq. (1.16) one can identify the linear combination of W_μ^1 and W_μ^2 given by $W_\mu = \frac{1}{\sqrt{2}}\left(W_\mu^1 + iW_\mu^2\right)$ as the field, that annihilates W^+ and creates W^- gauge bosons of weak interaction. The neutral field W_μ^3 is inadequate to describe Z boson, the neutral weak gauge boson, as it couples to both left and right chiral fields, while W_μ^3 interacts only with left chiral fields. So $SU(2)_L$ symmetry is insufficient to explain weak interaction, this led to the unification of electromagnetic and weak interaction. The gauge field B_μ is neutral and couples with both left and right chiral fields, hence, it should be one of the two linear combination of W_μ^3 and B_μ that describes Z boson while the other gives photon field A_μ [42]. Two orthogonal combinations of neutral gauge fields W_μ^3 and B_μ that give the physical fields Z_μ and A_μ, are given by

$$\begin{aligned} Z_\mu &= -B_\mu \sin\theta_W + W_\mu^3 \cos\theta_W\,, \\ A_\mu &= B_\mu \cos\theta_W + W_\mu^3 \sin\theta_W\,, \end{aligned} \tag{1.17}$$

where θ_W is known as weak mixing angle or Weinberg angle which relates the coupling constants g, g' and electromagnetic coupling e, as $g\sin\theta_W = g'\cos\theta_W = e$. In the basis of

physical gauge fields, interaction part of the Lagrangian is given by

$$\mathcal{L}_{\text{int}} = -\frac{g}{\sqrt{2}}\left[j^{\mu\dagger}W_\mu + \text{h.c.}\right] - \frac{g}{\cos\theta_w} j^\mu_{NC} Z_\mu - e j^\mu_{em} A_\mu \ , \tag{1.18}$$

where j_μ is the weak charged current

$$j^\mu = \bar{\nu}_e \gamma^\mu \frac{1}{2}\left(1-\gamma^5\right) e, \tag{1.19}$$

j^μ_{NC} is the weak neutral current

$$j^\mu_{NC} = \bar{\nu}_e \gamma^\mu \frac{1}{2}\left(g^\nu_V - g^\nu_A \gamma^5\right)\nu_e + \bar{e}\gamma^\mu \frac{1}{2}\left(g^e_V - g^e_A\gamma^5\right) e \ , \tag{1.20}$$

with

$$g^f_V = I^f_3 - 2\sin^2\theta_W q^f \ , \quad g^f_A = I^f_3 \ , \tag{1.21}$$

and j^μ_{em} is the electromagnetic current

$$j^\mu_{em} = q^e \bar{e}\gamma^\mu e \ , \tag{1.22}$$

where q^f is the electric charge of fermion f in units of e, for charged leptons it is -1, for up-type quark it is $\frac{2}{3}$ and for down-type quark $-\frac{1}{3}$. Similarly, quarks also posses same kind of interactions to preserve $SU(2)_L \times U(1)_Y$ symmetry. Hence, $SU(2)_L \times U(1)_Y$ symmetry defines charged and neutral weak currents and electromagnetic current.

The mass terms for fermions as well as that of gauge bosons are absent in the electroweak Lagrangian, as such terms do not respect $SU(2)_L$ symmetry. The fermion mass term, $m_\psi \bar{\psi}_L \psi_R$ is not invariant under SM symmetry as $SU(2)_L \times U(1)_Y$ transformations distinguish the left (ψ_L) and right (ψ_R) chiral projections of fermions. Hence, the symmetry demands all elementary fermions and gauge bosons to be massless but in reality all fermions and weak gauge bosons ($W^\pm$ and Z) are massive while gluons and photons are massless. Hence, to explain masses of fermions and weak gauge bosons $SU(2)_L \times U(1)_Y$ symmetry has to be broken but an explicit breaking of symmetry by mass terms of gauge bosons make the theory non-renormalizable hence, meaning less. Higgs mechanism is the resolution for the nonzero masses of particles where particle get mass when local gauge symmetry breaks spontaneously by the nonzero vacuum expectation value of Higgs field.

1.1.1 Higgs mechanism

Spontaneous breaking of global gauge symmetry: The Lagrangian describing a complex scalar field $\phi = \frac{1}{\sqrt{2}}(\phi_1 + i\phi_2)$ given by

$$\mathcal{L} = (\partial_\mu \phi)^* (\partial^\mu \phi) - \mu^2 \phi^* \phi - \lambda(\phi^* \phi)^2 \,, \tag{1.23}$$

is invariant under global $U(1)$ transformation of ϕ

$$\phi \to e^{i\alpha}\phi. \tag{1.24}$$

For $\mu^2 > 0$, the second and third terms in the above Lagrangian is the potential $V(\phi)$ of a scalar field with mass m and ground state at zero, as minimum value of the scalar potential corresponds to $\phi = 0$. But if $\mu^2 < 0$ it can not be the mass of the field as it has a wrong sign also $\phi = 0$ no longer gives a minima of the potential, which can be seen by looking into the conditions for minima

$$\frac{\partial V(\phi)}{\partial|\phi|} = 0 \Rightarrow \mu^2 + \lambda(\phi_1^2 + \phi_2^2) = 0, \tag{1.25}$$

$$\frac{\partial^2 V(\phi)}{\partial|\phi|^2} > 0 \Rightarrow \mu^2 + 3\lambda(\phi_1^2 + \phi_2^2) > 0. \tag{1.26}$$

Solutions of the first condition (1.25) are $\phi = 0$ and $(\phi_1^2 + \phi_2^2) = -(\mu^2/\lambda)$ while the second condition (1.26) is satisfied only for $(\phi_1^2 + \phi_2^2) = -(\mu^2/\lambda)$. Hence, all points in $\phi_1 - \phi_2$ plane that satisfy the condition $(\phi_1^2 + \phi_2^2) = -(\mu^2/\lambda)$ correspond to a minimum which is an outcome of $U(1)$ symmetry, as all those points are connected by $U(1)$ transformations. So there are many possible ground states for ϕ and one among them can be chosen as the ground state. The symmetry breaks down, once the choice is made hence, called spontaneous symmetry breaking. One can chose the ground state $\phi = v = \sqrt{-(\mu^2/\lambda)}$, e.g., $\phi_1 = v$ and $\phi_2 = 0$ as all the possible ground states are equivalent. The field $\phi(x)$ can be expressed in terms of fields $\eta(x)$ and $\xi(x)$ as a small fluctuation from its ground state v as

$$\phi(x) = \frac{1}{\sqrt{2}}\left[v + \eta(x) + i\xi(x)\right]. \tag{1.27}$$

The Lagrangian $\mathcal{L}$ can be expanded about the ground state by substituting Eq. (1.27) in (1.23) as

$$\mathcal{L} = \frac{1}{2}(\partial_\mu \xi)(\partial^\mu \xi) + \frac{1}{2}(\partial_\mu \eta)(\partial^\mu \eta) - (\lambda v^2 \eta^2 + \text{const} + \cdots) \,, \tag{1.28}$$

where the dots stand for cubic and quartic terms in η and ξ. The above Lagrangian (1.28), describes a massive real scalar field η with mass $\sqrt{2\lambda v^2}$ and a massless one ξ, known as

Goldstone boson [45]. One can see that when a local gauge symmetry breaks spontaneously the resulting massless fields are unphysical and serve as extra degrees of freedom required for gauge bosons to become massive [46, 47]. This is known as Higgs mechanism.

Spontaneous breaking of local $U(1)$ symmetry [47]: $U(1)$ local gauge symmetry demands the Lagrangian to be invariant under a transformation

$$\phi \to e^{i\alpha(x)}\phi \ , \tag{1.29}$$

hence, should be in the form

$$\mathcal{L} = (\partial_\mu + ieA_\mu)\phi^*(\partial^\mu - ieA^\mu)\phi - \mu^2\phi^*\phi - \lambda(\phi^*\phi)^2 - \frac{1}{4}F_{\mu\nu}F^{\mu\nu} \ , \tag{1.30}$$

where

$$F_{\mu\nu} = \partial_\mu A_\nu - \partial_\nu A_\mu \ , \tag{1.31}$$

and the gauge field A_μ transforms as

$$A_\mu \to A_\mu + \frac{1}{e}\partial_\mu\alpha(x) \ . \tag{1.32}$$

Substituting Eq. (1.27) into (1.30), one obtains

$$\begin{aligned} \mathcal{L} &= \frac{1}{2}(\partial_\mu\xi)(\partial^\mu\xi) + \frac{1}{2}(\partial_\mu\eta)(\partial^\mu\eta) - \lambda v^2\eta^2 + \frac{1}{2}e^2v^2A_\mu A^\mu \\ &- evA_\mu\partial^\mu\xi(x) - \frac{1}{4}F_{\mu\nu}F^{\mu\nu} + \text{h.o.} \ , \end{aligned} \tag{1.33}$$

which describes a massless fermion ξ and a massive fermion η along with massive gauge boson A_μ but has an extra degree of freedom compared to the Lagrangian in Eq. (1.30), which means one of the scalar fields is unphysical. The unphysical scalar field can be removed by proper gauge transformation. To see this one should choose the representation of ϕ as

$$\phi = \frac{1}{\sqrt{2}}\left(v + h(x)\right)e^{i\frac{\theta(x)}{v}} \ , \tag{1.34}$$

where both $h(x)$ and $\theta(x)$ are real scalar fields. The phase part of ϕ can be removed by the $U(1)$ transformation

$$\phi' \to e^{-i\frac{\theta(x)}{v}}\phi \ , \tag{1.35}$$

for which the Lagrangian is invariant along with the gauge field transformed as

$$A'_\mu \to A_\mu - \frac{1}{ev}\partial_\mu \theta(x) \; . \tag{1.36}$$

Substituting ϕ' in Eq. (1.30), yields

$$\mathcal{L} \;\; = \;\; \frac{1}{2}\left(\partial_\mu h(x)\right)^2 - \lambda v^2 h(x)^2 + \frac{1}{2}e^2 v^2 {A'_\mu}^2 - \frac{1}{4}F_{\mu\nu}F^{\mu\nu} + \text{h.o.} \; . \tag{1.37}$$

Now the theory is free of massless fields. In a similar way $SU(2)$ gauge boson masses are generated dynamically when the symmetry is broken by nonzero vacuum expectation value of Higgs doublet.

Spontaneous breaking of Local $SU(2)$ gauge symmetry: The Lagrangian describing the field ϕ, a $SU(2)$ doublet of complex scalar fields, which preserves local $SU(2)$ gauge symmetry is given by

$$\mathcal{L} = \left(\partial_\mu \phi + ig\boldsymbol{\tau}.\boldsymbol{W}_\mu \phi\right)^\dagger \left(\partial^\mu \phi + ig\boldsymbol{\tau}.\boldsymbol{W}^\mu \phi\right) - V(\phi) - \frac{1}{4}\boldsymbol{W}_{\mu\nu}.\boldsymbol{W}^{\mu\nu} \; , \tag{1.38}$$

where

$$\phi = \frac{1}{\sqrt{2}}\begin{bmatrix} \phi_1 + i\phi_2 \\ \phi_3 + i\phi_4 \end{bmatrix} \; , \tag{1.39}$$

and

$$V(\phi) = \mu^2 \phi^\dagger \phi + \lambda(\phi^\dagger \phi)^2 \; , \tag{1.40}$$

is the Higgs potential with $\mu^2 < 0$. Thus, it has the minimum at

$$\phi^\dagger \phi = \frac{1}{2}\left(\phi_1^2 + \phi_2^2 + \phi_3^3 + \phi_4^2\right) = -\frac{\mu^2}{\lambda} \; , \tag{1.41}$$

and one can chose the vacuum as

$$\phi_0 = \frac{1}{\sqrt{2}}\begin{bmatrix} 0 \\ v \end{bmatrix}, \tag{1.42}$$

and the invariance under $SU(2)$ transformation $\phi \to e^{i\boldsymbol{\alpha}.\boldsymbol{\tau}}\phi$ allows to expand ϕ about the vacuum as

$$\phi(x) = \frac{1}{\sqrt{2}}\begin{bmatrix} 0 \\ v + h(x) \end{bmatrix}. \tag{1.43}$$

Substituting ϕ in Eq. (1.38) gives

$$\mathcal{L} = \frac{1}{2}\left(\partial_\mu h(x)\right)^2 - \lambda v^2 h(x)^2 + \frac{1}{8}\left(W_\mu^\dagger W^\mu + W_\mu^{3\,2}\right) - \frac{1}{4}\boldsymbol{W}_{\mu\nu}.\boldsymbol{W}^{\mu\nu} + \text{h.o.}. \tag{1.44}$$

Thus, the particle content of the theory includes three massive gauge bosons, $W^{\pm}$, W^3 with mass $\frac{1}{2}gv$, a scalar with mass λv and no massless particles. This shows breaking of $SU(2)$ symmetry by a $SU(2)$ doublet Higgs generate mass for all three gauge bosons, this is the key for generating mass for three gauge bosons $W^{\pm}$ and Z of weak interaction.

1.1.2 Weinberg Salam model

Weinberg-Salam model explains mass generation of weak gauge bosons and fermions by applying Higgs mechanism to electroweak theory. Out of four gauge bosons of electroweak interaction one is massless implying a $U(1)$ symmetry is preserved even after the spontaneous breaking of $SU(2)_L \times U(1)_Y$ symmetry. The symmetry can be identified as $U(1)_{\text{em}}$, symmetry of electromagnetic interaction as it is the photon that remains massless. Hence, the Higgs field should break $SU(2)_L \times U(1)_Y$ to $U(1)_{\text{em}}$. The Higgs doublet with hypercharge +1 serves the purpose [42]. Nonzero vacuum expectation value of neutral component of Higgs doublet breaks electroweak symmetry and generates mass for weak gauge bosons keeping photons massless [42]. Interestingly the same Higgs field can generate mass for quarks and charged leptons.

A Higgs doublet with hypercharge $Y = 1$ is given by

$$\begin{bmatrix} \phi^+ \\ \phi^0 \end{bmatrix}, \tag{1.45}$$

where both ϕ^+ and ϕ^0 are complex fields with charge +1 and zero respectively. Since the photon is charge-less vacuum should be electrically neutral. Hence, the vacuum is chosen as

$$\langle \phi \rangle = \begin{bmatrix} 0 \\ \frac{v}{\sqrt{2}} \end{bmatrix}. \tag{1.46}$$

The term in the Lagrangian describing ϕ, relevant for mass generation of gauge bosons is given by

$$\mathcal{L}_{mass} = \left| \left(-ig\boldsymbol{\tau}.\boldsymbol{W}_\mu - i\frac{g'}{2}B_\mu \right) \langle \phi \rangle \right|^2. \tag{1.47}$$

Substituting the value of $\langle \phi \rangle$ from (1.46), in the above equation gives

$$\begin{aligned} \mathcal{L}_{mass} &= \frac{1}{8}(gv)^2 \left[\left(W^1_\mu + iW^2_\mu \right) \left(W^{1\mu} - iW^{2\mu} \right) \right] \\ &+ \frac{1}{8}(gv)^2 \left[W^3_\mu W^{3\mu} - 2\frac{g'}{g} W^3_\mu B^\mu + \left(\frac{g'}{g} \right)^2 B_\mu B^\mu \right], \end{aligned} \tag{1.48}$$

which in terms of physical gauge boson fields W_μ, Z_μ and A_μ is,

$$\mathcal{L}_{mass} = M_W^2 W_\mu^\dagger W^\mu + \frac{1}{2}\left[M_Z^2 Z_\mu Z^\mu + M_A^2 A_\mu A^\mu\right], \tag{1.49}$$

where

$$\begin{aligned} M_W &= \frac{1}{2}gv, \quad M_Z = \frac{1}{2}\frac{gv}{\cos\theta_W}, \\ M_A &= 0. \end{aligned}$$

Thus, weak gauge bosons become massive as electroweak symmetry breaks spontaneously by nonzero vacuum expectation value of Higgs doublet, while photon remains massless.
The above mass relations give the ratio

$$\frac{M_W}{M_Z} = \cos\theta_W \ , \tag{1.50}$$

predicting the mass of W bosons to be less than or equal to that of Z boson and relative strength of charged current and neutral current interaction in low energy limit, $\rho = \frac{M_W^2}{M_Z^2 \cos^2\theta_W}$ as one. Experimental value of ρ is found to be 0.9980 ± 0.0086, agreeing with the model. The mass of W boson is related to the Fermi constant G_F as

$$\frac{G_F}{\sqrt{2}} = \frac{g^2}{8M_W^2}. \tag{1.51}$$

Substituting $M_W^2 = \frac{1}{4}g^2v^2$ and $G_F = 1.16638 \times 10^{-5}$ in the above equation fixes the VEV of Higgs doublet, $\frac{v}{\sqrt{2}}$ to be 174 GeV.
Under $SU(2)_L \times U(1)_Y$, the product $\bar{L}_{\alpha L}\psi_{\beta R}$ of isospin doublet of left-handed leptons $L_{\alpha L}^T = (\nu_\alpha, l_\alpha)_L$ and right-handed leptons $l_{\beta R}$ for $\alpha, \beta = e, \mu, \tau$ transform as $(2, -1)$ i.e., the product is a doublet under $SU(2)_L$ with hypercharge, $Y = -1$, while the Higgs doublet transforms as $(2, 1)$, hence, the Yukawa interaction

$$\mathcal{L}_Y = -\sum_{\alpha,\beta=e,\mu,\tau} Y_{\alpha\beta}^l \bar{L}_{\alpha L}\phi l_{\beta R} + \text{h.c.} \ , \tag{1.52}$$

is invariant under $SU(2)_L \times U(1)_Y$ symmetry transformations thus, allowed by electroweak symmetry. Substituting ϕ as given in (1.43) in the above Yukawa Lagrangian gives

$$\mathcal{L}_Y = -\frac{1}{\sqrt{2}}(v + h)\,\bar{l}_L Y^l l_R + \text{h.c.} \ , \tag{1.53}$$

where the matrices $l_{L,R}$ are defined as

$$l_{L,R} = \begin{pmatrix} e_{L,R} \\ \mu_{L,R} \\ \tau_{L,R} \end{pmatrix},$$

and Y^l is the 3×3 matrix of Yukawa coupling with elements $\left(Y^l\right)_{\alpha\beta} = Y^l_{\alpha\beta}$. The first term in $\mathcal{L}_Y$ is mass term of charged leptons while second term is the interaction of charged lepton with Higgs. The mass term of charged lepton can be written as

$$\mathcal{L}_{mass} = \bar{l}_L M^l l_R, \tag{1.54}$$

where the mass matrix, $M_l = vY^l$ and the interaction term is given by

$$\mathcal{L}_{int} = \frac{1}{v}\bar{l}_L M l_R h. \tag{1.55}$$

In the similar way, up and down type quarks get mass through the Yukawa interaction,

$$\mathcal{L}^Q_y = -\sum_{i=1,2,3}\sum_{\beta=u,c,t} Y^U_{i\beta}\overline{Q}_{iL}\tilde{\phi}q_{\beta R} + Y^Q_{i\beta}\overline{Q}_{iL}\phi q_{\beta R} + \text{h.c.}, \tag{1.56}$$

where Q_{iL} is the quark doublet of i^{th} generation and

$$\tilde{\phi} = i\tau_2\phi^* = \frac{1}{\sqrt{2}}\begin{pmatrix} v + h(x) \\ 0 \end{pmatrix}. \tag{1.57}$$

Hence, the mass term for quarks is given by

$$\mathcal{L}_{mass} = \overline{q}^U_L M^U q^U_R + \overline{q}^D_L M^D q^D_R + \text{h.c.}, \tag{1.58}$$

with $M^U = vY^U$ and $M^D = vY^D$, where $q^U_{L,R}$ and $q^D_{L,R}$ are defined as

$$\begin{aligned} q^U_{L,R} &= \begin{pmatrix} u_{L,R} \\ c_{L,R} \\ t_{L,R} \end{pmatrix}, \\ q^D_{L,R} &= \begin{pmatrix} d_{L,R} \\ s_{L,R} \\ b_{L,R} \end{pmatrix}. \end{aligned} \tag{1.59}$$

Thus, all fermions except neutrino get mass as electroweak symmetry breaks due to nonzero VEV of Higgs doublet while neutrino remains massless. Fermion mass matrices M^l, M^U and

M^D can be diagonalized by bi-unitary transformations

$$V_L^{l\dagger} M^l V_R^l = M^{l\prime},$$
$$V_L^{U\dagger} M^U V_R^U = M^{U\prime},$$
$$V_L^{D\dagger} M^D V_R^D = M^{D\prime}.$$

Then in the mass diagonal basis lepton charged current is given by

$$j_\mu^\dagger = \bar{l}_L V_L^{l\dagger} \gamma_\mu \nu_L = \bar{l}_L \gamma_\mu V_L^{l\dagger} \nu_L = \bar{l}_L \gamma_\mu \nu_L', \tag{1.60}$$

where ν_L is a three element column matrix containing field of three flavors of neutrinos and $\nu_L' = V_L^{l\dagger} \nu_L$. One can choose the flavor eigenstates (eigenstates of charged weak interactions) as l_l and ν_L'. Since neutrinos are massless ν_L' also forms mass basis. Hence, in SM lepton flavor and mass basis is same, hence lepton flavor is conserved. But in the context of quark it is not possible to find simultaneous eigenstates of mass and flavor as both up-type and down-type quarks are massive. In mass basis charged weak current is given by

$$j_\mu = \bar{q}_L^U V_L^{U\dagger} \gamma_\mu V_L^D q_L^D = \bar{q}_L^U \gamma_\mu V q_L^D, \tag{1.61}$$

where $V = V_L^{U\dagger} V_L^D$ is the quark mixing matrix. The flavor basis can be chosen as $(q_L^U, q_L^{D\prime} = V q_L^D)$, thus it is possible to choose flavor eigenstates of up type quarks same as mass eigenstates then for down type quarks flavor states will be a linear combination of mass states. So the quark mixing is not related to V_L^U or V_L^D but the difference between two i.e., $V_L^{U\dagger} V_L^D$ and there will be no mixing if V_L^D is same as V_L^U. The quark mixing matrix known as CKM (Cabibbo-Kobayashi-Maskawa) matrix can be parameterized in terms of three mixing angles and one phase. In general an $N \times N$ unitary matrix can be parameterized in terms $\frac{1}{2}N(N-1)$ mixing angles and $\frac{1}{2}N(N+1)$ phases but, $2N-1$ phases can be removed by redefining phases of fields. Hence, for $N = 3$ there will be three mixing angles and one phase and the standard parameterization of CKM matrix is given by

$$V_{CKM} = \begin{pmatrix} c_{12}c_{13} & s_{12}c_{13} & s_{13}e^{-i\delta} \\ -s_{12}c_{23} - c_{12}s_{13}s_{23}e^{i\delta} & c_{12}c_{23} - s_{12}s_{13}s_{23}e^{i\delta} & c_{13}s_{23} \\ s_{12}s_{23} - c_{12}s_{13}c_{23}e^{i\delta} & -c_{12}s_{23} - s_{12}s_{13}c_{23}e^{i\delta} & c_{13}c_{23} \end{pmatrix}. \tag{1.62}$$

Similar situation arises in lepton sector also if neutrinos are massive. Since neutrinos are electrically neutral they can be either Dirac type or Majorana type. If neutrinos are Dirac type then lepton mixing matrix known as PMNS matrix can be parametrized in terms of

three mixing angles and one phase (Dirac phase), similar to CKM matrix. If neutrino are Majorana type then there will be two additional phases known as Majorana phases in mixing matrix. This is because Majorana fields do not respect $U(1)$ global symmetry, hence, phases in the mixing matrix can not be removed by redefining neutrino fields. So in the case of Majorana neutrinos lepton mixing matrix is given by [48]

$$V_{PMNS} = U_{PMNS} \cdot P_{\nu}, \tag{1.63}$$

where

$$U_{PMNS} = \begin{pmatrix} c_{12}c_{13} & s_{12}c_{13} & s_{13}e^{-i\delta_{CP}} \\ -s_{12}c_{23} - c_{12}s_{13}s_{23}e^{i\delta_{CP}} & c_{12}c_{23} - s_{12}s_{13}s_{23}e^{i\delta_{CP}} & c_{13}s_{23} \\ s_{12}s_{23} - c_{12}s_{13}c_{23}e^{i\delta} & -c_{12}s_{23} - s_{12}s_{13}c_{23}e^{i\delta} & c_{13}c_{23} \end{pmatrix},$$

and $\quad P_{\nu} = \text{diag}(e^{i\rho}, e^{i\sigma}, 1)$

with ρ and σ are Majorana phases. Physical consequences of lepton mixing is that, the flavor states of neutrino evolve with time hence, neutrinos change their flavor as they propagate, and this phenomenon is known as neutrino oscillation. Kamiokande and Sudbury experiments confirmed neutrino oscillation hence, brought out the fact that lepton mixing exists and neutrinos are massive.

1.2 Neutrino oscillations

Neutrino oscillation was suggested as a resolution to solar and atmospheric neutrino problems [49]. Solar and atmospheric neutrino problems refer to the mismatch in neutrino flux predicted by theory and measured by experiments. Neutrino oscillation was first proposed by Pontecorvo in analogy with $K^0 - \bar{K^0}$ oscillation [50], long before the solar and atmospheric neutrino problems were encountered. $K^0 - \bar{K^0}$ oscillation occurs because quark flavor states are admixture of mass states i.e., the mass matrix is non-diagonal in flavor basis. Analogously, neutrino oscillation occurs because flavor and mass bases are different, so it is essentially an effect of nonzero neutrino mass and mixing. Pontecorvo proposed oscillation between active neutrino and a fermion which is a singlet under SM symmetry group, a new concept introduced by him known as sterile neutrino, as there was only one active neutrino known at that time. Later with the discovery of muon neutrino, another flavor of neutrino, flavor oscillation were considered. During 1975 -76, theory of neutrino oscillation was developed in plane-wave approximation [24, 25] which gives various oscillation probabilities such as transition and survival probabilities. Transition probability is the probability of a neutrino to change its

flavor while survival probability is the probability of neutrino flavor to remain the same.
In the plane wave approximation, the time evolution of neutrino mass state in vacuum is given by

$$|\nu_i(t)\rangle = e^{-iE_i t}\,|\nu_i\rangle\,, \tag{1.64}$$

where E_i, the energy of i^{th} mass state is related to its mass m_i and momentum $\vec{p}$ by energy momentum relation

$$E_i = \sqrt{p^2 + m_i^2}\,. \tag{1.65}$$

The flavor state ν_α in terms of mass state is given by,

$$|\nu_\alpha\rangle = \sum_i U_{\alpha i}\,|\nu_i\rangle \qquad (\alpha = e, \mu, \tau), \tag{1.66}$$

where i varies from 1 to 3 and U is a 3×3 unitary matrix that relates mass and flavor eigenstates as

$$\begin{pmatrix} \nu_e \\ \nu_\mu \\ \nu_\tau \end{pmatrix} = U \begin{pmatrix} \nu_1 \\ \nu_2 \\ \nu_3 \end{pmatrix}. \tag{1.67}$$

Both flavor and mass states are orthonormal, hence,

$$\begin{aligned} \langle \nu_i | \nu_j \rangle &= \delta_{ij}\,, \\ \langle \nu_\alpha | \nu_\beta \rangle &= \delta_{\alpha\beta}\,. \end{aligned} \tag{1.68}$$

The state ν_α describes a neutrino with a definite flavor at time, $t = 0$ and after a time t it becomes $|\nu_\alpha(t)\rangle$, given by Eqs (1.64) and (1.66) as,

$$|\nu_\alpha(t)\rangle = \sum_i U_{\alpha i} e^{-iE_i t} \sum_\beta U^*_{\beta i}\,|\nu_\beta\rangle\,, \tag{1.69}$$

a superposition of flavor states. Hence, the probability of a neutrino created with definite flavor α at $t = 0$ to change its flavor to β at $t > 0$ is given by

$$P_{\nu_\alpha \to \nu_\beta}(t) = \left|\left\langle \nu_\beta | \nu_{\alpha(t)} \right\rangle\right|^2. \tag{1.70}$$

Substituting Eq. (1.67) in (1.70) along with the condition $\langle \nu_\alpha | \nu_\beta \rangle = \delta_{\alpha\beta}$ gives

$$P_{\nu_\alpha \to \nu_\beta}(t) = \sum_{i,j} U_{\alpha i} U^*_{\beta i} U^*_{\alpha j} U_{\beta j} e^{-i(E_i - E_j)t}\,. \tag{1.71}$$

In ultra-relativistic limit, the time traveled by neutrino $t \approx L$, the distance traveled by it as

its velocity is close to that of light and with the assumption that all mass states have the same momentum, the difference in energy is approximately,

$$E_i - E_j \approx \frac{\Delta m_{ij}^2}{2E}, \tag{1.72}$$

where $\Delta m_{ij}^2 = m_i^2 - m_j^2$ is the squared mass difference and $E \approx |\vec{p}|$. With this approximations the oscillation probability can be expressed as,

$$P_{\nu_\alpha \to \nu_\beta}(E, L) = \sum_{i,j} U_{\alpha i} U_{\beta i}^* U_{\alpha j}^* U_{\beta j} e^{-i\frac{\Delta m_{ij}^2 L}{2E}}. \tag{1.73}$$

The Eq. (1.73) gives oscillation probabilities for neutrino propagating through vacuum as a function of E, energy of neutrino and L, distance traveled by it which in an experiment is the distance between source and detector. Both E and L depend upon the experiment measuring oscillation probabilities while other quantities , $U_{\alpha i}$ and Δm_{ij}^2 on which oscillation probabilities depend upon are physical constants. The equation (1.73) for $\alpha \neq \beta$ gives transition probability and for $\alpha = \beta$ gives survival probability. The equation (1.73) can be rewritten as

$$P_{\nu_\alpha \to \nu_\beta}(E, L) = \sum_i |U_{\alpha i}|^2 |U_{\beta i}|^2 + 2 \sum_{i<j} \mathcal{R}e \left[U_{\alpha i} U_{\beta j}^* U_{\alpha j}^* U_{\beta i} e^{-i\frac{\Delta m_{ij}^2 L}{2E}} \right]. \tag{1.74}$$

Since U is a unitary matrix $\sum_i |U_{\alpha i}|^2 |U_{\beta i}|^2$ is given by,

$$\sum_i |U_{\alpha i}|^2 |U_{\beta i}|^2 = \delta_{\alpha\beta} - 2 \sum_{i<j} \mathcal{R}e \left[U_{\alpha i} U_{\beta j}^* U_{\alpha j}^* U_{\beta i} \right] . \tag{1.75}$$

Substituting (1.75) in (1.74) gives,

$$\begin{aligned} P_{\nu_\alpha \to \nu_\beta}(E, L) = \delta_{\alpha\beta} \quad &- \quad 4 \sum_{i<j} \mathcal{R}e \left[U_{\alpha i} U_{\beta j}^* U_{\alpha j}^* U_{\beta i} \right] \sin^2 \left[\frac{\Delta m_{ij}^2 L}{4E} \right] \\ &+ \quad 2 \sum_{i<j} \mathcal{I}m \left[U_{\alpha i} U_{\beta j}^* U_{\alpha j}^* U_{\beta i} \right] \sin \left[\frac{\Delta m_{ij}^2 L}{4E} \right]. \end{aligned} \tag{1.76}$$

The unitary matrix U is the PMNS matrix and the product $U_{\alpha i}^* U_{i\beta} U_{\alpha j} U_{i\beta}^*$ is invariant under rephasing transformation,

$$U_{\alpha i} = e^{i\psi_\alpha} U_{\alpha i} e^{i\psi_i}, \tag{1.77}$$

hence, U can be taken as U_{PMNS} even if neutrinos are Majorana type.

From Eq. (1.74) it is clear that oscillation probabilities in vacuum depend upon mass squared differences, mixing angles and Dirac phase but do not depend upon absolute mass of neutrinos

and Majorana phases. As a result of various neutrino oscillation experiments now we have clear idea about almost all oscillation parameters. Results from oscillation experiments show two of the three mixing angles θ_{23} and θ_{12} are large while θ_{13} is small and $\Delta m^2_{12} \ll |\Delta m^2_{13}|$. Sign of the mass squared difference, Δm^2_{13} is not known till the date leaving two possibilities, $m_1 < m_2 \ll m_3$ known as normal hierarchy (NH) and $m_3 \ll m_1 < m_2$ known as inverted hierarchy (IH) for neutrino mass spectrum. The best fit values and 3σ ranges of oscillation parameters are given in Table 1.2.

Mixing Parameters	Best Fit value	3σ Range
$\sin^2\theta_{12}$	0.323	$0.278 \to 0.375$
$\sin^2\theta_{23}$ (NH)	0.567	$0.392 \to 0.643$
$\sin^2\theta_{23}$ (IH)	0.573	$0.403 \to 0.640$
$\sin^2\theta_{13}$ (NH)	0.0234	$0.0177 \to 0.0294$
$\sin^2\theta_{13}$ (IH)	0.0240	$0.0183 \to 0.0297$
$\Delta m^2_{21}/10^{-5}$ eV^2	7.6	$7.11 \to 8.18$
$\lvert\Delta m_{31}\rvert^2/10^{-3}$ eV^2 (NH)	2.48	$2.30 \to 2.65$
$\lvert\Delta m_{31}\rvert^2/10^{-3}$ eV^2 (IH)	2.38	$2.20 \to 2.54$

Table 1.2: The best-fit values and the 3σ ranges of the neutrino oscillation parameters [51].

Data given in Table 1.2 shows atleast two of the three neutrinos are massive falsifying SM prediction of massless neutrino. Hence, explanation of results from neutrino oscillation experiments needs physics beyond SM, specifically a model for neutrino mass which predicts mass squared differences and mixing as given by experiments.

1.3 Outline of thesis

Flavor symmetries also known as family symmetries configure interactions between fermions of different generations. Therefore if flavor symmetry exists one can see its implications on fermion mass and mixing. Various neutrino oscillation experiments probe neutrino mixing and mass hierarchies. Data from these experiments support the idea of existence of flavor symmetry since, the particular form of lepton mixing given by experiments are close to some symmetry forms which are possible outcomes if flavor symmetries existed at high energies. This thesis aim to interpret the recent results on neutrino mass and mixing as an outcome of flavor symmetries.

Various seesaw mechanisms that generate tiny neutrino mass in beyond SM framework, neutrinoless double beta decay and some symmetry forms of lepton mixing matrix which are $\mu - \tau$ symmetric are discussed in chapter 2 of this thesis. Different forms of perturbations to these symmetry forms of lepton mixing matrix, that arise from charged lepton and neutrino sector and predict leptonic CP phase are presented in chapter 3. Chapter 4 discuss non-zero θ_{13} and leptonic CP phase with A_4 symmetry. A_4 realization of linear seesaw is given in chapter 5. Chapter 6 contains summary and conclusions of the thesis.

Chapter 2

Neutrino mass and mixing in beyond standard model

Neutrino is massless in the SM in all order of perturbation due to the absence of right handed neutrinos. Hence, an obvious way to generate neutrino mass is to add right handed neutrinos to SM. This will generate neutrino mass like other fermion masses but will not tell why neutrino mass is too small compared to the mass of other fermions especially to the mass of charged lepton, their isospin partners. The smallness of neutrino mass is addressed by various seesaw mechanisms, such as Type-I [52, 53], Type-II [54, 55], Type-III [56], Linear [57], and Inverse seesaw [58, 59] etc, which will be discussed in following sections.

2.1 Type-I seesaw

The addition of a right handed neutrino N_{Ri}, per generation in the SM model allows the gauge invariant Yukawa interaction,

$$L_Y = -\sum_{ij} Y^{\nu}_{ij} \bar{L}_{iL} \tilde{\phi} N_{jR} + \text{h.c.}, \tag{2.1}$$

which generates Dirac type mass for neutrino through Higgs mechanism. Right-handed neutrinos are singlet under $SU(2)_L$ group like all other right-handed fermions and are electrically neutral too. Then from the relation $Q = I_3 + Y/2$ it is clear that they have zero hypercharge, in short they are singlet under SM symmetry group. Since N_{iR}'s are singlets, the bare mass term,

$$\mathcal{L}_{\text{bare}} = -\frac{1}{2} \sum_{i,j=1}^{3} M_{Rij} \overline{\widehat{N}}_{iL} N_{jR}, \tag{2.2}$$

where $\widehat{N}_{iL}$ is the CP conjugate of N_{iR}, is also allowed by gauge symmetry. Mass terms of such forms are known as Majorana mass terms. After symmetry breaking, mass terms of

neutrinos in the basis $(\widehat{\nu}, N_R)^T$ can be written as,

$$\mathcal{L}_{mass} = -\frac{1}{2}\begin{pmatrix} \bar{\nu}_L & \bar{\hat{N}}_L \end{pmatrix}\begin{pmatrix} 0 & M_D \\ M_D^T & M_R \end{pmatrix}\begin{pmatrix} \hat{\nu}_R \\ N_R \end{pmatrix}, \tag{2.3}$$

where ν_L and N_R are N element column matrices of fields of N generations while $M_D = vY^\nu$ and M_R are $N \times N$ matrices. Then block diagonalizing the mass matrix,

$$M^\nu = \begin{pmatrix} 0 & M_D \\ M_D^T & M_R \end{pmatrix}, \tag{2.4}$$

decouples heavy and light neutrino mass terms. For single generation M^ν is 2×2 mass matrix given by,

$$M^\nu = \begin{pmatrix} 0 & M_D \\ M_D & M_R \end{pmatrix}, \tag{2.5}$$

can be diagonalized by orthogonal transformation

$$O^T M^\nu O = M^{\nu\prime}, \tag{2.6}$$

where O is an orthogonal matrix given by

$$O = \begin{pmatrix} \cos\theta & \sin\theta \\ -\sin\theta & \cos\theta \end{pmatrix}, \tag{2.7}$$

with $\tan 2\theta = \frac{2M_D}{M_R}$ and $M^{\nu\prime}$ is a diagonal matrix with elements

$$m_{1,2} = \frac{1}{2}\left(M_R \pm \sqrt{M_R^2 + 4M_D^2}\right). \tag{2.8}$$

For $M_R \gg M_D$ the eigenvalues become, $m_1 = -\frac{M_D^2}{M_R}$ and $m_2 = M_R$. Hence, light and heavy neutrino masses are given by, $m_{\text{light}} = -\frac{M_D^2}{M_R}$ and $m_{\text{heavy}} = M_R$, respectively. The light neutrino mass has wrong sign which can be removed by the transformation,

$$K^T M^{\nu\prime} K = \text{diag}\left(\frac{M_D^2}{M_R}, M_R\right), \tag{2.9}$$

where

$$K = \begin{pmatrix} i & 0 \\ 0 & 1 \end{pmatrix}. \tag{2.10}$$

Hence, the mass eigenstates are given by,

$$\begin{aligned} n_1 &= i\cos\theta(\nu_L - \hat{\nu}_R) - i\sin\theta(\hat{N}_L - N_R), \\ n_2 &= \sin\theta(\nu_L + \hat{\nu}_R) + \cos\theta(\hat{N}_L + N_R). \end{aligned} \tag{2.11}$$

Since $\hat{n}_1 = n_1$ and $\hat{n}_2 = -n_2$, they are fields of Majorana particles. Similarly for N generations, there will be $2N$ Majorana fermions. Here the mass of light neutrino is suppressed by M_R^{-1}. The Dirac type mass M_D is proportional to VEV of SM Higgs like other fermion masses, hence, they are expected to be of the order of other fermion masses. Let $M_D \sim m_\tau$, mass of the tau lepton, then to obtain neutrino mass of the order of 10^{-2}eV (Cosmological bound restricts mass of neutrino to be less than 0.08eV) requires $M_R \sim 10^7$GeV. Hence, in Type-I seesaw, smallness of light neutrino mass is ensured by the presence of very heavy right handed neutrinos.

For $N = 3$, the neutrino mass matrix M^ν will be 6×6, with each element in it is a 3×3 matrix and can be block diagonalized by the transformation,

$$M^{\nu\prime} = \Theta^T M^\nu \Theta, \tag{2.12}$$

where

$$\Theta = \begin{pmatrix} 1 - \frac{1}{2}\rho\rho^\dagger & \rho \\ -\rho^\dagger & 1 - \frac{1}{2}\rho^\dagger\rho \end{pmatrix}, \tag{2.13}$$

with $\rho = M_D M_R^{-1} \ll 1$. The matrix Θ is unitary upto second order in ρ. The block diagonalization of M^ν gives the light neutrino mass as [52, 53]

$$m_\nu = -M_D^T M_R^{-1} M_D, \tag{2.14}$$

and heavy neutrino mass matrix as M_R. Further diagonalization of m_ν gives mass of light neutrino as well as mass eigenstates. Similarly diagonalization of M_R gives mass and mass states of heavy neutrinos. For $N > 1$ the diagonalization is done in two steps starting with neutrino mass in flavor basis and ends up in mass basis. Hence, mass and flavor eigenstates of neutrinos are related by,

$$\begin{aligned} \nu_\alpha &\approx U_\nu \nu_i + \rho U_N N_i, \\ N_\alpha &\approx -\rho^\dagger U_\nu + U_N N_1, \end{aligned} \tag{2.15}$$

where U_α and U_M diagonalize light and heavy neutrino mass matrices, ν_α is a column matrix

that contains flavor states of light neutrinos,

$$\nu_\alpha = \begin{pmatrix} \nu_e \\ \nu_\mu \\ \nu_\tau \end{pmatrix},$$

and ν_i has mass eigenstates of light neutrinos as its elements,

$$\nu_i = \begin{pmatrix} \nu_1 \\ \nu_2 \\ \nu_3 \end{pmatrix}.$$

Similarly N_α and N_i are column matrices of flavor and mass states of heavy neutrinos. In neutrino oscillation experiments only the active neutrinos, ν_e, ν_μ and ν_τ can be detected hence, only probabilities for a flavor to oscillate to active neutrinos can be measured. Since the flavor states can oscillate to N_α's also, the sum of the probabilities deviate from one, which is known as non-unitarity effect and the strength of deviation from unity is given by $\rho^\dagger\rho$. The Majorana mass term violate $B - L$ by two unit hence, can account for baryon asymmetry of universe through leptogenesis. Right-handed neutrino can decay in to both leptons and antileptons. If rate of decay to lepton is different from the rate of decay to antilepton, that is if CP is violated in the decay of right-handed neutrino, then the out of equilibrium decay of right-handed neutrino generate lepton asymmetry. So type-I seesaw not only explains tiny mass of neutrino but also have the potential to explain the baryon asymmetry of the Universe.

2.1.1 Type-II seesaw

The Majorana mass term $\sum_{\alpha\beta} m^\nu_{\alpha\beta}\overline{\widehat{\nu}}_{\alpha L}\nu_{\beta L}$ is absent in the SM, as such terms transforms as $(3, -2)$ under $SU(2)_L \times U(1)_Y$ symmetry. Those type of mass terms can be generated dynamically through Higgs mechanism, if there exists a Higgs triplet $\boldsymbol{\Delta}$ with hypercharge 2 and posses non zero VEV [54, 55]. The relevant term in the Lagrangian is given by,

$$\mathcal{L}_Y = -\sum_{\alpha\beta} f^l_{\alpha\beta}\overline{\widehat{L}}_{\alpha L}\frac{1}{\sqrt{2}}\boldsymbol{\tau}\cdot\boldsymbol{\Delta}L_{\beta L} + \text{h.c.}, \tag{2.16}$$

where $\boldsymbol{\tau}\cdot\boldsymbol{\Delta}$ is the two dimensional representation of $\boldsymbol{\Delta}$ given by

$$\boldsymbol{\tau}\cdot\boldsymbol{\Delta} = \begin{pmatrix} \frac{\Delta^+}{\sqrt{2}} & \Delta^{++} \\ \Delta^0 & -\frac{\Delta^+}{\sqrt{2}} \end{pmatrix}. \tag{2.17}$$

As Δ^0 gets nonzero VEV $\frac{v_\Delta}{\sqrt{2}}$, the interaction given in (2.16) generates Majorana mass for neutrinos

$$\mathcal{L}_{mass} = \sum_{\alpha\beta} \overline{\widehat{\nu}}_{\alpha L} m^{\nu}_{\alpha\beta} \nu_{\beta L} + \text{h.c.}, \tag{2.18}$$

where

$$m^{\nu}_{\alpha\beta} = f^{l}_{\alpha\beta} \frac{v_\Delta}{\sqrt{2}}. \tag{2.19}$$

Here the smallness of neutrino mass is guaranteed by the smallness of v_Δ, in other words, the neutrino mass is small compared to other fermion mass as they have different origin. The Higgs triplet not only generates Majorana mass of neutrinos but also contributes to mass of gauge bosons W and Z and those contributions should be small enough to keep the prediction of relative strength of charged current interaction and neutral current interaction within the experimental bound. Since SM model prediction of this ratio falls within the error bar of experimental observation, this ratio set an upper bound on v_Δ. Mass of W and Z bosons in this scenario is given by

$$\begin{aligned} M_W &= \frac{1}{4} g^2 \left(v^2 + 2 v_\Delta^2 \right), \\ M_Z &= \frac{1}{4} \left(g^2 + g'^2 \right) \left(v^2 + 4 v_\Delta^2 \right), \end{aligned} \tag{2.20}$$

giving the relative strength of charged current and neutral current interaction as

$$\rho = \frac{1 + 2 v_\Delta^2 / v^2}{1 + 4 v_\Delta^2 / v^2}\,. \tag{2.21}$$

Substituting $\rho = 0.9980 \pm 0.0086$ set the upper bound on the ratio v_Δ / v as 0.07. To get the correct neutrino mass this ratio should be even smaller than the upper bound. The smallness of v_Δ can be seen by looking into the minimization of scalar potential. The scalar potential of the model is given by [60]

$$\begin{aligned} V(\phi, \Delta) = &- \mu^2 \phi^\dagger \phi + m_\Delta^2 \text{Tr} \left((\boldsymbol{\tau} \cdot \boldsymbol{\Delta})^\dagger \boldsymbol{\tau} \cdot \boldsymbol{\Delta} \right) + \left(\mu_\Delta \tilde{\phi}^\dagger (\boldsymbol{\tau} \cdot \boldsymbol{\Delta})^\dagger \phi + \text{h.c.} \right) \\ &- \lambda \left(\phi^\dagger \phi \right)^2 + \lambda_1^\Delta \left[\text{Tr} \left((\boldsymbol{\tau} \cdot \boldsymbol{\Delta})^\dagger \boldsymbol{\tau} \cdot \boldsymbol{\Delta} \right) \right]^2 + \lambda_2^\Delta \left[\text{Tr} \left((\boldsymbol{\tau} \cdot \boldsymbol{\Delta})^\dagger \boldsymbol{\tau} \cdot \boldsymbol{\Delta} \right) \right]^2 \\ &+ \lambda_1^{\phi\Delta} \phi^\dagger \phi \text{Tr} \left((\boldsymbol{\tau} \cdot \boldsymbol{\Delta})^\dagger \boldsymbol{\tau} \cdot \boldsymbol{\Delta} \right) + \lambda_2^{\phi\Delta} \phi^\dagger (\boldsymbol{\tau} \cdot \boldsymbol{\Delta}) (\boldsymbol{\tau} \cdot \boldsymbol{\Delta})^\dagger \phi, \end{aligned} \tag{2.22}$$

which on minimization with respect to v_Δ gives

$$v_\Delta \approx \frac{\mu_\Delta v^2}{\sqrt{2} m_\Delta^2}. \tag{2.23}$$

Hence, VEV of Higgs triplet is inversely proportional to the square of its mass. The triplet Higgs has to be very massive as it is not observed till date, hence, above formula guarantees the smallness of ν_Δ. In type-II seesaw, neutrino mixing is completely determined by the structure of f^l, which is arbitrary in the context of the model and heavy mass of triplet makes its VEV small enough to give tiny neutrino mass.

2.2 Type-III seesaw

Type-III seesaw [56] is implemented by adding fermion triplet with null hypercharge to SM particle content. To realize Type-III seesaw atleast two such triplets are required. New physics that come up with inclusion of fermion triplet

$$\Sigma = \begin{pmatrix} \frac{\Sigma^0}{\sqrt{2}} & \Sigma^+ \\ \Sigma^- & \frac{-\Sigma^0}{\sqrt{2}} \end{pmatrix}, \tag{2.24}$$

is given by

$$\mathcal{L} = -\frac{1}{2}\mathrm{Tr}\left[\overline{\Sigma} M_\Sigma \Sigma^c\right] - \tilde{\phi}^\dagger \overline{\Sigma}\sqrt{2} Y_\Sigma L + \mathrm{h.c.}, \tag{2.25}$$

which below electroweak scale generates mass terms as

$$\mathcal{L}_{mass} = -v\left(\frac{\overline{\Sigma^0}}{\sqrt{2}} Y_\Sigma \nu_L + \overline{\Sigma}^- Y_\Sigma l_L + \mathrm{h.c.}\right). \tag{2.26}$$

Hence, neutrino mass term is given by

$$\mathcal{L}^\nu_{mass} = -\frac{1}{2}\begin{pmatrix} \overline{\nu}_L & \overline{\Sigma}^{0c} \end{pmatrix}\begin{pmatrix} 0 & \sqrt{2}Y_\Sigma v \\ \sqrt{2}Y_\Sigma^T v & M_\Sigma \end{pmatrix}\begin{pmatrix} \nu_L^c \\ \Sigma^0 \end{pmatrix}. \tag{2.27}$$

For $M_\Sigma \gg v$, the above equation gives light neutrino mass as

$$m_\nu = Y_\Sigma^T M_\Sigma^{-1} Y_\Sigma v^2, \tag{2.28}$$

similar to Type-I seesaw formula. Hence, in Type-III seesaw the smallness of ratio of Dirac type mass to Majorana type mass ensures tiny mass for active neutrinos as in Type-I seesaw framework.

2.3 Linear and Inverse seesaw

Realization of linear [57] and inverse seesaw [58, 59] requires inclusion of singlet fermions known as sterile neutrinos (S_R), in addition to right-handed neutrinos. New physics arises

due to the presence of right-handed and sterile neutrinos are given by the Lagrangian

$$\mathcal{L}_{NP} = -\left(\overline{L}\tilde{\phi}N_R + \overline{L}\tilde{\phi}S_R + \overline{\widehat{N}}_R M_R N_R + \overline{\widehat{S}}_R \mu_S S_R + \text{h.c.}\right). \tag{2.29}$$

After symmetry breaking, the mass part of the above Lagrangian is given by

$$\mathcal{L}_{mass} = -\left(\overline{\nu}_L m_D N_R + \overline{\nu}_L m_{RS} S_R + \overline{\widehat{N}}_R M_R N_R + \overline{\widehat{S}}_R \mu_S S_R + \text{h.c.}\right). \tag{2.30}$$

So the full mass matrix for neutrinos in the basis $(\widehat{\nu}_L\, N_R, S_R)^T$ is given by

$$\mathbb{M} = \begin{pmatrix} 0 & m_{\rm D} & m_{\rm LS} \\ m_{\rm D}^{\rm T} & M_R & m_{RS} \\ m_{\rm LS}^{\rm T} & m_{RS}^{\rm T} & \mu_S \end{pmatrix}. \tag{2.31}$$

If all the off-diagonal elements of above mass matrix are vanishingly small and $m_{LS}, m_D \ll m_{RS}$, then active neutrinos receive mass through linear seesaw. For realization of linear seesaw mass matrix for neutrinos should be of the form

$$\mathbb{M}_{linear} = \begin{pmatrix} 0 & m_{\rm D} & m_{\rm LS} \\ m_{\rm D}^{\rm T} & 0 & m_{RS} \\ m_{\rm LS}^{\rm T} & m_{RS}^{\rm T} & 0 \end{pmatrix}. \tag{2.32}$$

Then the block diagonalization of $\mathbb{M}_{linear}$ separates out the mass terms of heavy and light neutrinos, giving light neutrino mass matrix as

$$m_\nu = \begin{pmatrix} m_{\rm D} & m_{\rm LS} \end{pmatrix} \begin{pmatrix} 0 & m_{\rm RS} \\ m_{\rm RS}^{\rm T} & 0 \end{pmatrix}^{-1} \begin{pmatrix} m_{\rm D}^{\rm T} \\ m_{\rm LS}^{\rm T} \end{pmatrix} = m_{\rm D} m_{RS}^{-1} m_{\rm LS}^{\rm T} + \text{ transpose}, \tag{2.33}$$

and the heavy neutrino mass matrix as

$$M = \begin{pmatrix} 0 & m_{\rm RS} \\ m_{\rm RS}^{\rm T} & 0 \end{pmatrix}, \tag{2.34}$$

which on diagonalization gives doubly degenerate mass eigenstates for heavy neutrinos due to vanishing off-diagonal elements of M.

Similarly, realization of inverse seesaw requires the mass matrix of neutrinos in the form given by

$$\mathbb{M}_{inverse} = \begin{pmatrix} 0 & m_{\rm D} & 0 \\ m_{\rm D}^{\rm T} & 0 & m_{RS} \\ 0 & m_{RS}^{\rm T} & \mu_S \end{pmatrix}, \tag{2.35}$$

with $\mu_S \ll m_D \ll m_{RS}$. In this case light neutrino mass matrix is given by

$$m_\nu = -m_{\rm D} {m_{\rm RS}^T}^{-1} \mu_S m_{RS}^{-1} m_D^T, \tag{2.36}$$

where as heavy neutrino mass matrix is

$$\begin{pmatrix} 0 & m_{RS} \\ m_{RS}^{\rm T} & \mu_S \end{pmatrix}, \tag{2.37}$$

which on diagonalization yields nearly doubly degenerate mass eigenstates for heavy neutrinos.

In Type-I, Type-II and Type-III seesaw where new particles are very heavy and in most of the cases beyond the reach of experiments but in linear and inverse seesaw the new particles can be in the energy range accessible to experiments. This is because in linear and inverse seesaw light neutrino mass can be in the required range due to small values of m_{LS} and μ_s respectively, even if the ratio $m_D m_{RS}^{-1}$ is quite high. So unlike other seesaw models linear and inverse seesaw models can be tested experimentally. The mass of active neutrinos generated by all these seesaw mechanisms are of Majorana type. Hence, neutrinos are their own antiparticles (Majorana fermions) hence, they can mediate neutrinoless double beta decay. As the name indicates it is the process in which two neutrinos inside a nucleus converted into two protons (double beta decay) without emitting neutrinos [61, 28, 62]. A brief discussion on neutrinoless beta decay is given in subsequent section.

2.4 Neutrinoless double beta decay

If neutrino is its own anti-particle then anti-neutrino emitted in beta decay ($n \to p + e + \overline{\nu}$) can be absorbed by neutron to convert into proton ($n + \nu_e \to p + e$) as shown in Fig. 2.1, resulting in to double beta decay without neutrino emission

$$(A + Z) \to (A + Z + 2) + 2e \ .$$

From Fig. 2.1 one can see that the amplitude of the process is proportional to $\Sigma_i U_{ei}^2 m_i$, the (1,1) element of active neutrino mass matrix in flavor basis since, mass of neutrinos (m_i) is very small compared to the momentum exchange in the process. Therefore, the half-life of neutrinoless double beta decay is proportional to $|M_{ee}|^2$, where $|M_{ee}| = |\Sigma_i U_{ei}^2 m_i|$ is called effective Majorana mass and U_{ei}'s are elements of first raw of PMNS matrix. Hence, $0\nu\beta\beta$ is sensitive to absolute mass of neutrinos, mixing angles, and Majorana phases as well as Dirac

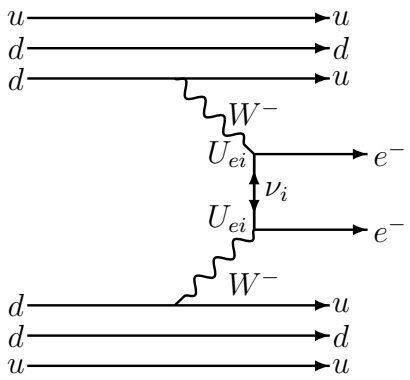

Figure 2.1: Feynman diagram for neutrinoless double beta decay

CP phase. Observation of neutrinoless double beta decay is a consistency test for all those seesaw mechanisms that generate Majorana type mass for active neutrinos.
Seesaw mechanisms well explain why neutrino masses are so small but do not give any idea about structure of mass matrix hence, do not explain neutrino mixing and mass spectrum. If there exists some symmetries across fermion generations (flavor symmetry) then that will reflect on neutrino mixing pattern thus, give predictions on mixing parameters. So in next section various symmetry forms which are possible outcome of various flavor symmetries are discussed.

2.5 Neutrino mixing patterns

All seesaw mechanism predicts neutrinos to be Majorana type hence, the mass matrix is symmetric, so there will be $N(N+1)$ parameters in the matrix. If it is only the SM symmetry that govern the interactions of elementary particles then all these parameters are independent of each other but number of free parameters reduce if there exist symmetry between generations known as flavor symmetry. The neutrino mixing pattern obtained from experiments favors the idea of flavor symmetries as the mixing pattern is very close to some standard mixing patterns such as Tribimaximal mixing (TBM) [63, 64, 65], Bimaximal mixing (BM) [66, 67], Hexagonal Mixing (HG) [68], Golden ratio A (GRA) [69, 70] and Golden ratio B (GRB) [71, 72] etc, that can be obtained if some flavor symmetries such as A_4, S_4 etc are assumed between the generations. All the above mentioned mixing patterns have $\sin^2\theta^{\nu}_{23} = \frac{1}{2}$ and $\sin^2\theta^{\nu}_{13} = 0$, which was good explanation for the trend of initial atmospheric oscillation data. Initially, data from atmospheric oscillation experiments supported maximal $\nu_\mu - \nu_\tau$ mixing simple solution of which is $\sin^2\theta^{\nu}_{23} = \frac{1}{2}$ and $\sin^2\theta^{\nu}_{13} = 0$. All these patterns which differ from

each other by the value of solar mixing angle $\sin^2\theta_{12}$ can be represented by.

$$U_\nu = \begin{pmatrix} \cos\theta_{12}^\nu & \sin\theta_{12}^\nu & 0 \\ -\frac{\sin\theta_{12}^\nu}{\sqrt{2}} & \frac{\cos\theta_{12}^\nu}{\sqrt{2}} & -\frac{1}{\sqrt{2}} \\ -\frac{\sin\theta_{12}^\nu}{\sqrt{2}} & \frac{\cos\theta_{12}^\nu}{\sqrt{2}} & \frac{1}{\sqrt{2}} \end{pmatrix} , \tag{2.38}$$

The general form of corresponding neutrino mass matrix in terms of the (complex) mass eigenvalues $m_1,\ m_2,\ m_3$ in the basis where the charged lepton mass matrix is diagonal is given by

$$m_\nu = U^* \cdot diag(m_1, m_2, m_3) \cdot U^\dagger, \tag{2.39}$$

where $U = U_\nu$ and substituting U_ν in the above equation gives

$$m_\nu = \begin{pmatrix} x & y & y \\ y & z & w \\ y & w & z \end{pmatrix} . \tag{2.40}$$

The parameters $x,\ y,\ z,\ w$ can be complex. This matrix is the most general one that is symmetric under 2-3 (or $\mu - \tau$) exchange, i.e.,

$$m_\nu = A_{23} \cdot m_\nu \cdot A_{23} \ , \tag{2.41}$$

where A_{23} is given by

$$A_{23} = \begin{pmatrix} 1 & 0 & 0 \\ 0 & 0 & 1 \\ 0 & 1 & 0 \end{pmatrix} . \tag{2.42}$$

The solar mixing angle θ_{12} is given by

$$\sin^2 2\theta_{12} = \frac{8|x^*y + y^*(w+z)|}{8|x^*y + y^*(w+z)|^2 + (|w+z|^2 - |x|^2)^2} \ . \tag{2.43}$$

For real parameters the above equation becomes

$$\sin^2 2\theta_{12} = \frac{8y^2}{(x-w-z)^2 + 8y^2} \ . \tag{2.44}$$

In the case of real values of $x,\ y,\ z$ and w, the value of solar mixing angle fixes one of the parameters in terms of other parameters of mass matrix. Hence, the mixing patterns differ by solar mixing angle leads to different neutrino mass matrices.

2.5.1 Tri-Bimaximal mixing

TBM mixing pattern fixes $\sin^2\theta_{12}$ as $\frac{1}{3}$, which is very close to the experimental value of the best measured mixing angle θ_{12}. It is the most plausible first order approximation to the experimental data. The simplest symmetry that in leading order leads to TBM is A4, the group of even permutations of 4 objects. Since TBM fixes $\sin^2 2\theta_{12} = \frac{8}{9}$, it leads to the relation $x + y = w + z$ between the parameters of mass matrix and gives mass matrix as

$$m_\nu = \begin{pmatrix} x & y & y \\ y & x+v & y-v \\ y & y-v & x+v \end{pmatrix}, \tag{2.45}$$

where $v = y - w$.

2.5.2 Bimaximal mixing

For Bimaximal mixing $\sin^2\theta_{12} = \frac{1}{2}$, thus, gives the relation between the parameters of mass matrix as $x = z + w$. Therefore, the mass matrix corresponding to BM takes the form

$$m_\nu = \begin{pmatrix} z+w & y & y \\ y & z & w \\ y & w & z \end{pmatrix}. \tag{2.46}$$

2.5.3 Golden ratio A and Golden ratio B

For GRA and GRB, $\sin^2\theta_{12}^\nu$ is $\frac{1}{2+r}$ and $\frac{3-r}{4}$ respectively, and r being golden ratio, i.e., $r = \frac{1+\sqrt{5}}{2}$. Neutrino mass matrix corresponds to GRA and GRB are given by

$$m_\nu = \begin{pmatrix} w+z-ry & y & y \\ y & z & w \\ y & w & z \end{pmatrix}, \tag{2.47}$$

where $r = 1.414$ for GRA and $r = 0.922$ for GRB.

2.5.4 Hexagonal mixing

Here $\sin^2\theta_{12}^\nu = \frac{1}{4}$, and the corresponding mass matrix is

$$m_\nu = \begin{pmatrix} x & y & y \\ y & \frac{1}{2}(x+2\sqrt{\frac{2}{3}}y+v) & \frac{1}{2}(x+2\sqrt{\frac{2}{3}}y-v) \\ y & \frac{1}{2}(x+2\sqrt{\frac{2}{3}}y-v) & \frac{1}{2}(x+2\sqrt{\frac{2}{3}}y+v) \end{pmatrix}, \tag{2.48}$$

where $v = z - w$.

Now it is known that the mixing angle θ_{13} is not so small and θ_{23} is not maximal. Therefore, all these forms do not explain the experimental result as such but, are good approximations to PMNS matrix at leading order. Possible forms of perturbations to these standard mixing patterns and their predictions are presented in the next chapter.

Chapter 3

Predicting Leptonic CP phase by considering deviations in charged lepton and neutrino sectors

3.1 Introduction

Understanding the origin of the patterns of neutrino masses and mixing, emerging from the neutrino oscillation data is one of the most challenging problems in neutrino physics. In fact, it is part of the more fundamental problem of particle physics of understanding the origin of masses and the mixing pattern in quark and lepton sector. The results from various neutrino oscillation experiments[18, 19, 20, 21], established the fact that the three flavors of neutrinos mix with each other as they propagate and form the mass eigenstates. As discussed in first chapter, the mixing is paremeterized in terms of three mixing angles, θ_{12}, θ_{23} and θ_{13} known as solar, atmospheric and reactor mixing angles respectively, one Dirac phase δ_{CP} and two Majorana phases. And the parameterization is given by [48]

$$V_{PMNS} = \begin{pmatrix} c_{12}c_{13} & s_{12}c_{13} & s_{13}e^{-i\delta_{CP}} \\ -s_{12}c_{23} - c_{12}s_{13}s_{23}e^{i\delta_{CP}} & c_{12}c_{23} - s_{12}s_{13}s_{23}e^{i\delta_{CP}} & c_{13}s_{23} \\ s_{12}s_{23} - c_{12}s_{13}c_{23}e^{i\delta} & -c_{12}s_{23} - s_{12}s_{13}c_{23}e^{i\delta} & c_{13}c_{23} \end{pmatrix} P_\nu \ ,$$

where

$$P_\nu = \mathrm{diag}(e^{i\rho}, e^{i\sigma}, 1),$$

ρ and σ are Majorana phases. The solar and atmospheric neutrino oscillation parameters are precisely known from various neutrino oscillation experiments. Recently, the reactor mixing angle has also been measured by the Double Chooz [73], Daya Bay [74, 75], RENO [76], and T2K [77, 78] experiments with a moderately large value. As θ_{13} is non-zero, there could be

CP-violation in the lepton sector, provided the CP violating phase δ_{CP} is not vanishingly small. After the discovery of sizable θ_{13}, much attention has been paid to determine the CP-violation effect in the lepton sector. The global analysis of various neutrino oscillation data has been performed by various groups [79, 80, 81, 82], and the hint for non-zero δ_{CP} was anticipated in Refs. [81, 82]. Including the data from T2K and Daya Bay, Forero *et al.* [83] performed a global fit and found a hint for non-zero value of δ_{CP}, with the best fit values as $\delta_{CP} \simeq 3\pi/2$. Hence, Many dedicated long-baseline experiments aim for precision measurement of δ_{CP} while Majorana phases are inaccessible to oscillation experiments.

Initially it was believed that the reactor mixing angle would be vanishingly small and θ_{23} is $\pi/4$, as a consequence the lepton mixing matrix is $\mu - \tau$ symmetric. Motivated by such anticipation, many models such as tri-bimaximal mixing (TBM) [63, 64, 65, 84], bi-maximal mixing (BM) [66, 67, 85, 86], golden ratio type A (GRA) [69, 70], golden ratio type B (GRB) [71, 72], hexagonal (HG) [68] mixing patterns were proposed to explain the neutrino mixing pattern which are generally based on some kind of discrete flavor symmetries like S_3, S_4, A_4, etc [87, 88, 89], thus, interpret the particular form of lepton mixing as an outcome of flavor symmetry. All those models predict θ_{13} to be zero and θ_{23} to be $\pi/4$, hence, have to be modified suitably to incorporate moderately large reactor mixing angle. Moreover, data from MINOS experiment hint towards deviation of θ_{23} from $\pi/4$. The effect of perturbations to such models are discussed in this chapter. Such discussions will help to understand the forms of perturbation that will make the model compatible with the experimental results, thus, the symmetries that can lead to the observed lepton mixing.

The theoretical prediction for the determination of CP phase in the neutrino mixing matrix depends on the approach, as well as the type of symmetries one uses to understand the pattern of neutrino mixing. Obviously a sufficiently precise measurement of δ_{CP} will serve as a very useful constraint for identifying the approaches and symmetries, if any. This chapter explores whether it is possible to constrain the CP phase δ_{CP} by considering perturbations to the leading lepton mixing matrices and if so, whether it is possible to verify such predictions with the data from ongoing NOνA experiment. In this chapter, perturbations with minimum number of parameters are considered and values of oscillation parameters used in this chapter are taken from [83].

The basic framework of the analysis is given in the next section. The deviation to the various mixing patterns due to perturbations originate from neutrino and charged lepton sectors are discussed in the following sections. The chapter ends with a summary and conclusions of the analysis.

3.2 Framework

It is well-known that the lepton mixing matrix arises from the overlapping of the matrices that diagonalize charged lepton and neutrino mass matrices, i.e.,

$$U_{\rm PMNS} = U_l^\dagger U_\nu \ . \tag{3.1}$$

The 3σ allowed values of PMNS matrix is given by

$$U_{PMNS} = \begin{pmatrix} 0.794 - 0.858 & 0.494 - 0.589 & 0.138 - 0.155 \\ -(0.374 - 0.574) & 0.418 - 0.639 & 0.61 - 0.784 \\ 0.203 - 0.403 & -(0.538 - 0.758) & 0.604 - 0.779 \end{pmatrix} , \tag{3.2}$$

where we have taken $\delta_{CP} = 0$ for simplicity. For the study of leptonic mixing, it is generally assumed that the charged lepton mass matrix is diagonal and hence, the corresponding mixing matrix U_l be an identity matrix. However, the neutrino mixing matrix U_ν has a specific form dictated by the symmetry which generally fixes the values of the three mixing angles in U_ν. The small deviations of the predicted values of the mixing angles from their corresponding measured values are considered in general, as perturbative corrections arising from symmetry breaking effects. Tri-bimaximal, bi-maximal, golden ratio type-A (GRA), type-B (GRB) and hexagonal (HG) are examples for such forms of U_ν. As shown in previous chapter, all these forms have $\theta_{23} = \pi/4$ and vanishing θ_{13} hence, take the form [90],

$$U_\nu^0 = \begin{pmatrix} \cos\theta_{12}^\nu & \sin\theta_{12}^\nu & 0 \\ -\frac{\sin\theta_{12}^\nu}{\sqrt{2}} & \frac{\cos\theta_{12}^\nu}{\sqrt{2}} & -\frac{1}{\sqrt{2}} \\ -\frac{\sin\theta_{12}^\nu}{\sqrt{2}} & \frac{\cos\theta_{12}^\nu}{\sqrt{2}} & \frac{1}{\sqrt{2}} \end{pmatrix} . \tag{3.3}$$

The superscript '0' is introduced to label the mixing matrix as the leading order matrix arising from certain discrete flavor symmetries. Where $\sin^2\theta_{12}^\nu$ takes the values 1/2, 1/3, 0.276, 0.345, and 0.25 respectively for TBM, BM, GRA, GRB and HG mixing patterns.
Thus, one possible way to generate corrections for the mixing angles such that all the mixing angles θ_{23}, θ_{12} and θ_{13} should be compatible with the observed experimental data, is to include suitable perturbative corrections to both the charged lepton and neutrino mixing matrices U_l and U_ν respectively. Such possibilities are explored in this chapter. While considering the corrections to the neutrino mixing matrix, the charged lepton mixing matrix is assumed to be identity matrix and for correction to the charged lepton mass matrix the neutrino mixing matrix is considered to be either of TBM/BM/GRA/GRB/HG forms. Furthermore, possible corrections to U_ν from higher dimensional operators and from renormalization group effects

will be neglected.

3.3 Deviation in Neutrino sector

In this section, the corrections to the neutrino mixing matrix are considered such that it can be written as

$$U_\nu = U_\nu^0 U_\nu^{corr}, \tag{3.4}$$

where U_ν^0 is one of the symmetry forms of the mixing matrix as described in Eq. (3.3) and U_ν^{corr} is a unitary matrix describing the correction to U_ν^0. An important requirement is that the correction due to the matrix U_ν^{corr} should allow sizable deviation of the angle θ_{13} from zero and also the required deviations to θ_{23} and θ_{12}, so that all the mixing angles should be compatible with their measured values. As discussed in Ref. [91], U_ν^{corr} can be expressed as $V_{23}V_{13}V_{12}$, where V_{ij} are the rotation matrices in (ij) plane and hence, can be parameterized by three mixing angles and one phase. In this chapter, we consider the simplest case of such perturbation which involves only minimal set of new independent parameters, i.e., we consider the deviations involving only two new parameters (one rotation angle and one phase), which basically correspond to perturbation induced by a single rotation. There are several variants of this approach exist in the literature, generally for TBM mixing pattern [92, 93, 94, 95]. The main difference between the previous studies and our work is that apart from predicting the values of the mixing angles compatible with their experimental range, we have also looked into the possibility of constraining the CP phase δ_{CP}, not only for TBM case, but also for other variety of mixing patterns.

3.3.1 Deviation due to (23) rotation

First, we would like to consider additional rotation in the (23) plane. Since the charged lepton mixing matrix is considered to be identity in this case, the PMNS mixing matrix can be obtained by multiplying the neutrino mixing matrix U_ν^0 with the (23) rotation matrix as follows

$$U_{PMNS} = U_\nu^0 \begin{pmatrix} 1 & 0 & 0 \\ 0 & \cos\phi & e^{-i\alpha}\sin\phi \\ 0 & -e^{i\alpha}\sin\phi & \cos\phi \end{pmatrix}, \tag{3.5}$$

where ϕ and α are arbitrary free parameters. The mixing angles $\sin^2\theta_{12}$, $\sin^2\theta_{23}$ and $\sin\theta_{13}$ can be obtained using the relations

$$\sin^2\theta_{12} = \frac{|U_{e2}|^2}{1-|U_{e3}|^2}, \qquad \sin^2\theta_{23} = \frac{|U_{\mu 3}|^2}{1-|U_{e3}|^2}, \qquad \sin\theta_{13} = |U_{e3}|. \tag{3.6}$$

Using Eqs. (3.3), (3.5) and (3.6), one obtains the mixing angles as

$$\sin\theta_{13} = \sin\theta_{12}^{\nu}\sin\phi\ , \tag{3.7}$$

$$\sin^2\theta_{12} = \frac{\sin^2\theta_{12}^{\nu}\cos^2\phi}{1-\sin^2\theta_{12}^{\nu}\sin^2\phi}\ , \tag{3.8}$$

$$\sin^2\theta_{23} = \frac{1}{2}\left[\frac{1-\sin^2\theta_{12}^{\nu}\sin^2\phi-\cos\theta_{12}^{\nu}\sin 2\phi\cos\alpha}{1-\sin^2\theta_{12}^{\nu}\sin^2\phi}\right]\ . \tag{3.9}$$

Thus, from Eqs. (3.7-3.9), one can see that by including the (23) rotation matrix as a perturbation, it is possible to have nonzero θ_{13}, deviation of $\sin^2\theta_{23}$ from 1/2 and $\sin^2\theta_{12}$ from $\sin^2\theta_{12}^{\nu}$. With Eqs. (3.7) and (3.8) one can obtain the relation between $\sin^2\theta_{12}$ and $\sin^2\theta_{13}$ as

$$\sin^2\theta_{12} = \frac{\sin^2\theta_{12}^{\nu}-\sin^2\theta_{13}}{1-\sin^2\theta_{13}}\ . \tag{3.10}$$

Thus, it can be seen that in this case one can have $\sin^2\theta_{12} < \sin^2\theta_{12}^{\nu}$, although the deviation is not significant. Therefore, the BM, GRA and HG forms of neutrino mixing patterns cannot accommodate the observed value of $\sin^2\theta_{12}$ within its 3σ range.

Furthermore, as we have a non-vanishing and largish θ_{13}, this in turn implies that it could in principle be possible to observe CP violation in the lepton sector analogous to the quark sector, provided the CP violating phase is not vanishingly small, in the long-baseline neutrino oscillation experiments. The Jarlskog invariant, which is a measure of CP violation, has the expression in the standard parameterization as

$$J_{\rm CP} \equiv {\rm Im}[U_{e1}U_{\mu 2}U_{\mu 1}^{*}U_{e2}^{*}] = \frac{1}{8}\sin 2\theta_{12}\sin 2\theta_{23}\sin 2\theta_{13}\cos\theta_{13}\sin\delta_{CP}\ , \tag{3.11}$$

and is sensitive to the Dirac CP violating phase. With Eq. (3.5), one can obtain the value of Jarlskog invariant as

$$J_{\rm CP} = -\frac{1}{4}\cos\theta_{12}^{\nu}\sin^2\theta_{12}^{\nu}\sin 2\phi\sin\alpha\ . \tag{3.12}$$

Thus, comparing the two Eqs. (3.11) and (3.12), one can obtain the expression for δ_{CP} as

$$\sin\delta_{CP} = -\frac{(1-\sin^2\theta_{12}^{\nu}\sin^2\phi)\sin\alpha}{[(1-\sin^2\theta_{12}^{\nu}\sin^2\phi)^2-\cos^2\theta_{12}^{\nu}\sin^2 2\phi\cos^2\alpha]^{1/2}}\ . \tag{3.13}$$

For numerical evaluation we constrain the parameter ϕ from the measured value of $\sin\theta_{13}$ and vary the phase parameter α within its allowed range, i.e., $-\pi \leq \alpha \leq \pi$. With Eq. (3.7) and using the 3σ range of $\sin^2\theta_{13}$ and the specified value of $\sin^2\theta_{12}^{\nu}$, we obtain the allowed range of ϕ for various mixing patterns as: $(10.9-14.2)^{\circ}$ for BM, $(13.3-17.5)^{\circ}$ for TBM,

$(14.8 - 19.2)^\circ$ for GRA, $(13.2 - 17.2)^\circ$ for GRB, and $(15.6 - 20.3)^\circ$ for HG pattern. With these input parameters, we present our results in Fig. 3.1 and Fig. 3.2 . The correlation plot between $\sin^2\theta_{12}$ and $\sin^2\theta_{13}$ is shown in Fig. 3.1 panel where the magenta, red, green, orange and blue plots correspond to BM, TBM, GRA, GRB and HG mixing patterns respectively. The horizontal and vertical dashed black lines correspond to the best fit values for $\sin^2\theta_{12}$ and $\sin^2\theta_{13}$, whereas the vertical dashed magenta lines represent the 3σ allowed range of $\sin^2\theta_{12}$ and the horizontal dot-dashed lines correspond to the same for $\sin^2\theta_{13}$. As discussed before, one can see from the figure that, the predicted values of the mixing angles $\sin^2\theta_{12}$ and $\sin^2\theta_{13}$ lie within their 3σ ranges only for TBM and GRB mixing patterns whereas the predicted value of $\sin^2\theta_{12}$ lies outside its 3σ range for BM, GRA and HG mixing patterns. With Eq. (3.13), we obtain the constraint on δ_{CP} as shown in the top panel of Fig. 3.2 for TBM case, where we have used the 3σ allowed range of the mixing angles θ_{12}, θ_{23} and θ_{13}. Using the predicted value of δ_{CP}, correlation between the Jarlskog invariant and $\sin^2\theta_{13}/\sin^2\theta_{23}$ are shown in the bottom panel of Fig. 3.2 for TBM case. The corresponding results for GRB mixing pattern are almost same as TBM case and hence, are not shown explicitly in the figures. However, the allowed ranges of δ_{CP} and J_{CP} are listed in Table 3.1. Since BM, GRA and HG mixing patterns cannot accommodate the observed mixing angles as discussed earlier in this section, the corresponding results are not listed.

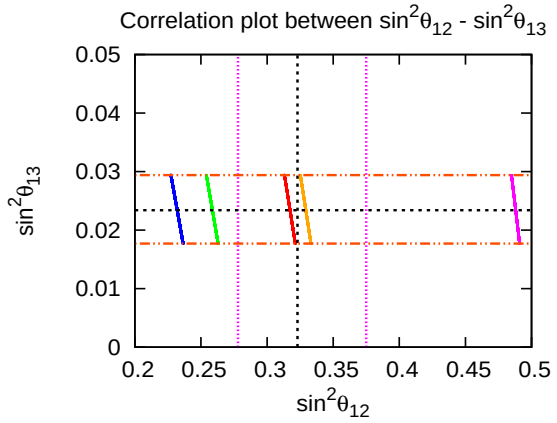

Figure 3.1: Correlation plots between $\sin^2\theta_{12}$ and $\sin^2\theta_{13}$ for BM (magenta), TBM (red), GRA (green), GRB (orange) and HG (blue) regions. The horizontal and vertical central lines represent the best fit values where as the dot-dashed orange and dashed magenta lines represent corresponding 3σ allowed ranges.

Our next objective is to speculate the possible experimental indications which could support or rule out our findings. As we know neutrino physics has now entered the precision era as far as the measured parameters are concerned. The currently running experiments T2K

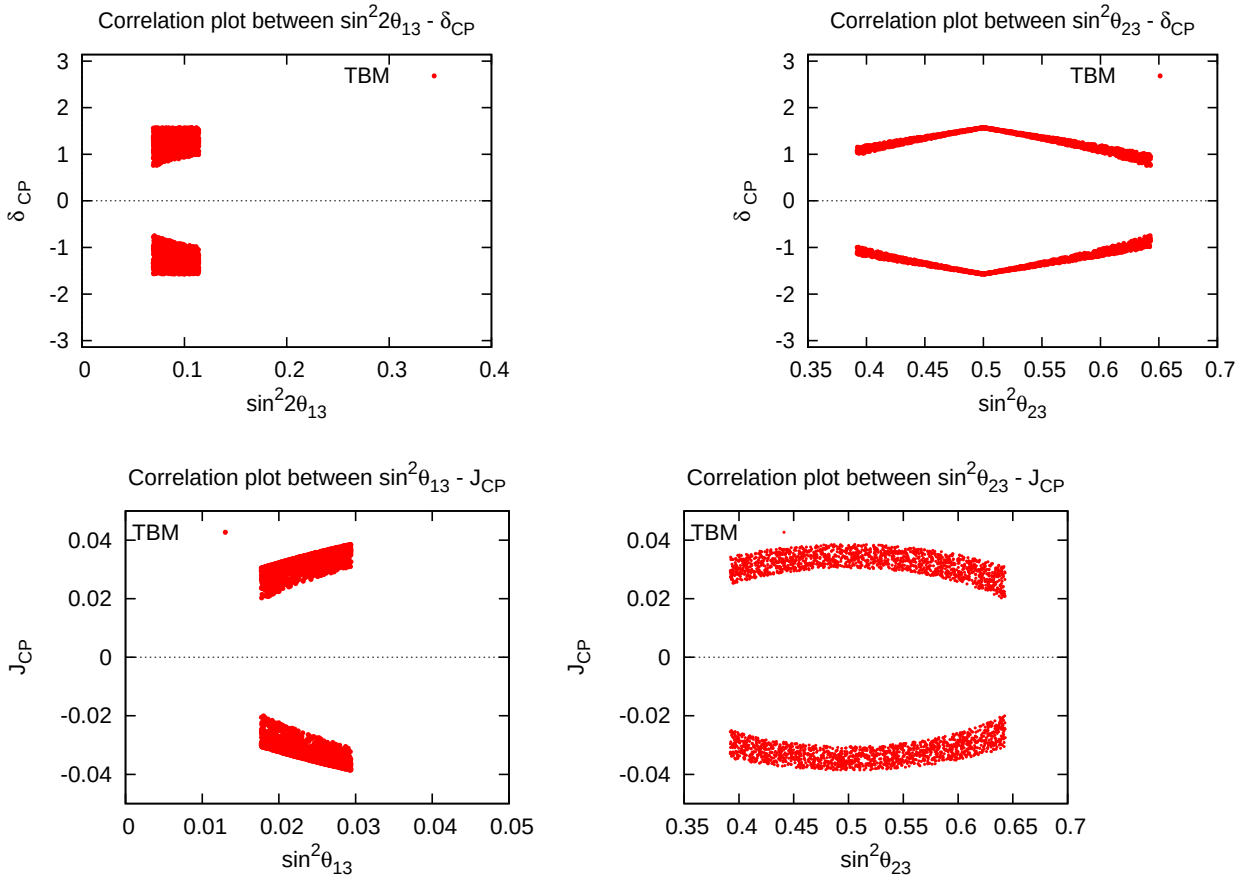

Figure 3.2: The constraints on δ_{CP} for TBM mixing pattern are shown in the top panel and on J_{CP} in the bottom panel.

and NOνA play a major role in this aspect. These experiments will provide the precise measurement of atmospheric neutrino mass square difference and the mixing angle θ_{23} through ν_μ disappearance channel. They also intend to measure θ_{13}, the CP violation phase δ_{CP} through ν_μ to ν_e appearance. Furthermore, NOνA can potentially resolve the mass-ordering through matter effects as it has a long-baseline. In this work, we would like to see whether the constraints obtained on δ_{CP} in our analysis could be probed in the NOνA experiment with 3 years of data taking with neutrino mode and then followed by another 3 years with antineutrino mode. For our study we do the simulations using GLoBES [96, 97].

3.3.2 Simulation details

NOνA (NuMI Off-axis ν_e Appearance) is an off-axis long-baseline experiment [98, 99], which uses Fermilab's NuMI $\nu_\mu/\bar{\nu}_\mu$ beamline. Its detector is a 14 kton totally active scintillator detector (TASD), placed at a distance of 810 km from Fermilab, near Ash River, which is 0.8° off-axis from the NuMI beam. It also has a 0.3 kton near detector located at the Fermilab site to monitor the unoscillated neutrino or anti-neutrino flux. It has already started data

taking from late 2014. The experiment is scheduled to have three years run in neutrino mode followed by three years run in anti-neutrino mode with a NuMI beam power of 0.7 MW and 120 GeV proton energy, corresponding to 6×10^{20} p.o.t per year. Apart from the precise measurement of θ_{13} and the atmospheric parameters, it aims to determine the unknowns such as neutrino mass ordering, leptonic CP-violation, and the octant of θ_{23} by the measurement of $\nu_\mu/\bar{\nu}_\mu \to \nu_e/\bar{\nu}_e$ oscillations.

For the simulation of NOνA experiment, the detector properties and other necessary details are taken from [100, 101]. We have used the following input true values of neutrino oscillation parameters in our simulations: $|\Delta m^2_{\text{eff}}| = 2.4 \times 10^{-3}$ eV^2, $\Delta m^2_{21} = 7.6 \times 10^{-5}$ eV^2, $\delta_{CP} = 0$, $\sin^2\theta_{12} = 0.32$, $\sin^2 2\theta_{13} = 0.1$ and $\sin^2\theta_{23} = 0.5$. The relation between the atmospheric parameter Δm^2_{eff} measured in MINOS and the standard oscillation parameter Δm^2_{31} in nature is given as [102]

$$\Delta m^2_{31} = \Delta m^2_{\text{eff}} + \Delta m^2_{21}(\cos^2\theta_{12} - \cos\delta_{CP}\sin\theta_{13}\sin 2\theta_{12}\tan\theta_{23}) \,, \tag{3.14}$$

where Δm^2_{eff} is taken to be positive for Normal Ordering (NO) and negative for Inverted Ordering (IO).

In order to obtain the allowed region for $\sin^2 2\theta_{13}$ and δ_{CP}, we generate the true event spectrum by keeping the above mentioned neutrino oscillation parameters as true values and generate the test event spectrum by varying the test values of $\sin^2 2\theta_{13}$ in the range [0.02:0.25] and that of δ_{CP} in its full range $[-\pi : \pi]$. Finally, we calculate $\Delta\chi^2$ by comparing the true and test event spectra. The obtained results in the $\sin^2 2\theta_{13} - \delta_{CP}$ plane are shown in Fig. 3.3, which are overlaid by our predicted value of δ_{CP}. The top panel shows the 1σ contours for the running of $(3\nu + 0\bar{\nu})$ years, with NO as the true hierarchy. The bottom left (right) panel represents $(3\nu + 3\bar{\nu})$ years of data taking with NO (IO) as the true hierarchy. In these plots, the inner regions (bubbles) correspond to 1σ contours whereas the outer curves represent 3σ contours. From these plots, one can see that our results are supported by NOνA data within 3σ C.L., however, with $(3\nu{+}3\bar{\nu})$ years of data taking, NOνA could marginally exclude these results at 1σ C.L.

Next we would like to briefly mention about the implications of future generation long baseline experiments such as Hyper-Kamiokande (T2HK) and Deep Underground Neutrino Experiment (DUNE) experiments in our predicted results. All the details for simulation of T2HK experiment are taken from [101] for $(3\nu{+}7\bar{\nu})$ years of running. The DUNE experiment which is basically slightly upgraded version of LBNE experiment, plans to use a 40 kton Liquid Argon detector. Except the detector volume other characteristics are taken from [103] for the simulation for $(5\nu{+}5\bar{\nu})$ years of data taking. We use the same true values of other input

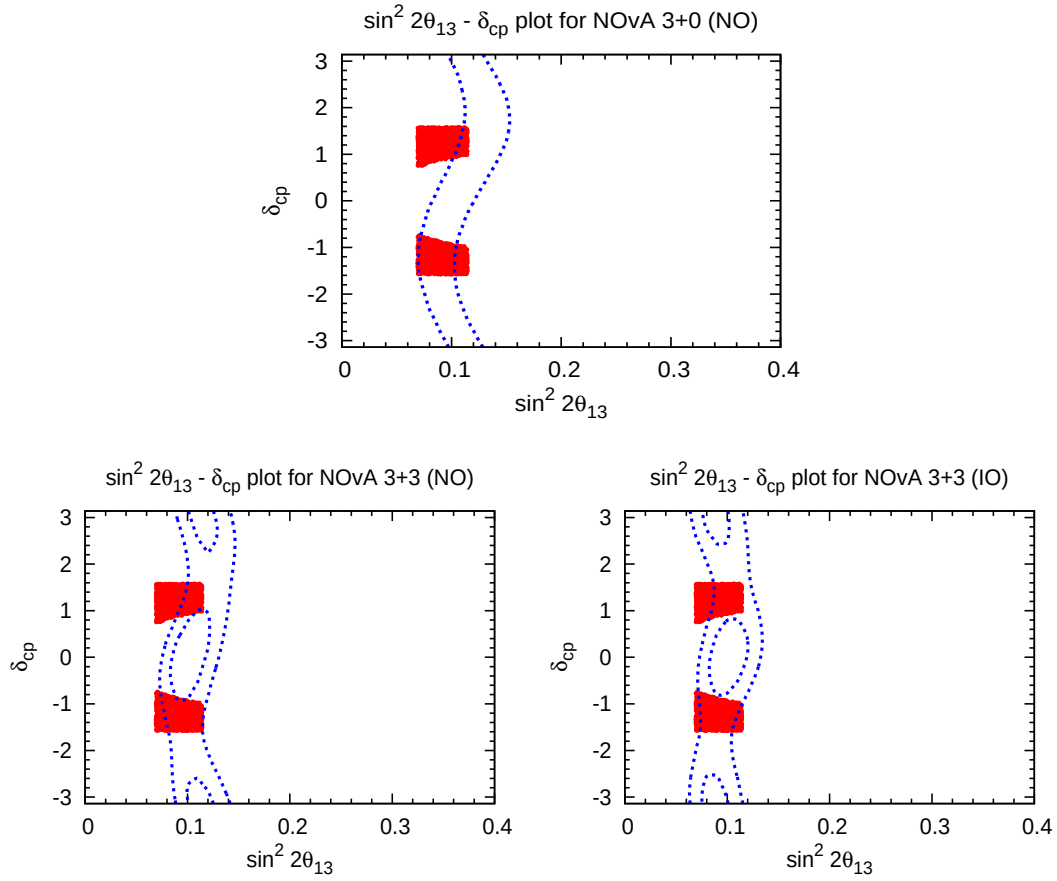

Figure 3.3: The correlation between δ_{CP} and $\sin^2 2\theta_{13}$ for TBM mixing pattern (red regions) superimposed on expected NOνA data where the blue dashed lines (top panel) represent the 1σ contours for 3 years of neutrino data taking with NO as test ordering, the blue lines in the bottom-left (NO as test ordering) and bottom-right (for IO as test ordering) panels represent the 1σ and 3σ contours for $(3\nu{+}3\bar{\nu})$ years of running.

parameters as done for NOνA experiment. The correlation plots between δ_{CP} and $\sin^2 2\theta_{13}$ are shown in Fig. 3.4, overlaid by our predicted values for TBM. The plots on the top (bottom) panel are for DUNE (T2HK) experiment with NO/IO as the true ordering as labeled in the plots. It can be seen from these figures that as the $\delta_{CP} - \sin^2 2\theta_{13}$ parameter space is severely constrained, our predicted results are expected to be precisely verified by these experiments.

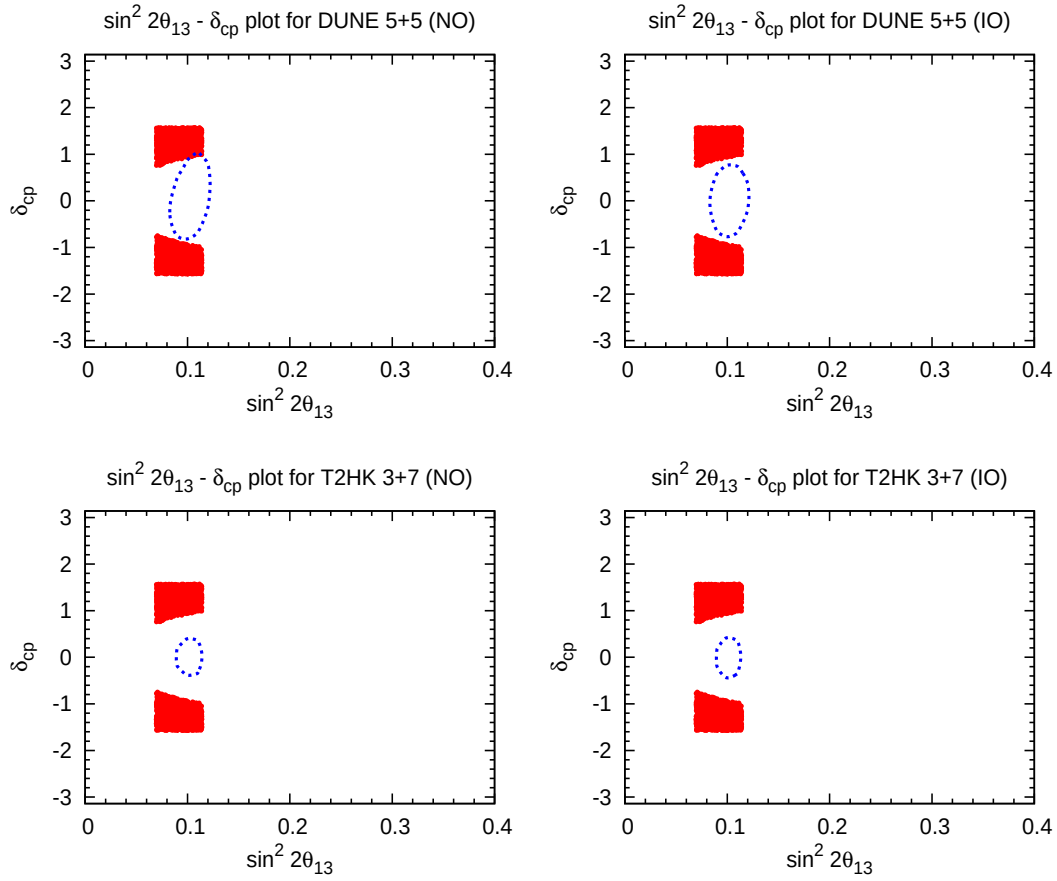

Figure 3.4: The correlation between δ_{CP} and $\sin^2\theta_{13}$ for TBM mixing pattern (red regions) superimposed on expected DUNE data (top panels) where the blue dashed lines represent the 3σ contours for $(5\nu{+}5\bar{\nu})$ years of data taking, while the bottom panels represent the T2HK results for $(3\nu{+}7\bar{\nu})$ years of running.

3.3.3 Deviation due to (13) rotation

Next we consider the corrections arising from an additional (13) rotation in the neutrino sector for which the rotation matrix can be given as

$$U_{PMNS} = U_{\nu}^{0} \begin{pmatrix} \cos\phi & 0 & e^{-i\alpha}\sin\phi \\ 0 & 1 & 0 \\ -e^{i\alpha}\sin\phi & 0 & \cos\phi \end{pmatrix}. \tag{3.15}$$

Deviation type	Neutrino mixing matrix pattern	δ_{CP} Range (in radian)	$\lvert J_{CP}\rvert$ Range
23 rotation to U_ν^0	TBM and GRB	$\pm(0.7-1.5)$	$(0.02-0.04)$
13 rotation to U_ν^0	TBM, GRA and GRB	$\pm(0-1.5)$	$(0-0.04)$
12 and 13 rotation to U_l	TBM and GRB	$\pm(1.2-1.55)$	$(0.03-0.04)$
	GRA	$\pm(0.6-1.5)$	$(0.02-0.04)$
	HG	$\pm(0-1.3)$	$(0-0.035)$
	BM	$\pm(0-0.8)$	$(0-0.03)$

Table 3.1: Predicted range of the CP phase δ_{CP} and the Jarlskog invariant $|J_{CP}|$ due to possible deviations for various neutrino mixing patterns.

Proceeding in the similar way as done in the previous case, we obtain the mixing angles using Eq. (3.6) as

$$\sin\theta_{13} = \cos\theta_{12}^{\nu}\sin\phi\,, \tag{3.16}$$

$$\sin^2\theta_{12} = \frac{\sin^2\theta_{12}^{\nu}}{1-\cos^2\theta_{12}^{\nu}\sin^2\phi}\,, \tag{3.17}$$

$$\sin^2\theta_{23} = \frac{1}{2}\left[\frac{\cos^2\phi+\sin\theta_{12}^{\nu}\sin 2\phi\cos\alpha+\sin^2\theta_{12}^{\nu}\sin^2\phi}{1-\cos^2\theta_{12}^{\nu}\sin^2\phi}\right]\,. \tag{3.18}$$

Analogously, the Jarlskog invariant and the CP violating phase δ_{CP} are given as

$$J_{CP} = -\frac{1}{8}\cos\theta_{12}^{\nu}\sin 2\theta_{12}^{\nu}\sin 2\phi\sin\alpha\,, \tag{3.19}$$

and

$$\sin\delta_{CP} = -\frac{(1-\cos^2\theta_{12}^{\nu}\sin^2\phi)\sin\alpha}{\left[(1-\cos^2\theta_{12}^{\nu}\sin^2\phi)^2-\sin^2\theta_{12}^{\nu}\sin^2 2\phi\cos^2\alpha\right]^{1/2}}\,. \tag{3.20}$$

In this case one obtains from Eqs. (3.16) and (3.17)

$$\sin^2\theta_{12} = \frac{\sin^2\theta_{12}^{\nu}}{1-\sin^2\theta_{13}}, \tag{3.21}$$

which implies that $\sin^2\theta_{12} > \sin^2\theta_{12}^{\nu}$. This in turn implies that BM and HG mixing patterns cannot accommodate the observed value of θ_{12} within its 3σ range.

From Eq. (3.16) and using the 3σ allowed range of $\sin^2\theta_{13}$ the allowed range of ϕ is found to be in the range $(9-15)^\circ$ for various mixing patterns. Now using this value of ϕ and varying the free phase parameter α in the range $-\pi \leq \alpha \leq \pi$, we obtain the correlation plots between $\sin^2\theta_{12}$ and $\sin^2\theta_{13}$ as shown in Fig. 3.5, where red, blue and green plots are for TBM, GRB and GRA mixing patterns. The correlation plot for HG and BM forms are not shown in the figure as they lie outside the allowed 3σ region of $\sin^2\theta_{12}$. The δ_{CP} phase is

very loosely constrained in this case as presented in Fig. 3.6. We also overlaid the predicted value of δ_{CP} for TBM over the NOνA simulated data. In this case also the predicted result is consistent with expected NOνA data. The correlation plots between δ_{CP} and $\sin^2\theta_{23}$, J_{CP} and $\sin^2\theta_{13}$ ($\sin^2\theta_{23}$), as well as between J_{CP} and δ_{CP} are also shown in the fig. 3.7. From the plots it can be seen that it could be possible to have large CP violation $\mathcal{O}(10^{-2})$ in the lepton sector.

It should be noted that for deviation due to (12) rotation matrix does not accommodate the observed value of θ_{13} as $U_{e3} = 0$, for such case.

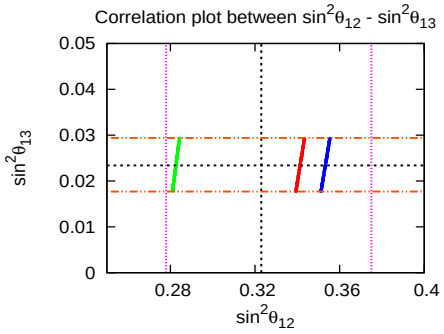

Figure 3.5: Correlation plots between $\sin^2\theta_{12}$ and $\sin^2\theta_{13}$ due to 13 deviation in the neutrino sector. The red, blue and green plots correspond to TBM, GRB and GRA mixing patterns.

3.4 Deviation in the charged lepton sector

In this section we will consider the deviation arising in the charged lepton sector. For the study of lepton mixing, it is generally assumed that the charged lepton mass matrix is diagonal and hence, the corresponding mixing matrix as an identity matrix. The deviation in the charged lepton sector and its possible consequences have been studied by various authors [72, 104, 105]. In Refs. [72, 104], the form for U_l is considered to be product of two orthogonal matrices describing rotations in (23) and (12) planes, which corresponds to two possible orderings, 'standard' with $U_l \propto R_{23}(\theta^l_{23})R_{12}(\theta^l_{12})$ and 'inverse' with $U_l \propto R_{12}(\theta^l_{12})R_{23}(\theta^l_{23})$. Using these forms for the lepton mixing matrix the values of δ_{CP} and the rephasing invariant J_{CP} have been predicted for the cases TBM, BM, LC, GRA, GRB and HG forms of neutrino mixing matrix U_ν. They have obtained the predictions for δ_{CP} as $\delta_{CP} \simeq \pi$ for BM (LC) and $\delta_{CP} \simeq 3\pi/2$ or $\pi/2$ for TBM, GRA, GRB and HG. Here, we consider the simplest case where the deviation matrix can be represented as a single rotation matrix in the (ij) plane, as done in the previous section for the neutrino sector.

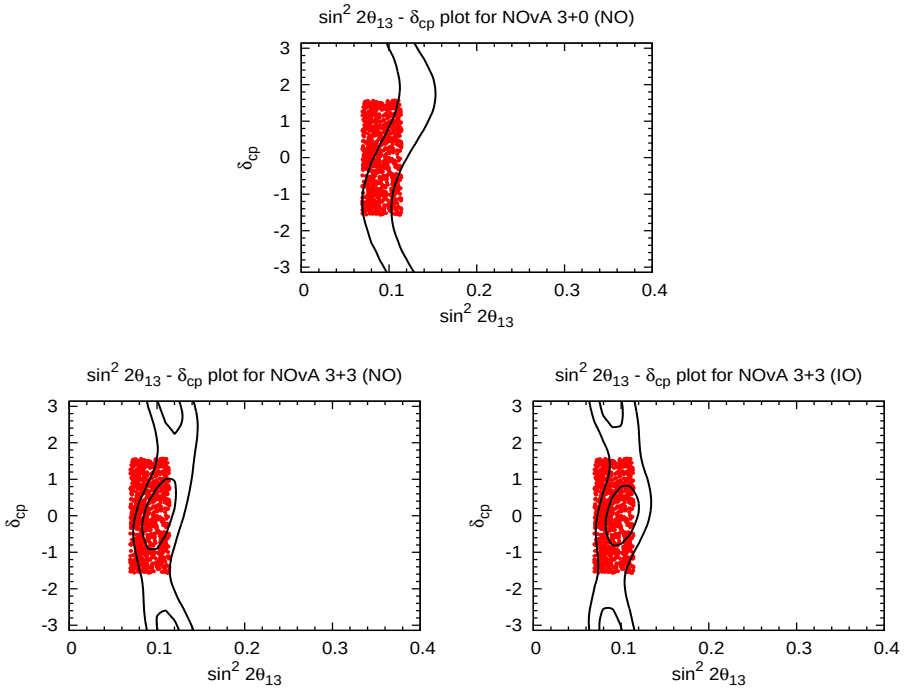

Figure 3.6: Correlation plots between δ_{CP} and $\sin^2 2\theta_{13}$ for TBM mixing pattern with 13 deviation in neutrino sector super imposed on expected NOνA data. The black solid lines represent the expected experimentally allowed parameter space (same as the dotted blue lines in Fig. 3.2.

Now considering the deviation to the charged lepton mixing matrix as a unitary rotation matrix either in (12), (23) or (13) plane, one can write the PMNS matrix as

$$U_{PMNS} = U_{ij}^{\dagger} U_{\nu}^{0} \,, \tag{3.22}$$

where U_{ij} is the rotation matrix in (ij) plane and U_{ν}^{0} is any one of the standard neutrino mixing matrix form TBM/BM/GRA/GRB/HG. However, corrections arising due to U_{23} rotation matrix is ruled out as it gives vanishing U_{e3}.

3.4.1 Deviation due to rotation in (12) and (13) sectors

Including the additional correction matrix U_{12} to the charged lepton sector, one can write the PMNS matrix as

$$U_{PMNS} = \begin{pmatrix} \cos\phi & -e^{-i\alpha}\sin\phi & 0 \\ e^{i\alpha}\sin\phi & \cos\phi & 0 \\ 0 & 0 & 1 \end{pmatrix} U_{\nu}^{0} \,. \tag{3.23}$$

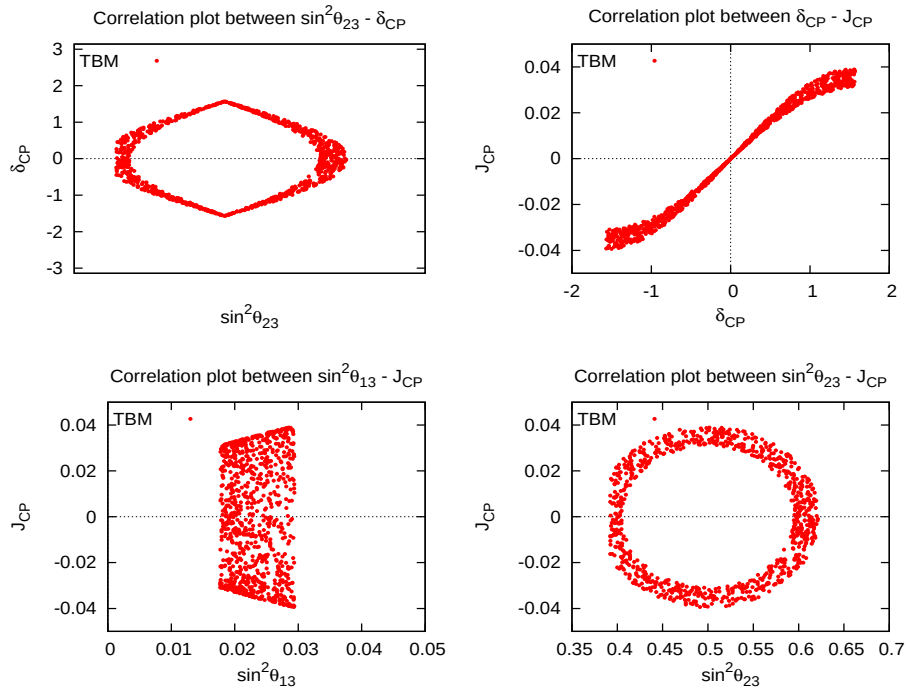

Figure 3.7: Correlation plots between different oscillation parameters due to (13) deviation in the neutrino sector. The plots represent the correlation between different mixing parameters as indicated in the plot labels for TBM mixing pattern.

In this case we get the mixing angles as

$$\sin\theta_{13} = \frac{\sin\phi}{\sqrt{2}}\,, \tag{3.24}$$

$$\sin^2\theta_{12} = \frac{2\sin^2\theta_{12}^{\nu}\cos^2\phi + \cos^2\theta_{12}^{\nu}\sin^2\phi - \frac{1}{\sqrt{2}}\sin 2\theta_{12}^{\nu}\sin 2\phi\cos\alpha}{1+\cos^2\phi}\,, \tag{3.25}$$

$$\sin^2\theta_{23} = \frac{\cos^2\phi}{1+\cos^2\phi}\,. \tag{3.26}$$

With Eqs. (3.24) and (3.26), we obtain the relation

$$\sin^2\theta_{23} = 1 - \frac{1}{2\cos^2\theta_{13}}\,, \tag{3.27}$$

which implies that $\sin^2\theta_{23} < 1/2$. The Jarlskog invariant in this case is found to be

$$J_{CP} = -\frac{1}{8\sqrt{2}}\sin 2\theta_{12}^{\nu}\sin 2\phi\sin\alpha\,, \tag{3.28}$$

and the CP violating phase as

$$\sin\delta_{CP} = -\frac{(1+\cos^2\phi)\sin 2\theta_{12}^{\nu}\sin\alpha}{2\sqrt{Y}}\,, \tag{3.29}$$

where

$$\begin{aligned} Y &= \left(2\sin^2\theta_{12}^{\nu}\cos^2\phi + \cos^2\theta_{12}^{\nu}\sin^2\phi - \frac{1}{\sqrt{2}}\sin 2\phi \sin 2\theta_{12}^{\nu}\cos\alpha\right) \\ &\times \left(1 + \cos 2\theta_{12}^{\nu}\cos^2\phi - \cos^2\theta_{12}^{\nu}\sin^2\phi + \frac{1}{\sqrt{2}}\sin 2\theta_{12}^{\nu}\sin 2\phi\cos\alpha\right). \end{aligned} \tag{3.30}$$

Proceeding in a similar fashion as in the previous cases and considering the 3σ allowed range of θ_{13}, one can obtain the allowed range of ϕ with Eq. (3.24) as $(10-15)^\circ$. Now varying the free parameters ϕ and α in their allowed ranges, we obtain the correlation plots between various mixing parameters as depicted in Fig. 3.8 and Fig. 3.9. It should be noted that the correlation plots between $\sin^2\theta_{13}$ and $\sin^2\theta_{23}$ remain same for all the forms of neutrino mixing matrix U_ν^0 as these mixing angles depend only on the free parameter ϕ and are independent of θ_{12}^{ν} (which takes different values for different mixing patterns). For the correlation plots between $\delta_{CP} - \sin^2 2\theta_{13}$ ($\sin^2\theta_{12}$) and $J_{CP} - \sin^2\theta_{13}$, the red, green, blue and magenta regions correspond to TBM, GRA, HG and BM mixing patterns. The GRB mixing pattern predicts the same constraints as TBM pattern and hence, the corresponding results are not shown in the plots. Furthermore, the CP violating phase is severely constrained in this scenario and the Jarlskog invariant is found to be significantly large as seen from the figure.

Next we consider deviation due to additional rotation in (13) sector. In this case the PMNS matrix is given as

$$U_{PMNS} = \begin{pmatrix} \cos\phi & 0 & -e^{-i\alpha}\sin\phi \\ 0 & 1 & 0 \\ e^{i\alpha}\sin\phi & 0 & \cos\phi \end{pmatrix} U_\nu^0. \tag{3.31}$$

The mixing angles obtained are

$$\begin{aligned} \sin\theta_{13} &= \frac{\sin\phi}{\sqrt{2}}, \\ \sin^2\theta_{23} &= \frac{1}{1+\cos^2\phi}, \\ \sin^2\theta_{12} &= \frac{2\sin^2\theta_{12}^{\nu}\cos^2\phi + \cos^2\theta_{12}^{\nu}\sin^2\phi - \frac{1}{\sqrt{2}}\sin 2\theta_{12}^{\nu}\sin 2\phi\cos\alpha}{1+\cos^2\phi}. \end{aligned} \tag{3.32}$$

In this case we obtain

$$\sin^2\theta_{23} = \frac{1}{2\cos^2\theta_{13}}, \tag{3.33}$$

which implies $\sin^2\theta_{23} > 1/2$. The Jarlskog invariant and the CP phase are found to be

$$J_{CP} = \frac{1}{8\sqrt{2}}\left(\sin 2\theta_{12}^{\nu}\sin 2\phi\sin\alpha\right), \tag{3.34}$$

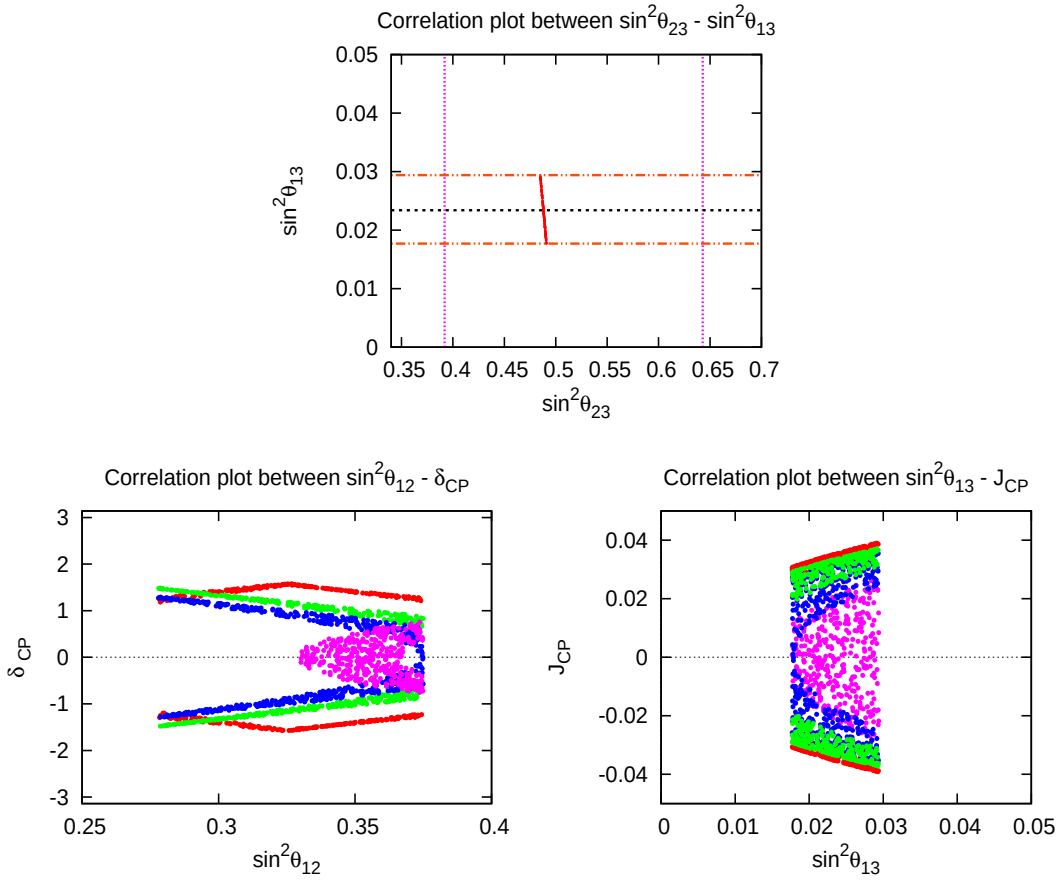

Figure 3.8: Correlation plots between different observables due to 12 deviation in the charged lepton sector. The description of the plots are indicated in the corresponding plot labels. In these plots the red, green, blue and magenta regions correspond to TBM, GRA, HG and BM mixing patterns.

$$\sin\delta_{CP} = \frac{\sin 2\theta_{12}^{\nu}\sin\alpha(1+\cos^2\phi)}{2\sqrt{Y}} \ . \tag{3.35}$$

Since the results for this deviation pattern are almost similar to the correction due to (12) rotation case, one obtains the same constraints on δ_{CP} as in the previous case, which are listed in Table 3.1.

3.5 Summary and Conclusions

The recent observation of moderately large reactor mixing angle θ_{13} has ignited a lot of interest to understand the mixing pattern in the lepton sector. It also opens up promising perspectives for the observation of CP violation in the lepton sector. The precise determination of θ_{13}, in addition to providing a complete picture of neutrino mixing pattern could be a signal of underlying physics responsible for lepton mixing and for the physics beyond the standard

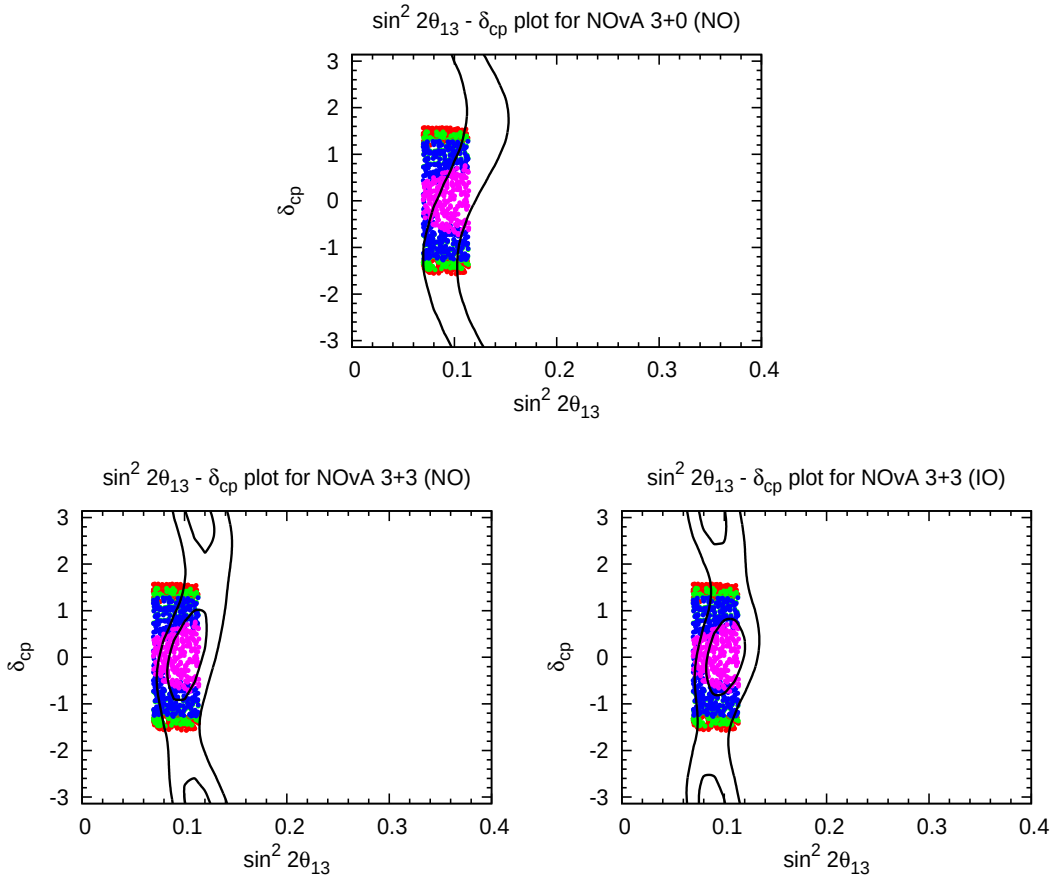

Figure 3.9: Correlation plots between δ_{CP} and $\sin^2 2\theta_{13}$ due to 12 deviation in the charged lepton sector super imposed on expected NOνA data. In these plots the red, green, blue and magenta regions correspond to TBM, GRA, HG and BM mixing patterns. The black solid lines correspond to the experimentally allowed contours.

model. In this context a number of neutrino mixing patterns like TBM/BM/GRA etc, were proposed based on some discrete flavor symmetries like S_3, A_4, $\mu - \tau$, etc. However, these symmetry forms of the mixing matrices predict vanishing reactor and maximal atmospheric mixing angles. To accommodate the observed value of relatively large θ_{13}, these mixing patterns should be modified by including appropriate perturbations. In this work, we have considered the simplest case of such perturbation which involves only minimal set of new independent parameters, i.e., one rotation angle and one phase, (which basically corresponds to perturbation induced by a single rotation), and found that it is possible to explain the observed neutrino oscillation data with such corrections. The predicted values of δ_{CP} are expected to be supported by the data from currently running NOνA experiment with (3ν $+3\bar{\nu}$) years of data taking. We have also shown that it is possible to predict the value of CP phase with such corrections. We have also found that sizable leptonic CP violation characterized by the Jarlskog invariant J_{CP}, i.e., $|J_{CP}| \sim 10^{-2}$ could be possible in these

scenarios.

Chapter 4

Non-zero θ_{13} and leptonic CP phase with A_4 Symmetry

4.1 Introduction

In the previous chapter, we have seen that some forms of neutrino mixing patterns relay on certain flavor symmetries which are proposed to explain initial neutrino oscillation data inticating vanishing reactor mixing angle, and with suitable modifications can accommodate moderatly large reactor mixing angle measured by recent experiments. Out of all those forms, TBM best resembles lepton mixing and gives positive results for all forms of corrections considered in chapter 3. There are many models which explain TBM mixing pattern on the basis of A_4 symmetry [106] with a certain set of Higgs scalars and vacuum alignments. The A_4 discrete symmetry group, the group of even permutations of four elements has attracted a lot of attention since it is the smallest one which admits one three-dimensional representation and three inequivalent one-dimensional representations. Then, the choice of the A_4 symmetry is natural since there are three families of fermions, i.e, the left-handed leptons can be unified in triplet representation of A_4 while the right-handed leptons can be assigned to A_4 singlets. This set-up was first proposed in Ref. [107] to study the lepton masses and mixing obtaining nearly degenerate neutrino masses and allowing realistic charged leptons masses after the A_4 symmetry is spontaneously broken. Later A_4 symmetry was proved to be very successful in generating Tribimaximal mixing pattern for lepton mixing.

TBM predict $\sin^2\theta_{12}$ to be 0.333 against its best-fit value 0.297 and the prediction comes within the 3σ range. Also the prediction of 0.5 for $\sin^2\theta_{23}$ also comes within the 3σ range. It is only the mixing angle θ_{13}, which is quite different from the experimental value. So θ_{13} might be non-zero at leading order itself while perturbative corrections slightly modifies other mixing angles. One of such forms with non-zero θ_{13} is a special case of deviation from

TBM due to an additional 23 rotation in neutrino sector. The 23 rotation is parameterized in terms of two parameters, one mixing angle (θ) and one phase (ϕ). For $\phi = \pi/2$, the resulting mixing matrix will have $\theta_{23} = \pi/4$, $\theta_{12}, \theta_{13} \neq 0$ and $\delta_{CP} = \pm\pi/2$. Such forms are known as cobimaximal mixing.

Supersymmetric models based on A_4 family symmetry, combined with the generalized CP symmetry [108], can also predict trimaximal (TM) lepton mixing (in which either only the first column or only the second column of the lepton mixing matrix is assumed to take the TBM form), together with either zero CP violation or $\delta_{CP} = \pm\pi/2$. Also models based on S_4 family symmetry and generalized CP symmetry [109] predict trimaximal lepton mixing and the Dirac CP phase is predicted to be either conserved or maximally broken. In Ref. [110], a minimal extension of the simplest A_4 model has been considered, which not only can induce non-zero θ_{13} value consistent with the recent observations, but also can correlate the CP violation in neutrino oscillation with the octant of the atmospheric mixing angle θ_{23}.

In this chapter, we would like to present a model based on A_4 symmetry which gives cobimaximal mixing in neutrino sector at leading order. We also consider perturbations in neutrino sector due to higher order corrections, which can be represented as five-dimensional operators. These corrections modify the mixing parameters slightly hence, the deviation of θ_{23} from $\pi/4$, indicated by recent experiments can be incorporated. The best-fit values and 3σ ranges of neutrino oscillation parameters taken from Ref. [51] are given in Table 4.1.

Mixing Parameters	Best Fit values	3σ Range
$\sin^2\theta_{12}$	0.323	$0.278 \to 0.375$
$\sin^2\theta_{23}$ (NH)	0.567	$0.393 \to 0.643$
$\sin^2\theta_{23}$ (IH)	0.573	$0.403 \to 0.640$
$\sin^2\theta_{13}$ (NH)	0.0226	$0.0190 \to 0.0262$
$\sin^2\theta_{13}$ (IH)	0.0229	$0.0193 \to 0.0265$
$\delta_{\rm CP}$ (NH)	1.41π	$(0 \to 2\pi)$
$\delta_{\rm CP}$ (IH)	1.48π	$(0 \to 2\pi)$
$\Delta m^2_{21}/10^{-5}\text{eV}^2$	7.60	$7.11 \to 8.18$
$\Delta m^2_{31}/10^{-3}\text{eV}^2$(NH)	2.48	$2.30 \to 2.65$
$\Delta m^2_{31}/10^{-3}\text{eV}^2$(IH)	-2.38	$-2.54 \to -2.20$

Table 4.1: The best-fit values and the 3σ ranges of the neutrino oscillation parameters from Ref. [51].

The details of the model is presented in section 4.2.In section 4.3, we describe the higher order corrections in neutrino sector while in sections 4.3 and 4.4, we discuss the vacuum alignment and lepton flavor violating muon decay $\mu \to e\gamma$ in the context of the model. We conclude our discussion in section 4.6.

4.2 The Model

The model is based on A_4 group [107], which is the group of even permutation of four objects and is the smallest non-Abelian discrete group with triplet irreducible representation. It has four irreducible representations: 1, $1'$, $1''$ and 3, with the multiplication rule

$$3 \times 3 = 1 + 1' + 1'' + 3 + 3 \ . \tag{4.1}$$

A_4 group has two generators represented by S and T, which obey the relations,

$$S^2 = T^3 = (ST)^3 = 1 \ . \tag{4.2}$$

The representation of S is 1 under 1, $1'$ and $1''$ while that of T are 1, ω and ω^2 respectively under 1, $1'$ and $1''$. There are two possible bases for three dimensional representations of S and T, one in which S is diagonal while in other T is diagonal. The direct product of two triplets, $a \sim (a_1, a_2, a_3)$ and $b \sim (b_1, b_2, b_3)$ in S diagonal basis is given by

$$\begin{aligned}
1 &= a_1b_1 + a_2b_2 + a_3b_3 \ , \\
1' &= a_1b_1 + \omega^2 a_2b_2 + \omega a_3b_3 \ , \\
1'' &= a_1b_1 + \omega a_2b_2 + \omega^2 a_3b_3 \ , \\
3 &\sim (a_2b_3, a_3b_1, a_1b_2) \ , \\
3 &\sim (a_3b_2, a_1b_3, a_2b_1) \ ,
\end{aligned} \tag{4.3}$$

while that in T diagonal basis is

$$\begin{aligned}
1 &\sim a_1b_1 + a_2b_3 + a_3b_2 \ , \\
1' &\sim a_3b_3 + a_1b_2 + a_2b_1 \ , \\
1'' &\sim a_2b_2 + a_3b_1 + a_1b_3 \ , \\
3_S &\sim \frac{1}{3}\begin{pmatrix} 2a_1b_1 - a_2b_3 - a_3b_2 \\ 2a_3b_3 - a_1b_2 - a_2b_1 \\ 2a_2b_2 - a_1b_3 - a_3b_1 \end{pmatrix} \ , \\
3_A &\sim \frac{1}{2}\begin{pmatrix} a_2b_3 - a_3b_2 \\ a_1b_2 - a_2b_1 \\ a_3b_1 - a_1b_3 \end{pmatrix} \ ,
\end{aligned} \tag{4.4}$$

where 3_S is symmetric and 3_A is antisymmetric under the exchange of a and b. In this chapter, we have followed Eq. (4.3) for the calculation of direct product of A_4 triplets. As we know in this basis, A_4 allows the charged-lepton mass matrix to be diagonalized by the Cabibbo-Wolfenstein matrix [111]

$$U_\omega = \frac{1}{\sqrt{3}} \begin{pmatrix} 1 & 1 & 1 \\ 1 & \omega & \omega^2 \\ 1 & \omega^2 & \omega \end{pmatrix} , \tag{4.5}$$

where $\omega = e^{2\pi i/3} = -1/2 + i\sqrt{3}/2$.

In this work, our discussion is limited to the leptonic sector. The particle content of the model includes, in addition to standard model fermions (i.e., the lepton doublets l_{iL} and charged lepton singlets l_{iR}), three right-handed neutrinos (ν_{iR}), four Higgs doublets (ϕ_i, ϕ_0) and three Higgs singlets (χ_i). They belong to four irreducible representations of A_4 as given in Table 4.2.

Particle	$SU(2)_L$	$U(1)_Y$	A_4
l_{iL}	2	-1	3
l_{1R}	1	-2	1
l_{2R}			$1'$
l_{3R}			$1''$
ν_{iR}	1	0	3
ϕ_i	2	1	3
ϕ_0	2	1	1
χ_i (real gauge singlet)	1	0	3

Table 4.2: Particle content of the model along with their quantum numbers.

Here A_4 symmetry is accompanied by an additional $U(1)_X$ symmetry as discussed in Ref. [106], which prevents the existence of Yukawa interactions of the form $\bar{l}_{iL}\nu_{iR}\tilde{\phi}_i$ and $\bar{l}_{iL}l_{iR}\phi_0$ as l_{iL}, l_{iR}, $\tilde{\phi}_0$ have quantum number $X = 1$, and all other fields have $X = 0$. The phenomenologically disallowed Nambu-Goldstone boson does not arise in this case as $U(1)_X$ symmetry does not break spontaneously but explicitly. Thus, the Yukawa Lagrangian for the leptonic sector is given as [112]

$$\begin{aligned} \mathcal{L} = &- \left\{ \left[\lambda_1 \left(\bar{l}_{iL}\phi_i \right) l_{1R} \right] + \left[\lambda_2 \left(\bar{l}_{iL}\phi_i \right)'' l_{2R} \right] + \left[\lambda_3 \left(\bar{l}_{iL}\phi_i \right)' l_{3R} \right] \right\} \\ &- \left\{ \lambda_0 \left[\left(\bar{l}_{iL}\nu_{iR} \right) \tilde{\phi}_0 \right] + \frac{1}{2} \left[M \left(\bar{\nu}_{iR}\hat{\nu}_{iR} \right) \right] + \lambda_\chi \left[\left(\bar{\nu}_{iR}\hat{\nu}_{iR} \right)_3 \chi_i \right] \right\} + \text{h.c.} , \end{aligned} \tag{4.6}$$

where $\hat{\nu}_{iR}$ are antiparticles of ν_{iR} and $\left(\bar{l}_{iL}\phi_i \right)'$, $\left(\bar{l}_{iL}\phi_i \right)''$ and $\left(\bar{\nu}_{iR}\hat{\nu}_{iR} \right)_3$ are $1'$, $1''$ and triplet

representations of A_4 respectively. As the scalars ϕ_i, ϕ_0 and χ_i get vacuum expectation values v_i, v_0 and ω_i respectively, the above Lagrangian becomes

$$\mathcal{L} = -\bar{l}_L M_l l_R - \bar{\nu}_L M_D \nu_R - \frac{1}{2}\bar{\nu}_R M_R \hat{\nu}_R + \text{h.c.}\ , \tag{4.7}$$

where M_l, M_D and M_R are charged-lepton, Dirac neutrino and right-handed neutrino mass matrices and have the forms

$$M_l = \begin{pmatrix} \lambda_1 v_1 & \lambda_2 v_1 & \lambda_3 v_1 \\ \lambda_1 v_2 & \lambda_2 v_2 \omega^2 & \lambda_3 v_2 \omega \\ \lambda_1 v_3 & \lambda_2 v_3 \omega & \lambda_3 v_3 \omega^2 \end{pmatrix}, \tag{4.8}$$

$$M_D = \lambda_0 v_0 I, \tag{4.9}$$

where I is the identity matrix and

$$M_R = \begin{pmatrix} M & \lambda_\chi \omega_3 & \lambda_\chi \omega_2 \\ \lambda_\chi \omega_3 & M & \lambda_\chi \omega_1 \\ \lambda_\chi \omega_2 & \lambda_\chi \omega_1 & M \end{pmatrix}. \tag{4.10}$$

For the vacuum alignment $v_i = v$, the charged lepton sector can be diagonalized by the transformation:

$$U_\omega \cdot M_l \cdot I = \begin{pmatrix} \sqrt{3} v \lambda_1 & 0 & 0 \\ 0 & \sqrt{3} v \lambda_2 & 0 \\ 0 & 0 & \sqrt{3} v \lambda_3 \end{pmatrix}, \tag{4.11}$$

where U_ω is the Cabibbo-Wolfenstein matrix given in Eq. (4.5). The light neutrino mass is given by the type-I seesaw formula

$$M_\nu = -M_D^T \cdot M_R^{-1} \cdot M_D\ . \tag{4.12}$$

Since M_D is proportional to an identity matrix, the neutrino mixing matrix will be the one which diagonalizes the right-handed neutrino mass matrix M_R. The Majorana mass matrix M_R can be parameterized as

$$M_R = \begin{pmatrix} A & C & D \\ C & A & B \\ D & B & A \end{pmatrix}, \tag{4.13}$$

in a basis where charged-lepton mass matrix is not diagonal. However, in the charged lepton mass diagonal basis $M_R^d = U_\omega^\dagger \cdot M_R \cdot U_\omega^*$ and can be diagonalized by tri-bimaximal (TBM) mixing matrix for $D = C = 0$, which we don't need as it gives vanishing θ_{13}. Even if these conditions are not satisfied some of the off-diagonal elements of M_R become zero in TBM

basis and one can go to the TBM basis through the transformation

$$M'_R = U_T^\dagger \cdot M_R \cdot U_T^* = \begin{pmatrix} A+B & \frac{1}{\sqrt{2}}(D+C) & 0 \\ \frac{1}{\sqrt{2}}(D+C) & A & \frac{i}{\sqrt{2}}(D-C) \\ 0 & \frac{i}{\sqrt{2}}(D-C) & B-A \end{pmatrix}, \tag{4.14}$$

where

$$U_T = \begin{pmatrix} 0 & 1 & 0 \\ \frac{1}{\sqrt{2}} & 0 & \frac{i}{\sqrt{2}} \\ \frac{1}{\sqrt{2}} & 0 & \frac{-i}{\sqrt{2}} \end{pmatrix}. \tag{4.15}$$

With the condition $D = -C$, M'_R becomes

$$\begin{pmatrix} A+B & 0 & 0 \\ 0 & A & i\sqrt{2}D \\ 0 & i\sqrt{2}D & B-A \end{pmatrix}, \tag{4.16}$$

which can be diagonalized by U_R, having the form

$$U_R = \begin{pmatrix} 1 & 0 & 0 \\ 0 & c & is \\ 0 & is & c \end{pmatrix}, \tag{4.17}$$

where s and c stand for $\sin\theta$ and $\cos\theta$ respectively and satisfy the relation

$$\frac{cs}{c^2 - s^2} = \frac{\sqrt{2}D}{B} = \frac{\sqrt{2}\omega_2}{\omega_1}\ . \tag{4.18}$$

It should be noted that, this ratio should be real, since $\omega_{1,2}$ are VEV of real scalar fields χ_i. The condition $C = -D$ can be realized with the vacuum alignment $\langle\chi_i\rangle = (\omega_1, \omega_2, -\omega_2)$ as discussed in [113]. Thus, the lepton mixing matrix becomes

$$U = U_\omega \cdot U_T \cdot U_R\ , \tag{4.19}$$

which basically known as co-bimaximal mixing matrix and predicts the mixing angles and CP violating Dirac phase as $\theta_{13} \neq 0$, $\theta_{23} = \pi/4$ and $\delta_{CP} = \pm\pi/2$. Also, the mixing angles θ_{12} and θ_{13} are not independent and one can express $\sin^2\theta_{12}$ in terms of $\sin^2\theta_{13}$ as

$$\sin^2\theta_{12} = \frac{1 - 3\sin^2\theta_{13}}{3(1 - \sin^2\theta_{13})}, \quad \text{with} \quad \sin\theta_{13} = \frac{s}{\sqrt{3}}\ . \tag{4.20}$$

To illustrate these results, we show in Fig. 4.1 the variation of $\sin^2\theta_{13}$ with θ (left panel) and the correlation plot between $\sin^2\theta_{13}$ and $\sin^2\theta_{12}$ (right panel). From the figure it can be seen

that the observed values of solar (θ_{12}) and reactor (θ_{13}) mixing angles can be accommodated in this model.

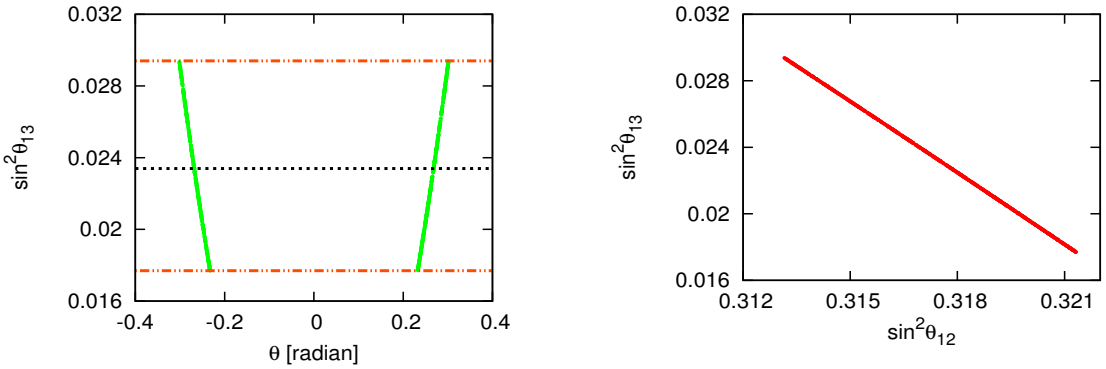

Figure 4.1: Variation of $\sin^2\theta_{13}$ with θ (left panel) and the correlation plots between $\sin^2\theta_{12}$ and $\sin^2\theta_{13}$ (right panel). The black dashed line in the left panel denotes the central value of $\sin^2\theta_{13}$ and the red dot-dashed lines represent the corresponding 3σ values.

4.3 Perturbation in neutrino sector

In this section, we will consider the perturbations to mass matrices due to higher order corrections. Prominent corrections come from five-dimensional operator $\lambda_{ij}\bar{\nu}_{iR}\hat{\nu}_{jR}\chi_i\chi_j$ which modifies right-handed neutrino mass matrix. Charged lepton and Dirac neutrino masses also receive corrections from $\lambda'_{jk}\bar{l}_{il}\phi_i l_{jR}\chi_i$ and $\lambda'_{jk}\bar{l}_{il}\tilde{\phi}_0\nu_{jR}\chi_i$ respectively, and here we are neglecting those corrections since they allow the mixing of χ_i with other fields.

All elements of Majorana mass matrix M_R receive corrections which is proportional to $\omega_1^2+\omega_2^2$ for diagonal elements and $\omega_1\omega_2$ for off diagonal elements. Since $0.04 < (\omega_2/\omega_1) < 0.22$, obtained from Eq. (4.18), using the allowed value of $s = \sqrt{3}\sin\theta_{13}$, we neglect corrections to off-diagonal elements.

$$\delta M_R \simeq \begin{pmatrix} \lambda_{11}\omega_1^2 & 0 & 0 \\ 0 & \lambda_{22}\omega_1^2 & 0 \\ 0 & 0 & \lambda_{33}\omega_1^2 \end{pmatrix} . \tag{4.21}$$

These corrections will modify the light neutrino mass matrix and the inverse of modified light neutrino mass matrix in TBM basis can be parameterized as

$$M_\nu^{-1} = \begin{pmatrix} B+A & 0 & 0 \\ 0 & A & i\sqrt{2}D \\ 0 & i\sqrt{2}D & B-A \end{pmatrix} + \begin{pmatrix} \frac{1}{2}(\lambda_{22}+\lambda_{33}) & 0 & \frac{i}{2}(\lambda_{33}-\lambda_{22}) \\ 0 & \lambda_{11} & 0 \\ \frac{i}{2}(\lambda_{33}-\lambda_{22}) & 0 & \frac{-1}{2}(\lambda_{33}+\lambda_{22}) \end{pmatrix} \omega_1^2 . \tag{4.22}$$

Hence, in the charged lepton diagonal basis light neutrino mass matrix can be diagonalized

by

$$U = U_\omega \cdot U_T \cdot U_R \cdot U_{13} \ , \tag{4.23}$$

where

$$U_{13} = \begin{pmatrix} c' & 0 & s'e^{-i\phi} \\ 0 & 1 & 0 \\ -s'e^{i\phi} & 0 & c' \end{pmatrix} . \tag{4.24}$$

with $s' = \sin\theta'$ and $c' = \cos\theta'$.

To obtain mixing angles we compare lepton mixing matrix U (4.23) with PMNS matrix (1.63), i.e.,

$$U = U_{PMNS} \ . \tag{4.25}$$

The mixing angles $\sin^2\theta_{12}$, $\sin^2\theta_{23}$ and $\sin^2\theta_{13}$ are related to the elements of U as

$$\sin^2\theta_{12} = \frac{|U_{12}|^2}{1-|U_{13}|^2}, \quad \sin^2\theta_{23} = \frac{|U_{23}|^2}{1-|U_{13}|^2}, \quad \sin^2\theta_{13} = |U_{13}|^2 \ , \tag{4.26}$$

where U_{ij} is the ij^{th} element of the lepton mixing matrix U. Now using Eqs. (4.5), (4.15), (4.23) and (4.26), we obtain

$$\sin^2\theta_{13} = \frac{1}{3}\left[2s'^2 - 2\sqrt{2}sc's'\sin\phi + s^2c'^2\right] \ , \tag{4.27}$$

$$\sin^2\theta_{12} = \frac{1-s^2}{3-\left(2s'^2 - 2\sqrt{2}sc's'\sin\phi + s^2c'^2\right)} \ , \tag{4.28}$$

$$\sin^2\theta_{23} = \frac{1}{2} + \frac{\sqrt{3}cc's'\cos\phi}{3-\left(2s'^2 - 2\sqrt{2}sc's'\sin\phi + s^2c'^2\right)} \ , \tag{4.29}$$

Another important parameter is J_{CP}, the Jarlskog invariant, which is a measure of CP violation, is found to have the value in this model as

$$\begin{aligned} J_{CP} &= \mathrm{Im}\left[U_{11}U_{22}U_{21}^*U_{12}^*\right] \\ &= \frac{c}{6\sqrt{3}}\left[\sqrt{2}sc'^2 - \left(1+c^2\right)c's'\sin\phi - \sqrt{2}ss'^2\right] . \end{aligned} \tag{4.30}$$

In standard parametrization, the value of J_{CP} is

$$J_{CP} = \frac{1}{8}\sin 2\theta_{12}\sin 2\theta_{23}\sin 2\theta_{13}\cos\theta_{13}\sin\delta_{CP} \ . \tag{4.31}$$

Comparing Eqs. (4.30) and (4.31), we obtain

$$\sin\delta_{CP} = \frac{\sqrt{2}s(c'^2 - s'^2) - c's'(1+c^2)\sin\phi}{\sqrt{X'(2-X'+s^2)\left(1-\frac{Y'^2}{(3-X')^2}\right)}} \ , \tag{4.32}$$

where

$$X' = \left[2s'^2 - 2\sqrt{2}sc's'\sin\phi + s^2c'^2\right] ,$$
$$Y' = 2\sqrt{3}cc's'\cos\phi \, . \tag{4.33}$$

To show that the model predicts the mixing angles compatible with the observed data,we

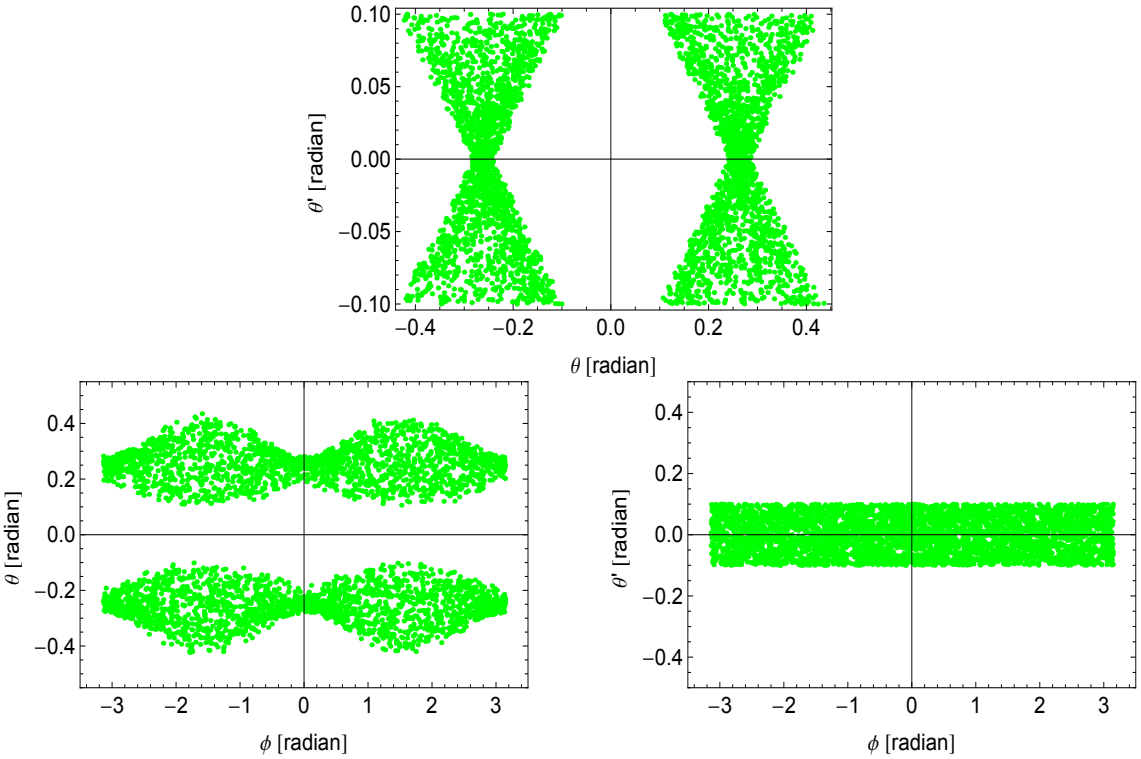

Figure 4.2: Allowed parameter space in $\theta' - \theta$ (left panel), $\theta - \phi$ (right panel) and $\theta' - \phi$ planes compatible with the observed data.

obtain the allowed parameter space compatible with the 3σ range of the observed data by varying the parameters s between $[-1, 1]$, s' between $[-0.1, 0.1]$ and ϕ between $[-\pi, \pi]$, we show the allowed parameter space in various planes in Fig. 4.2. Using these allowed values of different parameters, we show the correlation plots between $\sin^2\theta_{13}$ and $\sin^2\theta_{23}$ (left panel), $\sin^2\theta_{13}$ and $\sin^2\theta_{12}$ (right panel) and between $\sin^2\theta_{13}$ and δ_{CP}/J_{CP} (bottom panel) in Fig. 4.3. From these plots it can be seen that by including higher order correction to right handed neutrino mass matrix, it is possible to accommodate the observed data.

4.4 Vacuum alignment

We have assumed the vacuum alignment $\langle\phi_i\rangle = v(1, 1, 1)$, $\langle\phi_0\rangle = v_0$, $\langle\chi\rangle = (\omega_1, \omega_2, -\omega_2)$ to obtain the structure of mass matrices in lepton sector. One can obtain such vacuum

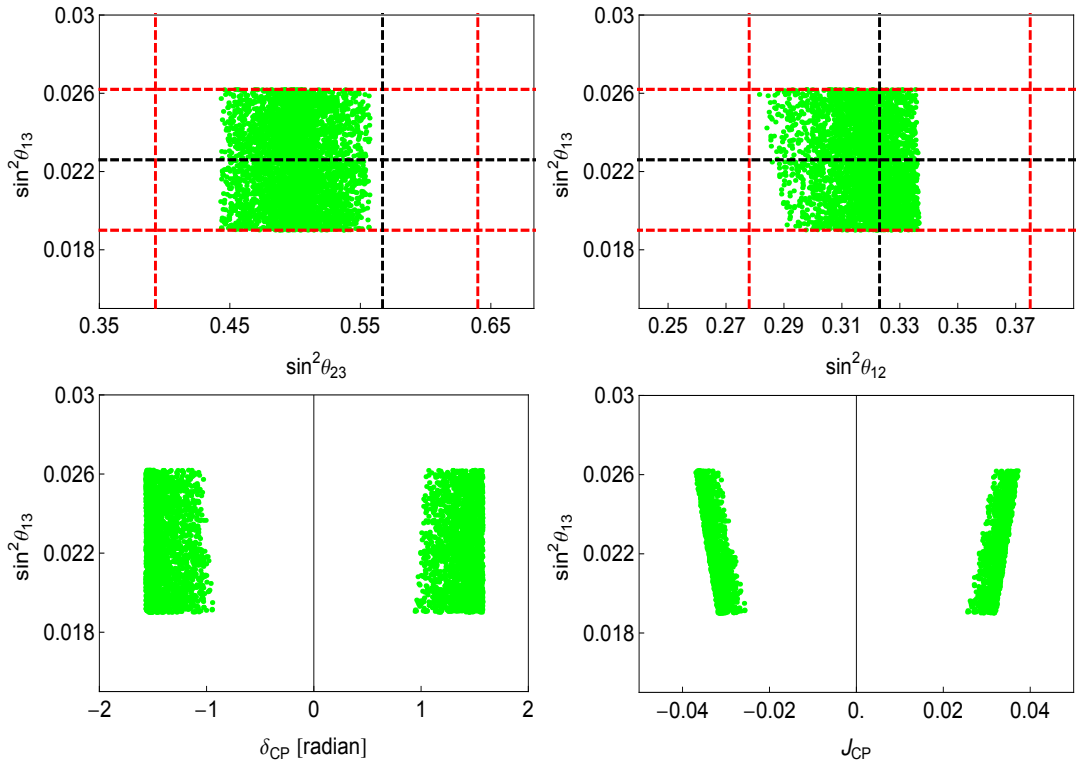

Figure 4.3: Correlation plots between $\sin^2\theta_{13}$ and $\sin^2\theta_{23}$ (left panel), and $\sin^2\theta_{13}$ and $\sin^2\theta_{12}$ (right panel) and between $\sin^2\theta_{13}$ and δ_{CP}/J_{CP} (bottom panel) including the corrections.

alignment in the limit χ decouples from rest of the fields. The complete scalar potential is given by

$$V = V(\phi_i) + V(\chi_i) + V(\phi_0) + V(\phi_i, \chi_i) + V(\phi_i, \phi_0), \tag{4.34}$$

with

$$\begin{aligned} V(\phi_i) &= \mu_{\phi_i}^2 \sum_j \phi_j^\dagger \phi_j + \frac{\lambda_1^{\phi_i}}{2}\left(\sum_j \phi_j^\dagger \phi_j\right)^2 \\ &+ \lambda_2^{\phi_i}\left(\phi_1^\dagger\phi_1 + \omega\phi_2^\dagger\phi_2 + \omega^2\phi_3^\dagger\phi_3\right)\left(\phi_1^\dagger\phi_1 + \omega^2\phi_2^\dagger\phi_2 + \omega\phi_3^\dagger\phi_3\right) \\ &+ \lambda_3^{\phi_i}\left[\left(\phi_2^\dagger\phi_3\right)\left(\phi_3^\dagger\phi_2\right) + \left(\phi_3^\dagger\phi_1\right)\left(\phi_1^\dagger\phi_3\right) + \left(\phi_1^\dagger\phi_2\right)\left(\phi_2^\dagger\phi_1\right)\right] \\ &+ \left\{\frac{\lambda_4^{\phi_i}}{2}\left[\left(\phi_2^\dagger\phi_3\right)^2 + \left(\phi_3^\dagger\phi_1\right)^2 + \left(\phi_1^\dagger\phi_2\right)^2\right] + \text{h.c.}\right\}, \end{aligned} \tag{4.35}$$

$$\begin{aligned} V(\chi_i) &= \mu_{\chi_i}^2 \sum_j \chi_j\chi_j + \delta^{\chi_i}\chi_1\chi_2\chi_3 + \lambda_1^{\chi_i}\left(\sum_j \chi_j\chi_j\right)^2 \\ &+ \lambda_2^{\chi_i}\left(\chi_1\chi_1 + \omega\chi_2\chi_2 + \omega^2\chi_3\chi_3\right)\left(\chi_1\chi_1 + \omega^2\chi_2\chi_2 + \omega\chi_3\chi_3\right) \\ &+ \lambda_3^{\chi_i}\left[(\chi_2\chi_3)^2 + (\chi_3\chi_1)^2 + (\chi_1\chi_2)^2\right], \end{aligned} \tag{4.36}$$

$$V(\phi_0) = \mu_{\phi_0}^2 \phi_0^\dagger\phi_0 + \lambda_1^{\phi_0}\left(\phi_0^\dagger\phi_0\right)^2, \tag{4.37}$$

$$\begin{aligned} V(\phi_i,\chi_i) &= \delta^{\phi_i\chi_i}\left(\phi_2^\dagger\phi_3\chi_1+\phi_3^\dagger\phi_1\chi_2+\phi_1^\dagger\phi_2\chi_3\right)+\lambda_1^{\phi_i\chi_i}\sum_{j,k}\phi_j^\dagger\phi_j\chi_k\chi_k \\ &+ \lambda_2^{\phi_i\chi_i}\left(\phi_1^\dagger\phi_1+\omega\phi_2^\dagger\phi_2+\omega^2\phi_3^\dagger\phi_3\right)\left(\chi_1\chi_1+\omega^2\chi_2\chi_2+\omega\chi_3\chi_3\right) \\ &+ \lambda_3^{\phi_i\chi_i}\left(\phi_2^\dagger\phi_3\chi_2\chi_3+\phi_3^\dagger\phi_1\chi_3\chi_1+\phi_1^\dagger\phi_2\chi_1\chi_2\right)+\text{h.c.}, \end{aligned} \tag{4.38}$$

$$\begin{aligned} V(\phi_i,\phi_0) &= \lambda_1^{\phi_i\phi_0}\left(\sum_j\phi_j^\dagger\phi_j\right)\phi_0^\dagger\phi_0+\lambda_2^{\phi_i\phi_0}\left(\sum_j\phi_j^\dagger\phi_0\ \phi_0^\dagger\phi_j\right) \\ &+ \left[\lambda_3^{\phi_i\phi_0}\left(\phi_1^\dagger\phi_0\phi_2^\dagger\phi_3+\phi_2^\dagger\phi_0\phi_3^\dagger\phi_1+\phi_3^\dagger\phi_0\phi_1^\dagger\phi_2\right)\right. \\ &+ \left.\lambda_4^{\phi_i\phi_0}\left(\phi_1^\dagger\phi_0\phi_3^\dagger\phi_2+\phi_2^\dagger\phi_0\phi_1^\dagger\phi_3+\phi_3^\dagger\phi_0\phi_2^\dagger\phi_1\right)+\text{h.c.}\right]\ , \end{aligned} \tag{4.39}$$

$$V(\chi_i,\phi_0) = \lambda^{\phi_0\chi_i}\left(\sum_j\chi_j\chi_j\right)\phi_0^\dagger\phi_0. \tag{4.40}$$

The last term in Eq. (4.39) breaks $U(1)_X$ symmetry explicitly and removes Goldstone boson which occurs due to the spontaneous breaking of $U(1)_X$ symmetry. The vacuum alignment, $\langle\phi_0\rangle = u$, $\langle\phi_i\rangle = (v,v,v)$ and $\langle\chi_i\rangle = (w_1,w_2,-w_2)$ assumed in the model is a possible minimum of the scalar potential for $V(\phi_i,\chi_i)=0$. A vanishing $V(\phi_i,\chi_i)$ can be achieved in the limit χ_i decouples from rest of the field as mentioned in Ref. [106]. The decoupling of χ_i requires $\lambda_\chi \to 0$, $\lambda^{\phi_0\chi_i}\to 0$. To generate an acceptable neutrino mass spectrum λ_χ has to be nonzero but can be small. A small but nonzero λ_χ will generate a sufficiently small $V(\phi_i,\chi_i)$, which will be too small to alter vacuum alignment considerably. In this limit the minimization condition on u is given by

$$\begin{aligned} &\mu_{\phi_0}^2 u+2\lambda_1^{\phi_0}(u^*u)u+\lambda_1^{\phi_i\phi_0}\left(\mid v_1\mid^2+\mid v_2\mid^2+\mid v_3\mid^2\right)u+\lambda_2^{\phi_i\phi_0}\left(\sum_{j,k}v_j^*v_k\right)u \\ &+\lambda_3^{\phi_i\phi_0{}^*}\left[v_1v_2v_3^*+v_2v_3v_1^*+v_3v_1v_2^*\right]+\lambda_4^{\phi_i\phi_0{}^*}\left[v_1v_3v_2^*+v_2v_1v_3^*+v_3v_2v_1^*\right]=0\ . \end{aligned} \tag{4.41}$$

The above Eq. (4.41) has a solution

$$u=\frac{\lambda_3^{\phi_i\phi_0{}^*}\left[v_1v_2v_3^*+v_2v_3v_1^*+v_3v_1v_2^*\right]+\lambda_4^{\phi_i\phi_0{}^*}\left[v_1v_3v_2^*+v_2v_1v_3^*+v_3v_2v_1^*\right]}{\mu_{\phi_0}^2+\left(\lambda_1^{\phi_i\phi_0}+\lambda_2^{\phi_i\phi_0}\right)\left(\sum_j|v_j|^2\right)}, \tag{4.42}$$

for $|u|^2 \ll |v_i|^2$.

Thus, for this case, i.e., for $|u|^2 \ll |v_i|^2$ minimization conditions on v_i are given as

$$\begin{aligned}\frac{\partial V}{\partial v_i^*} &= \mu_{\phi_i}^2 v_i + \lambda_1^{\phi_i} v_i \sum_j |v_j|^2 + \lambda_2^{\phi_i} v_i \left(2|v_i|^2 - \sum_{j\neq i} |v_j|^2\right) \\ &\quad + \lambda_3^{\phi_i} v_i \left(\sum_{j\neq i} |v_j|^2\right) + \lambda_4^{\phi_i} v_i^* \sum_{j\neq i} v_j^2 = 0 \,.\end{aligned} \tag{4.43}$$

Considering $\lambda_4^{\phi_i}$ as real, one can get the solution

$$v_i = v = \sqrt{\frac{-\mu_{\phi_i}^2}{3\lambda_1^{\phi_i} + 2\left(\lambda_3^{\phi_i} + \lambda_4^{\phi_i}\right)}} \,, \tag{4.44}$$

which is allowed.

Minimization conditions on w_i is given by

$$\frac{\partial V}{\partial w_1} = 2\left[\mu_{\chi_i}^2 + \lambda_2^{\chi_i\prime}\left(w_2^2 + w_3^2\right)\right] w_1 + \delta^{\chi_i} w_2 w_3 + 4\lambda_1^{\chi_i\prime} w_1^3 = 0 \,, \tag{4.45}$$

$$\frac{\partial V}{\partial w_2} = 2\left[\mu_{\chi_i}^2 + \lambda_2^{\chi_i\prime}\left(w_1^2 + w_3^2\right)\right] w_2 + \delta^{\chi_i} w_1 w_3 + 4\lambda_1^{\chi_i\prime} w_2^3 = 0 \,, \tag{4.46}$$

$$\frac{\partial V}{\partial w_3} = 2\left[\mu_{\chi_i}^2 + \lambda_2^{\chi_i\prime}\left(w_2^2 + w_1^2\right)\right] w_3 + \delta^{\chi_i} w_2 w_1 + 4\lambda_1^{\chi_i\prime} w_3^3 = 0 \,, \tag{4.47}$$

one of the solutions of above set of equations is $w_1 \neq 0$, $w_3 = -w_2 \neq 0$, which is the vacuum alignment condition for $\langle\chi_i\rangle$.

4.5 Effect of additional Higgs doublets on lepton flavor violating decay $\mu \to e\gamma$

Since $|\ u\ |^2 \ll v^2$, one can neglect the mixing between ϕ_i and ϕ_0 and the mass-squared matrices in the Re$[\phi_i^0]$, Im$[\phi_i^0]$, and $\phi_i^\pm$ bases have the same form [107]

$$M^2 = \begin{pmatrix} a & b & b \\ b & a & b \\ b & b & a \end{pmatrix}, \tag{4.48}$$

where $a = 2\left(\lambda_1^{\phi_i} + 2\lambda_2^{\phi_i}\right)v^2$, $-4\lambda_4^{\phi_i}v^2$, $-2(\lambda_3^{\phi_i} + \lambda_4^{\phi_i})v^2$ and $b = 2\left(\lambda_1^{\phi_i} - \lambda_2^{\phi_i} + \lambda_3^{\phi_i} + \lambda_4^{\phi_i}\right)v^2$, $2\lambda_4^{\phi_i}v^2$, $\left(\lambda_3^{\phi_i} + \lambda_4^{\phi_i}\right)v^2$ for Re$[\phi_i^0]$, Im$[\phi_i^0]$, and $\phi_i^\pm$ respectively. Hence, there are three linear combinations of ϕ_i's, $\phi = \frac{1}{\sqrt{3}}(\phi_1 + \phi_2 + \phi_3)$, $\phi' = \frac{1}{\sqrt{3}}(\phi_1 + \omega\phi_2 + \omega^2\phi_3)$ and

$\phi'' = \frac{1}{\sqrt{3}}(\phi_1 + \omega^2\phi_2 + \omega\phi_3)$ with vacuum expectation values $\sqrt{3}v$, 0, and 0 respectively. The Higgs doublet ϕ with mass-squared eigenvalues $\left(3\lambda_1^{\phi_i} + 2\lambda_3^{\phi_i} + 2\lambda_4^{\phi_i}\right)v^2$, 0, 0 for Re$[\phi^0]$, Im$[\phi^0]$ and $\phi^{\pm}$ can be identified as standard model Higgs doublet which gives masses to charged leptons. One can see this by expressing Yukawa interactions of ϕ_i's with leptons in charged lepton mass diagonal basis

$$\begin{aligned}\mathcal{L} &= \left(\frac{m_e}{\sqrt{3}v}\overline{(\nu_e, e)}_L e_R + \frac{m_\mu}{\sqrt{3}v}\overline{(\nu_\mu, \mu)}_L \mu_R + \frac{m_\tau}{\sqrt{3}v}\overline{(\nu_\tau, \tau)}_L \tau_R\right)\phi \\ &+ \left(\frac{m_e}{\sqrt{3}v}\overline{(\nu_\mu, \mu)}_L e_R + \frac{m_\mu}{\sqrt{3}v}\overline{(\nu_\tau, \tau)}_L \mu_R + \frac{m_\tau}{\sqrt{3}v}\overline{(\nu_e, e)}_L \tau_R\right)\phi' \\ &+ \left(\frac{m_e}{\sqrt{3}v}\overline{(\nu_\tau, \tau)}_L e_R + \frac{m_\mu}{\sqrt{3}v}\overline{(\nu_e, e)}_L \mu_R + \frac{m_\tau}{\sqrt{3}v}\overline{(\nu_\mu, \mu)}_L \tau_R\right)\phi''.\end{aligned} \tag{4.49}$$

The Higgs doublets ϕ' and ϕ'' contributes to flavor violating decays such as $\mu \to e\gamma$. The prominent contribution comes from ϕ' and the branching ratio is given by [107],

$$\text{Br}\,(\mu \to e\gamma) = \frac{9}{32\pi^2} m_\tau^4 \left(\frac{M_R^2 - M_I^2}{M_R^2 M_I^2}\right)^2 \left(\frac{v_0^2}{3v^2}\right)^2 , \tag{4.50}$$

where $M_R^2 = 2\left(3\lambda_2^{\phi_i} - \lambda_3^{\phi_i} - \lambda_4^{\phi_i}\right)v^2$, $M_I^2 = -6\lambda_4^{\phi_i}v^2$ are mass-squared eigenvalues of $\frac{1}{\sqrt{3}}(\text{Re}[\phi_1] + \omega\text{Re}[\phi_2] + \omega^2\text{Re}[\phi_3])$ and $\frac{1}{\sqrt{3}}(\text{Im}[\phi_1] + \omega\text{Im}[\phi_2] + \omega^2\text{Im}[\phi_3])$ respectively and $v_0^2 = \left(1/2\sqrt{2}G_F\right)$. The predicted branching ratio will be below the experimental upper limit Br $(\mu \to e\gamma) < 4.2 \times 10^{-13}$ [114] for

$$\left(\frac{M_R^2 - M_I^2}{M_R^2 M_I^2}\right)^{\frac{1}{2}} < 1.56 \times 10^{-3}\ \text{GeV}^{-1}\ . \tag{4.51}$$

4.6 Summary and Conclusions

There are many models in the literature that give tri-bimaximal (TBM) form for neutrino mixing by extending SM symmetry with A_4 symmetry. Many models have shown that the perturbations from higher order corrections can account for the difference in the mixing angle predicted by TBM and that obtained from oscillation data from various experiments. But deviation of the mixing angle θ_{13} predicted by TBM from the observed value is quite high compared to other mixing parameters as TBM predict vanishing θ_{13} while experiments measure moderately large value. Hence, it is appropriate to consider θ_{13} non-zero at leading order mixing matrix itself while other mixing angles are close to that of TBM and co-bimaximal mixing matrix is an example. In this regard, we considered a model based on A_4 symmetry,

which gives co-bimaximal form ($\theta_{23} = \pi/4$, $\delta_{CP} = \pm\pi/2$ and $\theta_{13} \neq 0$) for the leading order neutrino mixing matrix. We found that higher order corrections in neutrino sector coming from effective dimensional-five operators after spontaneous breaking of A_4 symmetry, modify leading order mixing matrix. And the mixing angles, thus obtained are found to be within the 3σ ranges of their experimental values. The CP violating phase δ_{CP} is found to be around the region $\pm\pi/2$, and the upper limit on the Jarlskog invariant is $\mathcal{O}(10^{-2})$. There are four Higgs doublets ϕ_0, and ϕ_i, for $i = 1, 2, 3$ in this model. One of the three linear combinations (ϕ) of ϕ_i behaves exactly as standard model Higgs doublet while neutral component of the other two (ϕ', ϕ'') contribute to the lepton flavor violating decays such as $\mu \to e\gamma$.

Chapter 5

A_4 realization of Linear Seesaw and Neutrino Phenomenology

5.1 Introduction

As discussed before, results from various neutrino oscillation experiments show atleast two of the three active neutrinos are massive but in the SM neutrinos do not have Dirac mass like other fermions due to the absence of right handed neutrinos. So neutrino mass generation in the SM is generally expected to arise from a dimension-five operator [115] known as Weinberg operator, which violates lepton number. However, in the context of SM very little is known about the origin of this operator and the underlying mechanism or its flavor structure. The seesaw mechanisms, type-I, type-II and type-III discussed in chapter 2 are tree level realizations of Weinberg operator in beyond the standard model framework. All of them include some heavy particles that mediate Weinberg operator, in addition to SM particles. For example, in type-I seesaw setting [116, 117], a detailed discussion of which is given previously in chapter 2 of this thesis, SM is extended by including the right-handed neutrinos to its particle content. And these right handed neutrinos mediate Weinberg operator, therefore the mass of active neutrinos are inversely proportional to that of right handed neutrinos. The inclusion of right-handed neutrinos N_{R_i}, not only generates the Dirac mass term but also leads to Majorana mass for the right handed neutrinos, which is of the form $\overline{N}_{R_i} N^c_{R_i}$ and violates $B-L$ symmetry. The smallness of active neutrino mass is ensured by the high value of Majorana mass of the right handed neutrino. In these cases, if Dirac mass of neutrinos are of the order of lightest charged lepton mass i.e., electron mass, the Majorana mass has to be in TeV range to get the observed value of active neutrino mass [53]. But if such models have to be embedded in Grand Unified Theories (GUTs) where both Quarks and Leptons are treated on the same footing, the Dirac mass of neutrinos will be of the order of that of

up-type quark [118] and the observed value of active neutrino mass requires Majorana mass to be of the order of 10^{15} GeV, which is beyond the access of present and future experiments. In a similar way, we have seen in chapter 2 that in type-II seesaw mechanism new particle involved is very heavy.

Many possibilities were proposed to have not so heavy Majorana mass and the existence of other type of neutrinos called sterile neutrinos (S) is one among them [119]. Now the neutrino mass can be expressed in the form of a 3×3 matrix with each element represents a matrix. Depending on the position of the zero elements in the mass matrix in the basis (ν, N_R, S), active neutrinos receive masses through two different mechanisms called inverse seesaw [119, 120] and linear seesaw [57], which are discussed earlier in chapter 2. In all those cases, the smallness of neutrino mass is not only depends on the ratio of Dirac mass to heavy neutrino mass but also depends on another parameter, 13 element of neutrino mass matrix in the case of linear seesaw and 33 element of neutrino mass matrix in the case of inverse seesaw hence, allows to have heavy neutrinos in TeV range and bound on the ratio comes from non-unitarity effect.

All those seesaw mechanisms require some of the elements of mass matrix to be zero or very small but none of them are prevented by SM symmetry. All those terms except 33 element in the matrix will be prohibited if the SM symmetry is extended to $SU(2)_L \times SU(2)_R \times SU(3)_C$, since in those symmetry groups right handed neutrinos are no longer singlets. But linear seesaw requires 33 element of the mass matrix to be zero or very small which is difficult to obtain with gauge symmetry, as sterile neutrinos are singlets in all gauge groups. But such terms will be absent if there is flavor symmetry under which sterile neutrinos have non trivial representation.

Here we consider the realization of linear seesaw with A_4 symmetry, since A_4 symmetry is proved to be successful in generating variants of tribimaximal mixing for lepton mixing that can accomodate recent results from neutrino oscillation experiments. We extend SM symmetry with $A_4 \times Z_4 \times Z_3$ along with an extra global symmetry $U(1)_X$, as discussed in Ref. [121]. The SM particle content has been extended by introducing three RH neutrinos, N_{R_i} and three singlet fermions, S_{R_i} along with the flavon fields (ϕ_S, ϕ_T, ξ, ξ', ρ, ρ'), to understand the flavor structure of the lepton mixing. The proposed model gives almost similar result as in [121] in the context of neutrino oscillation, but has a different physics aspect in the case of heavy neutrinos. In [121], the active neutrinos get their mass through inverse seesaw with the prediction of six nearly degenerate heavy neutrinos but in our case there are three very different mass state with each state is nearly doubly degenerated. Also, our proposed scenario is very much suitable for Leptogenesis as discussed in [39, 122], where the analytic

expression for CP asymmetry and corresponding baryon asymmetry for the case of three pairs of nearly degenerate heavy neutrinos can be found. In Ref. [122], the contributions of the absorptive part of Higgs self-energy to CP violation in heavy particle decays termed as ϵ-type CP violation, has been discussed elaborately. Such contributions are neglected in many cases as they are small compared to ϵ'-type, the CP violation in heavy neutrino decays due to the overlapping of tree-level with one-loop vertex diagram. They have provided the formalism to deal with mixing of states during the decay of the particles and have shown that there is resonant enhancement of ϵ-type CP violation, if mixing states are nearly degenerate. The CP asymmetries due to both types of CP violations for a model with a pair of nearly degenerate heavy neutrinos are also calculated and it was shown that the CP asymmetry due to ϵ-type CP violation is about 100 times more than that of due to ϵ'-type, which in turn predicts the correct baryon asymmetry of the Universe.

The next section of this chapter presents the model framework of linear seesaw while the A_4 realization of linear seesaw and its implication to neutrino oscillation parameters and discussion on Leptogenesis are present in the subsequent sections. And the chapter ends with summary and conclusions.

5.2 The model framework for linear seesaw

We consider the minimal extension of Standard Model gauge group $\mathcal{G}_{\rm SM} \equiv SU(2)_L \times U(1)_Y$, omitting the $SU(3)_C$ structure for simplicity, with two types of singlet neutrinos, which are complete singlet under $\mathcal{G}_{\rm SM}$, for implementation of linear seesaw. We denote these neutral fermion singlets as right-handed sterile neutrinos N_{R_i} and S_{R_i}. Both these neutral fermion species have Yukawa coupling with the lepton doublet L. In addition, one can write down a mixing term connecting these two species of neutrinos. The bare Majorana mass terms for N_{R_i} and S_{R_i} are either assumed to be zero or forbidden by some symmetry arguments. The leptonic Lagrangian for linear seesaw mechanism is given by

$$\begin{aligned} -\mathcal{L} &= y\overline{L}\tilde{H}N_{\rm R} + h\overline{L}\tilde{H}S_{\rm R} + \overline{N_R}m_{RS}S^c_{\rm R} + \text{ h.c.} \\ &= \overline{\nu}_{\rm L}m_{\rm D}N_{\rm R} + \overline{\nu}_{\rm L}m_{\rm LS}S_{\rm R} + \overline{N}_{\rm R}m_{RS}S^c_{\rm R} + \text{ h.c. .} \end{aligned} \tag{5.1}$$

The full mass matrix for neutral leptons in the basis $N = (\nu_{\rm L},\ N^c_{\rm R},\ S^c_{\rm R})^{\rm T}$ is given as

$$\mathbb{M} = \begin{pmatrix} 0 & m_{\rm D} & m_{\rm LS} \\ m^{\rm T}_{\rm D} & 0 & m_{RS} \\ m^{\rm T}_{\rm LS} & m^{\rm T}_{RS} & 0 \end{pmatrix}. \tag{5.2}$$

The resulting mass formula for light neutrinos is governed by linear seesaw mechanism

$$m_\nu = m_{\rm D} m_{RS}^{-1} m_{\rm LS}^{\rm T} + \text{ transpose} \,. \tag{5.3}$$

5.3 An A_4 realization of linear seesaw

In this section, we wish to present an A_4 realization of linear seesaw which has been discussed in the previous section. The particle content of the model and their representations under flavor symmetries are presented in Table 5.1[1]. We introduce an extra global symmetry $U(1)_X$ which is broken explicitly but softly by the term $\mu^2_{\rho\xi}\rho\xi$+h.c., in the Higgs potential to prevent Goldstone boson [106]. This term not only breaks $U(1)_X$ symmetry but also gives non-zero vacuum expectation value to ρ, $\langle\rho\rangle = \mu^2_{\rho\xi}\langle\xi\rangle/m^2_\rho$. Here $\mu_{\rho\xi}$ has mass dimension one and it is natural to assume that $\mu_{\rho\xi}$ is very small to m_ρ, the mass of ρ since, $\mu^2_{\rho\xi}\rho\xi$ + h.c. breaks $U(1)_X$ symmetry while all other terms in the Higgs potential respect all symmetries of the model. Therefore, vacuum expectation value of ρ is very small compared to that of ξ, i.e., $\langle\rho\rangle \ll \langle\xi\rangle$.

Fields	e_R	μ_R	τ_R	L	H	N_R	S_R	ϕ_T	ϕ_S	ξ	ξ'	ρ	ρ'
A_4	1	$1''$	$1'$	3	1	3	3	3	3	1	$1'$	1	1
Z_4	$-i$	$-i$	$-i$	$-i$	1	i	1	1	i	i	i	$-i$	-1
Z_3	1	1	1	1	1	1	ω	1	ω	ω	ω	ω^2	1
X	-1	-1	-1	-1	0	0	0	0	0	0	0	-1	-1

Table 5.1: The particle content and their charge assignments for an A_4 realization of linear seesaw mechanism.

The Yukawa Lagrangian for the charged lepton sector is given as

$$\mathcal{L}_l = -\left\{\left[\frac{\lambda_e}{\Lambda}\left(\bar{L}\phi_T\right) H e_R\right] + \left[\frac{\lambda_\mu}{\Lambda}\left(\bar{L}\phi_T\right)' H \mu_R\right] + \left[\frac{\lambda_\tau}{\Lambda}\left(\bar{L}\phi_T\right)'' H \tau_R\right]\right\} .$$

After giving non-zero vacuum expectation values (VEVs) to SM Higgs as well as flavon fields and breaking all symmetries, the mass matrix for charged leptons is found to be

$$M_l = v\frac{v_T}{\Lambda}\text{diag}\left(\lambda_e, \lambda_\mu, \lambda_\tau\right), \tag{5.4}$$

[1]The implication of linear seesaw can be found in [39].

where the VEVs of the scalar fields are given as

$$v = \langle H \rangle, \quad v_T = \langle \phi_T \rangle \ . \tag{5.5}$$

For linear seesaw mechanism, the Lagrangian involved in the generation of the mass matrices for an A_4 flavor symmetric framework can be written as

$$-\mathcal{L}_\nu = \mathcal{L}_{\nu N} + \mathcal{L}_{NS} + \mathcal{L}_{\nu S} \ , \tag{5.6}$$

where

$$\mathcal{L}_{\nu N} = y_1 \overline{L} \widetilde{H} N_R \frac{\rho'}{\Lambda} \ , \tag{5.7}$$

$$\mathcal{L}_{\nu S} = y_2 \overline{L} \widetilde{H} S_R \frac{\rho}{\Lambda} \ , \tag{5.8}$$

$$\mathcal{L}_{NS} = \left(\lambda^{\phi}_{NS} \phi_s + \lambda^{\xi}_{NS} \xi + \lambda^{\xi'}_{NS} \xi' \right) \overline{N_R} S^c_R \ . \tag{5.9}$$

It should be noted that the terms $\mathcal{L}_{\nu N}$, $\mathcal{L}_{\nu S}$ and $\mathcal{L}_{NS}$ represent the contributions for Dirac neutrino mass connecting $\nu_L - N_R$, $\nu_L - S_R$ mixing and $N_R - S^c_R$ mixing terms. If one looks at the mass formula for light neutrinos governed by linear seesaw mechanism given in Eq. (5.3), one can use the mass hierarchy as $m_{RS} \gg m_D, m_{LS}$. That is the reason why we forbid $\overline{\nu} N$ and $\overline{\nu} S$ terms at tree level and generate them by dimension five operator, while the heavy mixing term $N - S$ is generated at tree level.
Using the following vevs for the scalar and flavon fields

$$\langle \phi_S \rangle = v_S(1,1,1), \quad \langle \xi \rangle = v_\xi, \ \langle \xi' \rangle = v_{\xi'}, \quad \langle \rho \rangle = v_\rho, \quad \langle \rho' \rangle = v_{\rho'} \ ,$$

the various mass matrices are found to be

$$m_{\rm D} = y_1 v \frac{v_{\rho'}}{\Lambda} \begin{pmatrix} 1 & 0 & 0 \\ 0 & 0 & 1 \\ 0 & 1 & 0 \end{pmatrix} \ , \tag{5.10}$$

$$m_{\rm LS} = y_2 v \frac{v_\rho}{\Lambda} \begin{pmatrix} 1 & 0 & 0 \\ 0 & 0 & 1 \\ 0 & 1 & 0 \end{pmatrix},$$

$$m_{RS} = \frac{a}{3} \begin{pmatrix} 2 & -1 & -1 \\ -1 & 2 & -1 \\ -1 & -1 & 2 \end{pmatrix} + b \begin{pmatrix} 1 & 0 & 0 \\ 0 & 0 & 1 \\ 0 & 1 & 0 \end{pmatrix} + d \begin{pmatrix} 0 & 0 & 1 \\ 0 & 1 & 0 \\ 1 & 0 & 0 \end{pmatrix}, \tag{5.11}$$

where $a = \lambda^{\phi}_{NS} v_S$, $b = \lambda^{\xi}_{NS} v_\xi$ and $d = \lambda^{\xi'}_{NS} v_{\xi'}$.

The first term in Eq. (5.11) comes from $\lambda_1\phi_s\left(\overline{N_R}S_R^c\right)_{3s}$, where $\left(\overline{N_R}S_R^c\right)_{3s}$ is a triplet which is symmetric under exchange of N_R and S_R. The product of two triplets can also form a triplet which is antisymmetric under the exchange of the particles. In linear seesaw, the mass of the light neutrino is represented as $m_\nu = m_{\rm D}m_{\rm RS}^{-1}m_{\rm LS}^T$+transpose, and as seen from Eq. (5.10) the mass matrices $m_{\rm D}$ and $m_{\rm LS}$ are symmetric and are related as $m_{\rm D} \propto m_{\rm LS}$. Hence, in $m_\nu = m_{\rm D}^T(m_{\rm RS}^{-1} + m_{\rm RS}^{-1^T})m_{\rm LS}$, the antisymmetric part cancels out and only symmetric part survives.

5.4 Neutrino Masses and Mixing

For calculational convenience one can rewrite the $m_{\rm RS}$ mass matrix (5.11) as

$$m_{RS} = \begin{pmatrix} 2a/3+b & -a/3 & -a/3 \\ -a/3 & 2a/3 & -a/3+b \\ -a/3 & -a/3+b & 2a/3 \end{pmatrix} + \begin{pmatrix} 0 & 0 & d \\ 0 & d & 0 \\ d & 0 & 0 \end{pmatrix}. \tag{5.12}$$

Thus, with Eqs. (5.3), (5.10) and (5.11), one can obtain the the light neutrino mass

$$\begin{aligned} m_\nu &= m_{\rm D}m_{RS}^{-1}m_{\rm LS}^T + \text{transpose} \\ &= k_1k_2\begin{pmatrix} 1 & 0 & 0 \\ 0 & 0 & 1 \\ 0 & 1 & 0 \end{pmatrix} m_{RS}^{-1} \begin{pmatrix} 1 & 0 & 0 \\ 0 & 0 & 1 \\ 0 & 1 & 0 \end{pmatrix}, \end{aligned} \tag{5.13}$$

where the parameters k_1 and k_2 are related to the vevs through

$$k_1 = \sqrt{2}y_1 v\frac{v_{\rho'}}{\Lambda}\,, \qquad k_2 = \sqrt{2}y_2 v\frac{v_\rho}{\Lambda}.$$

Hence, the inverse of light neutrino mass matrix is given by

$$m_\nu^{-1} = \frac{1}{k_1k_2}\begin{pmatrix} 2a/3+b & -a/3 & -a/3 \\ -a/3 & 2a/3 & -a/3+b \\ -a/3 & -a/3+b & 2a/3 \end{pmatrix} + \frac{1}{k_1k_2}\begin{pmatrix} 0 & d & 0 \\ d & 0 & 0 \\ 0 & 0 & d \end{pmatrix}, \tag{5.14}$$

which in TBM basis will have the form, i.e., $m_\nu^{-1'} = U_{\rm TBM}^T m_\nu^{-1} U_{\rm TBM}$,

$$m_\nu^{-1'} = \begin{pmatrix} a+b-d/2 & 0 & -\frac{\sqrt{3}}{2}d \\ 0 & b+d & 0 \\ -\frac{\sqrt{3}}{2}d & 1 & a-b+d/2 \end{pmatrix}. \tag{5.15}$$

The inverse mass matrix $m_\nu^{-1'}$ can be diagonalized by U_{13}^*. Hence, the matrix m_ν^{-1} can be diagonalized by $U_{TBM} \cdot U_{13}^*$, and thus, the matrix m_ν can be diagonalized by $U_{TBM} \cdot U_{13}$, while m_{RS} by $U_{TBM} \cdot U_{13}^T$. The complex unitary matrix U_{13} has the form

$$U_{13} = \begin{pmatrix} \cos\theta & 0 & \sin\theta e^{-i\psi} \\ 0 & 1 & 0 \\ -\sin\theta e^{i\psi} & 0 & \cos\theta \end{pmatrix}, \tag{5.16}$$

where the parameters θ and ψ are expressed in terms of the mass matrix parameters $d/b = \lambda_1 e^{\phi_{db}}$, $a/b = \lambda_2 e^{\phi_{ab}}$ as

$$\tan 2\theta = -\frac{\sqrt{3}\lambda_1 \cos\phi_{db}}{(\lambda_1 \cos\phi_{db} - 2)\cos\psi + (2\lambda_2 \sin\phi_{ab})\sin\psi} , \tag{5.17}$$

and

$$\tan\psi = \frac{\sin\phi_{db}}{\lambda_2 \cos(\phi_{ab} - \phi_{db})} . \tag{5.18}$$

The eigenvalues of m_ν and m_{RS} are related to each other as

$$\tilde{m}_i = \frac{k_1 k_2}{\tilde{M}_i} . \tag{5.19}$$

where $\tilde{m}_i$ and $\tilde{M}_i$ are i^{th} eigenvalues of m_ν and m_{RS} respectively. The eigenvalues of m_{RS} can be expressed as

$$\begin{aligned} \tilde{M}_1 &= b\left[\lambda_2 e^{i\phi_{ab}} - \sqrt{1 + \lambda_1^2 e^{2i\phi_{db}} - \lambda_1 e^{i\phi_{db}}}\right], \\ \tilde{M}_2 &= b\left[1 + \lambda_1 e^{i\phi_{db}}\right], \\ \tilde{M}_3 &= b\left[\lambda_2 e^{i\phi_{ab}} + \sqrt{1 + \lambda_1^2 e^{2i\phi_{db}} - \lambda_1 e^{i\phi_{db}}}\right], \end{aligned} \tag{5.20}$$

which give the mass of the heavy neutrinos as $M_i = |\tilde{M}_i|$. Explicitly, one can write the heavy neutrino masses as

$$\begin{aligned} M_1 &= |b| M_1' = |b| \left[(\lambda_2 \cos\phi_{ab} - C)^2 + (\lambda_2 \sin\phi_{ab} - D)^2\right]^{1/2}, \\ M_2 &= |b| M_2' = |b| \left[1 + \lambda_1^2 + 2\lambda_1 \cos\phi_{db}\right]^{1/2}, \\ M_3 &= |b| M_3' = |b| \left[(\lambda_2 \cos\phi_{ab} + C)^2 + (\lambda_2 \sin\phi_{ab} + D)^2\right]^{1/2} , \end{aligned} \tag{5.21}$$

where

$$\begin{aligned} C &= \pm\left[\frac{A+\sqrt{A^2+B^2}}{2}\right]^{1/2}, \qquad D = \pm\left[\frac{-A+\sqrt{A^2+B^2}}{2}\right]^{1/2}, \\ A &= 1+\lambda_1^2\cos 2\phi_{db}-\lambda_1\cos\phi_{db}\,, \quad B = \lambda_1^2\sin 2\phi_{db}-\lambda\sin\phi_{db}\,, \end{aligned} \tag{5.22}$$

and the phases ϕ_is as

$$\begin{aligned} \phi_1 &= \tan^{-1}\left[\frac{\lambda_2\sin\phi_{ab}-D}{\lambda_2\sin\phi_{ab}-C}\right], \\ \phi_2 &= \tan^{-1}\left[\frac{\lambda_1\sin\phi_{db}}{1+\lambda_1\cos\phi_{db}}\right], \\ \phi_3 &= \tan^{-1}\left[\frac{\lambda_2\sin\phi_{ab}+D}{\lambda_2\sin\phi_{ab}+C}\right]. \end{aligned} \tag{5.23}$$

Thus, the active neutrino masses $m_i = |\tilde{m}_i|$ and the matrix which diagonalizes active neutrino mass matrix U_ν, are given by

$$\begin{aligned} m_i &= \frac{|k_1 k_2|}{M_i}, \\ U_\nu &= U_{TBM}\cdot U_{13}\cdot P\,, \end{aligned} \tag{5.24}$$

with $P = \mathrm{diag}(e^{-i\phi_1/2}, e^{-i\phi_2/2}, e^{-i\phi_3/2})$.
The lepton mixing matrix, known as PMNS matrix is given by [123, 48]

$$U_{PMNS} = U_l^\dagger\cdot U_\nu\,, \tag{5.25}$$

where U_l and U_ν are the matrices which diagonalize charged lepton and neutrino mass matrices. Here $U_l = I$ and $U_\nu = U_{TBM}\cdot U_{13}\cdot P$, hence,

$$U_{PMNS} = U_{TBM}\cdot U_{13}\cdot P, \tag{5.26}$$

which is proved to be in good agreement with the experimental observations [91, 124]. The PMNS matrix can be parameterized in terms of three mixing angles (θ_{13}, θ_{23} and θ_{12}) and three phases (one Dirac phase δ_{CP}, and two Majorana phases ρ and σ) as

$$U_{\rm PMNS} = \begin{pmatrix} c_{12}c_{13} & s_{12}c_{13} & s_{13}e^{-i\delta_{CP}} \\ -s_{12}c_{23}-c_{12}s_{13}s_{23}e^{i\delta_{CP}} & c_{12}c_{23}-s_{12}s_{13}s_{23}e^{i\delta_{CP}} & c_{13}s_{23} \\ s_{12}s_{23}-c_{12}s_{13}c_{23}e^{i\delta_{CP}} & -c_{12}s_{23}-s_{12}s_{13}c_{23}e^{i\delta_{CP}} & c_{13}c_{23} \end{pmatrix} P_\nu\,, \tag{5.27}$$

where $c_{ij} = \cos\theta_{ij}$ and $s_{ij} = \sin\theta_{ij}$ and $P_\nu = \text{diag}(e^{i\rho}, e^{i\sigma}, 1)$. From Eqs. (5.26) and (5.27), one can find

$$\begin{aligned}
\sin\theta &= \sqrt{\frac{3}{2}}\sin\theta_{13} \\
\sin\delta_{\rm CP} &= -\frac{\sin\psi}{\sqrt{1 - \dfrac{3(2-3\sin^2\theta_{13})}{(1-\sin^2\theta_{13})^2}\sin^2\theta_{13}\cos^2\psi}} \approx -\sin\psi\ .
\end{aligned} \tag{5.28}$$

The above expressions relate the parameters of the model, i.e., θ and ψ to the mixing observables $\sin^2\theta_{13}$ and δ_{CP} respectively. Since $\sin^2\theta_{13}$ is known more precisely than $\delta_{\rm CP}$, in our calculation we fix θ by fixing $\sin^2\theta_{13}$ at its best fit value while considering all possible value of ψ for which $\delta_{\rm CP}$ falls within its 3σ experimental range.

5.5 Numerical results

Using Eqs. (5.19) and (5.21), the light neutrino masses are found to be

$$m_i = \frac{|k_1 k_2|}{M_i} = \frac{|k_1 k_2|}{|b|}\frac{1}{M_i'}\ . \tag{5.29}$$

Since only the mass squared differences, Δm^2_{21} (solar mass squared difference) and $|\Delta m^2_{32}|$ (atmospheric mass squared difference) are measured in neutrino oscillation experiments, we calculate the mass squared differences from Eq. (5.29) as

$$\begin{aligned}
\Delta m^2_{21} &= \left|\frac{k_1 k_2}{b}\right|^2 \left(\frac{1}{M_2'^2} - \frac{1}{M_1'^2}\right)\ , \\
\left|\Delta m^2_{31}\right| &= \left|\frac{k_1 k_2}{b}\right|^2 \left|\left(\frac{1}{M_3'^2} - \frac{1}{M_1'^2}\right)\right|\ .
\end{aligned} \tag{5.30}$$

Substituting the set of Eqs. (5.21) in the above equations, we find the ratio of the two mass squared differences as

$$\begin{aligned}
r &= \frac{\Delta m^2_{21}}{|\Delta m^2_{31}|} = \left[\frac{(\lambda_2\cos\phi_{ab} + C)^2 + (\lambda_2\sin\phi_{ab} + D)^2}{1 + \lambda_1^2 + 2\lambda_1\cos\phi_{db}}\right] \\
&\times \left[\frac{(\lambda_2\cos\phi_{ab} - C)^2 + (\lambda_2\sin\phi_{ab} - D)^2 - (1 + \lambda_1^2 + 2\lambda_1\cos\phi_{db})}{4\lambda_2|C\cos\phi_{ab} + D\sin\phi_{ab}|}\right]\ .
\end{aligned} \tag{5.31}$$

Now using equations (5.17), (5.18), (5.21), (5.22) and 5.31, and by fixing the parameters ϕ_{db}, ψ and θ, one can find numerical values of M_i''s. Once M_i''s are known $\left|\dfrac{k_1 k_2}{b}\right|$ can be

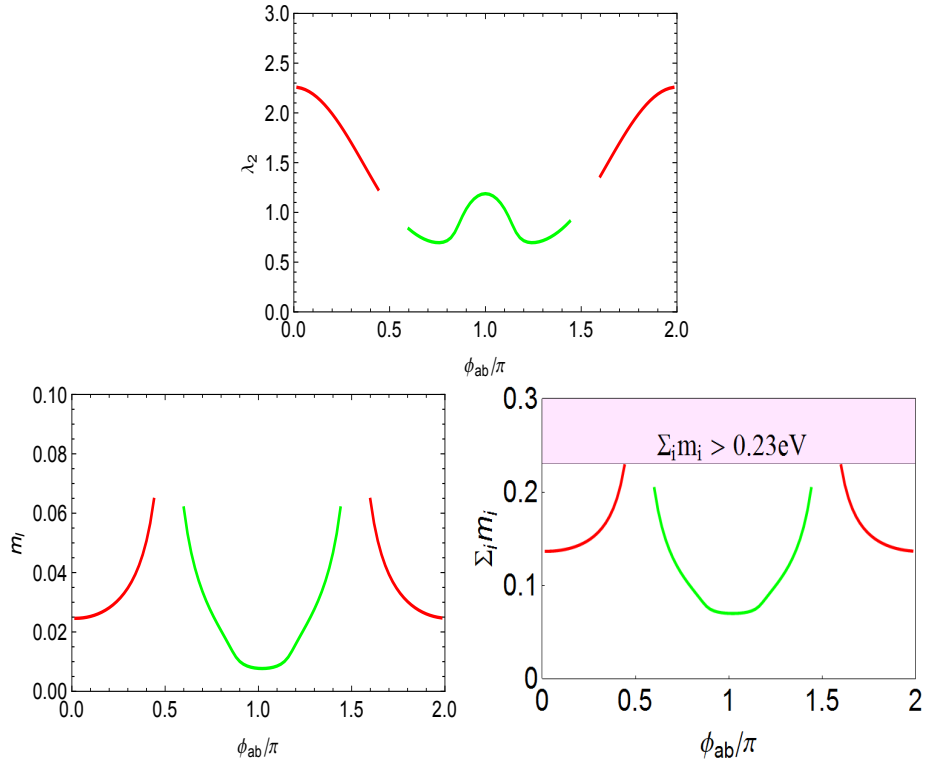

Figure 5.1: Variation of λ_2, the lightest neutrino mass (m_l) and $\Sigma_i m_i$ with ϕ_{ab}, red lines are for inverted hierarchy and green lines are for normal hierarchy.

calculated from (5.30) as

$$\left|\frac{k_1 k_2}{b}\right| = \sqrt{\frac{\Delta m^2_{21}}{\left(\frac{1}{M_2'^2} - \frac{1}{M_1'^2}\right)}} = \sqrt{\left|\frac{\Delta m^2_{31}}{\left(\frac{1}{M_3'^2} - \frac{1}{M_1'^2}\right)}\right|}\,, \tag{5.32}$$

which will also give the absolute value of light neutrino masses as all the quantities on the right hand side of (5.29) are now known.

We now rewrite the expression $\tan\psi$ (5.18) in terms of ϕ_{db} as

$$\phi_{db} = 0, \pi, \quad \text{for } \tan\psi = 0\,, \tag{5.33}$$

and

$$\phi_{ab} = \phi_{db} + \cos^{-1}\left(\frac{\sin\phi_{db}}{\lambda_2 \tan\psi}\right), \quad \text{for } \tan\psi \neq 0, \tag{5.34}$$

and consider the following cases to see the implications.

5.5.1 Correlation between model parameters with $\tan\psi = 0$

In this case ϕ_{db} will be either 0 or π, and for $\phi_{db} = 0$ one can obtain from Eq. (5.17)

$$\lambda_1 = \frac{2\tan 2\theta}{\sqrt{3} + \tan 2\theta} \,, \tag{5.35}$$

and the ratio of the mass square differences r satisfies the relation

$$r = 0.03 = \left[\frac{\lambda_2^2 + 2\lambda_2 C\cos\phi_{ab} + C^2}{(1+\lambda_1)^2}\right]\left[\frac{\lambda_2^2 - 2\lambda_2 C\cos\phi_{ab} + C^2 - (1+\lambda_1)^2}{4\lambda_2|C\cos\phi_{ab}|}\right], \tag{5.36}$$

where $C = \sqrt{\frac{1-\lambda_1+\lambda_1^2}{2}}$. The eigenvalues of m_{RS} in this case become

$$\begin{aligned} M_1 &= |b|\sqrt{\lambda_2^2 - 2\lambda_2 C\cos\phi_{ab} + C^2} \,, \\ M_2 &= |b|(1+\lambda_1) \,, \\ M_3 &= |b|\sqrt{\lambda_2^2 + 2\lambda_2 C\cos\phi_{ab} + C^2} \,. \end{aligned} \tag{5.37}$$

Now from Eq. (5.36), using the measured values of r (0.03), variation of the parameter λ_2, the lightest neutrino mass (m_l) and the sum of active neutrino masses $\sum m_i$ with ϕ_{ab} are shown in Fig. 5.1.

While for $\phi_{db} = \pi$

$$\lambda_1 = \frac{2\tan 2\theta}{\sqrt{3} - \tan 2\theta} \,, \tag{5.38}$$

and the ratio of the mass square differences r satisfies the relation

$$r = 0.03 = \left[\frac{\lambda_2^2 + 2\lambda_2 C\cos\phi_{ab} + C^2}{(1-\lambda_1)^2}\right]\left[\frac{\lambda_2^2 - 2\lambda_2 C\cos\phi_{ab} + C^2 - (1-\lambda_1)^2}{4\lambda_2|C\cos\phi_{ab}|}\right], \tag{5.39}$$

with $C = \sqrt{\frac{1+\lambda_1+\lambda_1^2}{2}}$, and the eigenvalues of m_{RS} are given as

$$\begin{aligned} M_1 &= |b|\sqrt{\lambda_2^2 - 2\lambda_2 C\cos\phi_{ab} + C^2} \,, \\ M_2 &= |b|(1-\lambda_1) \,, \\ M_3 &= |b|\sqrt{\lambda_2^2 + 2\lambda_2 C\cos\phi_{ab} + C^2} \,. \end{aligned} \tag{5.40}$$

Analogous to Fig. 5.1, the variation of various parameters with ϕ_{ab} is shown in Fig. 5.2. From the plots it can be seen that for normal ordering, the allowed parameter space is severely constrained.

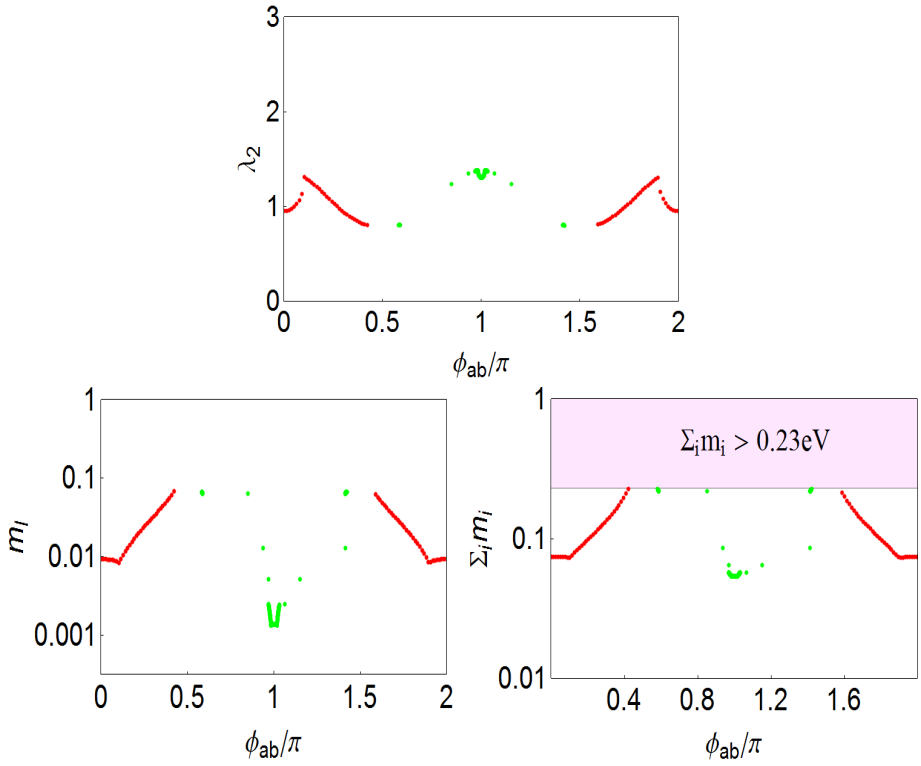

Figure 5.2: Variation of λ_2, m_l and $\Sigma_i m_i$ with ϕ_{ab}, red points are for inverted hierarchy and green points are for normal hierarchy.

5.5.2 Correlation between model parameters with $\tan\psi \neq 0$.

With $\tan\psi \neq 0$, the analytic expression for λ_1 is given by

$$\lambda_1 = \frac{2\lambda_2 \tan 2\theta \cos\phi_{ab} \sin\psi}{\sin\phi_{ab}\left[\sqrt{3} + \tan 2\theta \cos\psi\right]} \,. \tag{5.41}$$

We obtain the correlation plots between various parameters as given in Fig. 5.3 and Fig. 5.4, by varying ϕ_{db} between 0 to 2π and δ_{CP} in its 3σ range $(0 - 0.17\pi) \oplus (0.76\pi - 2\pi)$ while fixing $\sin^2\theta_{13}$ at its best fit value [125].

Comment on Neutrinoless double beta decay: The experimental observation of neutrinoless double beta decay would not only ascertain the Lepton Number Violation (LNV) in nature but it can also give absolute scale of lightest active neutrino mass. The experimental non-observation of such a event puts a bound on half-life of this process on various isotopes which can be translated as a bound on particle physics parameter called as Effective Majorana Mass. In the linear seesaw model, the light Majorana neutrinos contribute to neutrinoless double beta decay while the heavy pseudo-Dirac neutrinos give suppressed contribution.

The measure of LNV can be understood with the key parameter called Effective Majorana

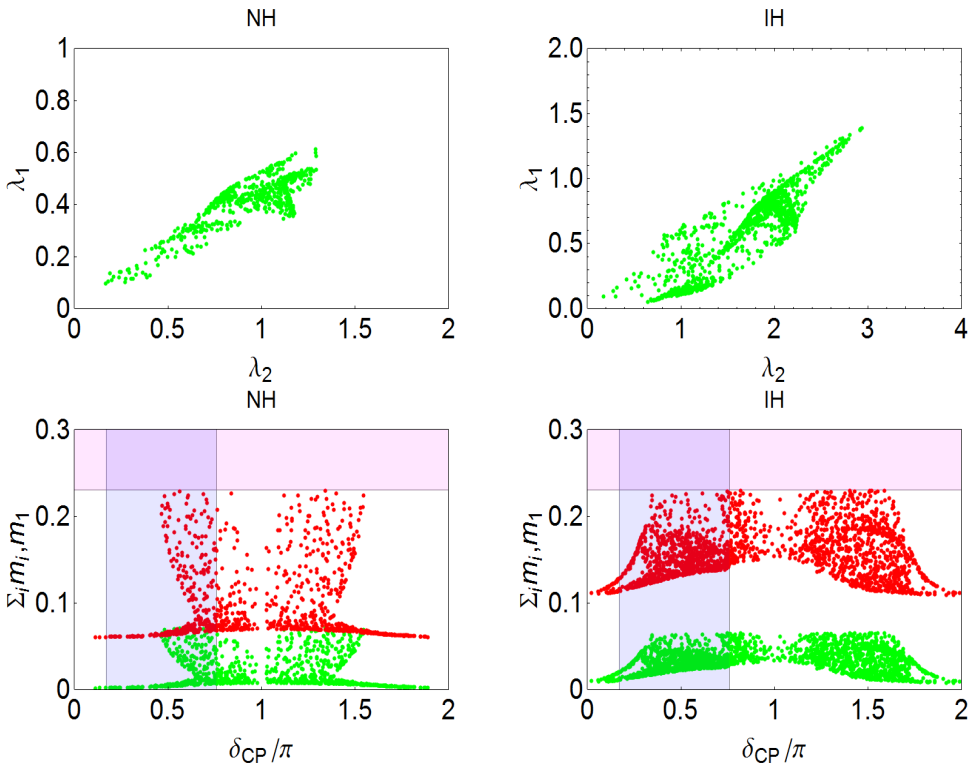

Figure 5.3: Correlation plots between λ_1 and λ_2 for normal hierarchy (top left panel), for inverted hierarchy (top right panel) and between $\Sigma_i m_i$, m_i and δ_{CP} in the bottom left (right) panel for normal (inverted) hierarchy. The vertical and horizontal bands represents the values of δ_{CP} beyond its 3σ range and $\Sigma_i m_i > 0.23$ eV, the upper bound on sum of active neutrino masses given by Planck data, respectively.

Mass which is defined as

$$|M_{ee}| \equiv |m^{\nu}_{ee}| \quad = \quad \left| U^2_{e1}\, m_1 + U^2_{e2}\, m_2 e^{i\rho} + U^2_{e3}\, m_3 e^{i\sigma} \right|. \tag{5.42a}$$

The light neutrino mass eigenvalues m_1, m_2, m_3 depend on input model parameters. These input model parameters are constrained to their allowed range in order to satisfy the oscillation data giving correct values of mass-squared differences and mixing. The Majorana phases ρ and σ are related to ϕ_{ab} and ϕ_{db} in some way and thus, they are constrained to take limited value. The element of PMNS mixing matrix derived from the knowledge of tribimaximal mixing multiplied by rotation matrix in 13 plane. The estimation of Effective Majorana mass parameter using these already constrained input model parameters with the variation of lightest neutrino mass in displayed in Fig. 5.5 where left-panel is for NH and right-panel is for IH pattern of light neutrino masses.

The current limit on half-life (or translated bound on effective Majorana Mass parameter m^{ν}_{ee}) from GERDA Phase-I [126] is $T^{0\nu}_{1/2}(^{76}\mathrm{Ge}) > 2.3 \times 10^{25}$ yr implies $|m_{ee}| \leq 0.21\,\mathrm{eV}$ and from KamLAND-Zen [127] as $T^{0\nu}_{1/2}(^{136}\mathrm{Xe}) > 1.07 \times 10^{26}$ yr implies $|m_{ee}| \leq 0.15\,\mathrm{eV}$.

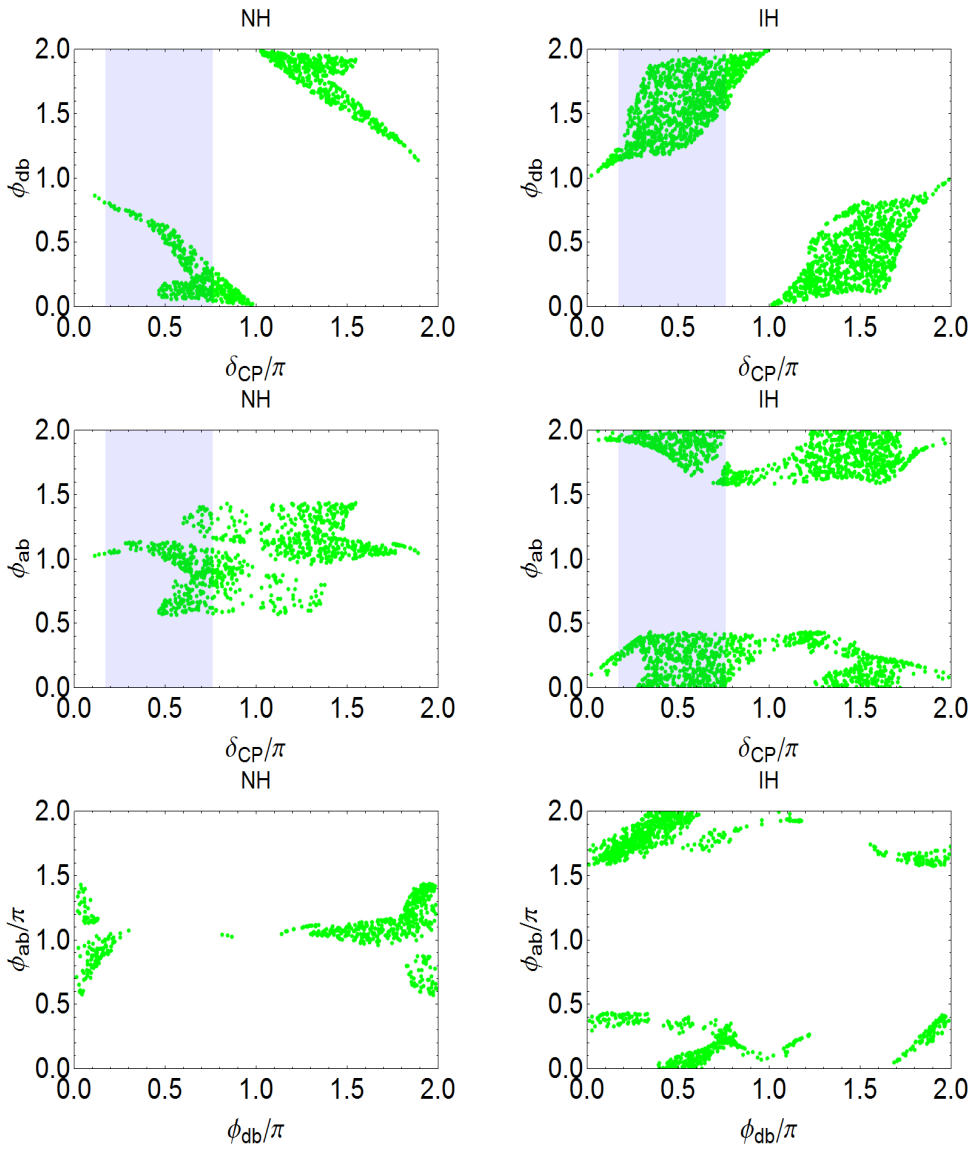

Figure 5.4: Correlation plots between ϕ_{db}, ϕ_{ab} and δ_{CP} for normal (left panel) and inverted (right panel) hierarchy. The vertical band represents the values of δ_{CP} beyond its 3σ range.

There is also bound from CUORE experiment on effective Majorana mass parameter as $|m_{ee}| \leq 0.073\,\text{eV}$ [128]. The expected reach of the future planned $0\nu\beta\beta$ experiments including nEXO experiment gives $T^{0\nu}_{1/2}(^{136}\text{Xe}) \approx 6.6 \times 10^{27}$ yr [129]. The variation of effective mass parameter in green points with lightest neutrino mass is shown in Fig. 5.5 for $\tan\psi = 0$ and the same is plotted in Fig. 5.6 for $\tan\psi \neq 0$. The left-panel is for NH pattern and right-panel is for IH pattern of light neutrino masses. The horizontal lines represent the bounds on Effective Majorana mass from various neutrinoless double beta decay experiments while the vertical shaded region are disfavoured from Planck data. The present bound is $m_\Sigma < 0.23$ eV from Planck+WP+highL+BAO data (Planck1) at 95% C.L. and $m_\Sigma < 1.08$ eV from Planck+WP+highL (Planck2) at 95% C.L. [15, 130].

This plot shows that quasi-degenerate pattern of light neutrinos are disfavoured if we consider

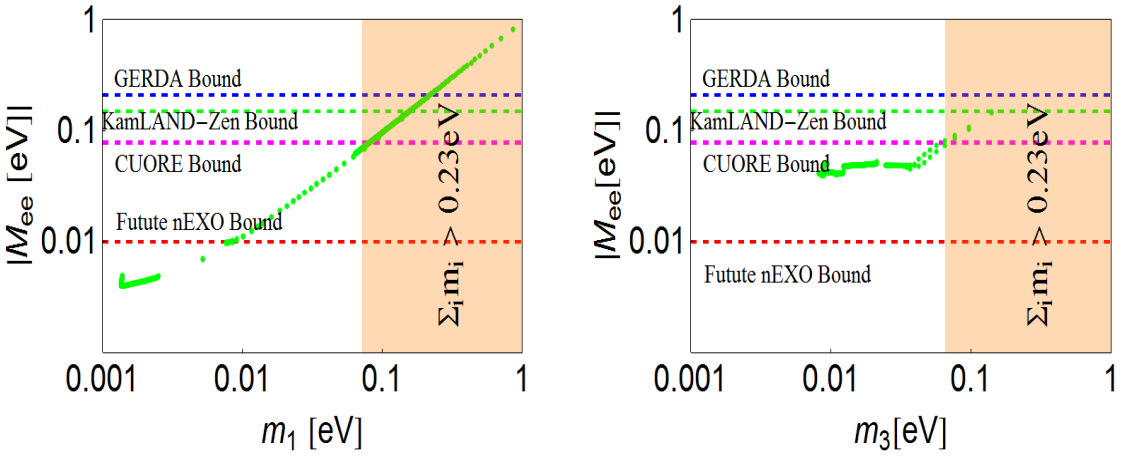

Figure 5.5: Variation of Majorana parameter M_{ee} which is an observable in neutrino less double beta decay with lightest neutrino mass for the case of normal(left panel) and inverted hierarchy(right panel) for $\tan\psi = 0$.

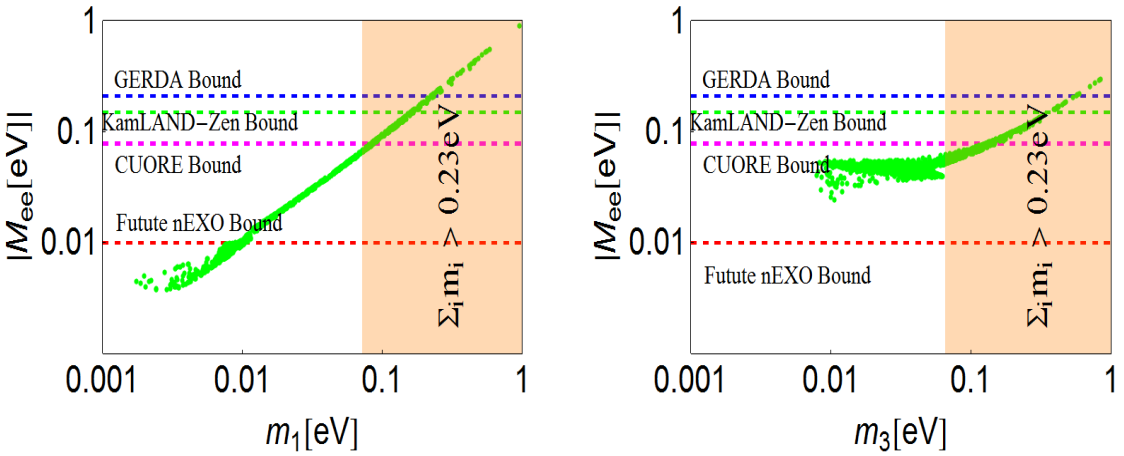

Figure 5.6: Variation of effective Majorana parameter M_{ee} which is a measure of lepton number violation with lightest neutrino mass for the case of normal (left panel) and inverted hierarchy (right panel) for $\tan\psi \neq 0$.

the bound on sum of light neutrino masses from cosmology. The current bound on Effective mass parameters from GERDA Phase-I and KamLAND-Zen proves that NH and IH pattern of light neutrinos are not sensitive. However, the future planned nEXO experiment is sensitive to both pattern of light neutrinos.

5.6 Leptogenesis

It is well known that leptogenesis is one of the most elegant frameworks for dynamically generating the observed baryon asymmetry of the Universe. In the resonance leptogenesis scenarios, since the mass difference between two or more heavy neutrinos is much smaller than their masses and comparable to their widths, the CP asymmetry in their decays occurs

primarily through self-energy effects (ϵ-type) rather than vertex effect (ϵ'-type) and gets resonantly enhanced. In the present A_4 realization, since the mass splitting between the two heavy neutrinos is rather tiny, it provides the opportunity for resonant leptogenesis, which will be discussed in this section.

During the calculation of light neutrino masses and mixing, we have neglected the higher order terms in the Lagrangian $\mathcal{L}_\nu$ as displayed in Eq. (5.6), which are given with extra dimension six operators as follows

$$-\left\{\left[\lambda_{N\phi}\phi_S+\lambda_{N\xi}\xi+\lambda_{N\xi'}\xi'\right]\frac{\rho\rho'}{\Lambda^2}\overline{N}_R N^c_R+\left[\lambda_{S\phi}\phi^\dagger_S+\lambda_{S\xi}\psi^\dagger+\lambda_{S\xi'}\xi'^\dagger\right]\frac{\rho\rho'^\dagger}{\Lambda^2}\overline{S}_R S^c_R\right\}, \quad (5.43)$$

as these extra terms do not make much difference in those calculations, but they make tiny mass splitting in doubly degenerate mass states of heavy neutrinos. Including these additional terms, the Majorana mass matrix $\mathbb{M}_2$ becomes

$$\mathbb{M}_2=\begin{pmatrix} m_R & m_{RS} \\ m^T_{RS} & m_S \end{pmatrix}, \quad (5.44)$$

where

$$\begin{aligned} m_R &= \frac{v_\rho v_{\rho'}}{\Lambda^2}\begin{pmatrix} \frac{2}{3}\lambda_{N\phi}v_S+\lambda_{N\xi}v_\xi & -\frac{1}{3}\lambda_{N\phi}v_S & -\frac{1}{3}\lambda_{N\phi}v_S \\ -\frac{1}{3}\lambda_{N\phi}v_S & \frac{2}{3}\lambda_{N\phi}v_S & -\frac{1}{3}\lambda_{N\phi}v_S+\lambda_{N\xi}v_\xi \\ -\frac{1}{3}\lambda_{N\phi}v_S & -\frac{1}{3}\lambda_{N\phi}v_S+\lambda_{N\xi}v_\xi & \frac{2}{3}\lambda_{N\phi}v_S \end{pmatrix} \\ &+ \frac{v_\rho v_{\rho'}}{\Lambda^2}\begin{pmatrix} 0 & 0 & \lambda_{N\xi'}v_{\xi'} \\ 0 & \lambda_{N\xi'}v_{\xi'} & 0 \\ \lambda_{N\xi'}v_{\xi'} & 0 & 0 \end{pmatrix}, \end{aligned}$$

and

$$\begin{aligned} m_S &= \frac{v_\rho v_{\rho'}}{\Lambda^2}\begin{pmatrix} \frac{2}{3}\lambda_{S\phi}v_S+\lambda_{S\xi}v_\xi & -\frac{1}{3}\lambda_{S\phi}v_S & -\frac{1}{3}\lambda_{S\phi}v_S \\ -\frac{1}{3}\lambda_{S\phi}v_S & \frac{2}{3}\lambda_{S\phi}v_S & -\frac{1}{3}\lambda_{S\phi}v_S+\lambda_{S\xi}v_\xi \\ -\frac{1}{3}\lambda_{S\phi}v_S & -\frac{1}{3}\lambda_{S\phi}v_S+\lambda_{S\xi}v_\xi & \frac{2}{3}\lambda_{S\phi}v_S \end{pmatrix} \\ &+ \frac{v_\rho v_{\rho'}}{\Lambda^2}\begin{pmatrix} 0 & 0 & \lambda_{S\xi'}v_{\xi'} \\ 0 & \lambda_{S\xi'}v_{\xi'} & 0 \\ \lambda_{S\xi'}v_{\xi'} & 0 & 0 \end{pmatrix}. \end{aligned} \quad (5.45)$$

The mass matrix $\mathbb{M}_2$ can be approximately block diagonalized by the unitary matrix $\frac{1}{\sqrt{2}}\begin{pmatrix} I & -I \\ I & I \end{pmatrix}$

and becomes

$$\begin{aligned}\mathbb{M}_2' &= \begin{pmatrix} m_{RS}+\dfrac{m_R+m_S}{2} & m_S-m_R \\ m_S-m_R & -m_{RS}+\dfrac{m_R+m_S}{2} \end{pmatrix} \\ &\approx \begin{pmatrix} m_{RS}+\dfrac{m_R+m_S}{2} & 0 \\ 0 & -m_{RS}+\dfrac{m_R+m_S}{2} \end{pmatrix}, \end{aligned} \tag{5.46}$$

with eigenvalues

$$\begin{aligned} M_1'^{\pm} &\approx M_1\left(1\pm\frac{v_\rho v_{\rho'}}{\Lambda^2}\frac{m_1'}{M_1}\right), \\ M_2'^{\pm} &\approx M_2\left(1\pm\frac{v_\rho v_{\rho'}}{\Lambda^2}\frac{m_2'}{M_2}\right), \\ M_3'^{\pm} &\approx M_3\left(1\pm\frac{v_\rho v_{\rho'}}{\Lambda^2}\frac{m_3'}{M_3}\right), \end{aligned} \tag{5.47}$$

where

$$\begin{aligned} m_1' &= 2\mathrm{Re}\left\{\left[a'-\left(\frac{bb'-\frac{1}{2}(bd'+b'd)+dd'}{\sqrt{b^2-bd+d^2}}\right)\right]e^{-i\phi_1}\right\}, \\ m_2' &= 2\mathrm{Re}\left[(b'+d')\,e^{-i\phi_2}\right], \\ m_3' &= 2\mathrm{Re}\left\{\left[a'+\left(\frac{bb'-\frac{1}{2}(bd'+b'd)+dd'}{\sqrt{b^2-bd+d^2}}\right)\right]e^{-i\phi_3}\right\}, \\ a' &= \frac{1}{2}(\lambda_{N\phi}+\lambda_{S\phi})\,v_S, \quad b'=\frac{1}{2}(\lambda_{N\xi}+\lambda_{S\xi})\,v_\xi, \\ d' &= \frac{1}{2}(\lambda_{N\xi'}+\lambda_{S\xi'})\,v_{\xi'}, \end{aligned} \tag{5.48}$$

and ϕ_i is the phase associated with $\tilde{M}_i$. The above set of equations show that m_i' can be of the order of M_i since a, a' are of the order of v_S, b, b' are of the order of v_ξ and d, d' are of the order of $v_{\xi'}$.

The decay of nearly degenerate heavy neutrinos creates lepton asymmetry, and is given as [39]

$$\begin{aligned} \epsilon_{N_i^\pm} = &- \frac{1}{4\pi A_{N_i^\pm}}\left[\left(\frac{\tilde{m}_D}{v}\right)^\dagger\left(\frac{\tilde{m}_D}{v}\right)-\left(\frac{\tilde{m}_{LS}}{v}\right)^\dagger\left(\frac{\tilde{m}_{LS}}{v}\right)\right]_{ii}\mathrm{Im}\left[\frac{\tilde{m}_D^\dagger\tilde{m}_{LS}}{v^2}\right]_{ii} \\ &\times \frac{r_{N_i}}{{r_{N_i}}^2+\dfrac{1}{64\pi^2}{A_{N_i^\pm}}^2}, \end{aligned} \tag{5.49}$$

where

$$A_{N_i^\pm} = \frac{1}{2}\left[\left(\frac{\tilde{m}_D^\dagger}{v} \pm \frac{\tilde{m}_{LS}^\dagger}{v}\right)\left(\frac{\tilde{m}_D}{v} \pm \frac{\tilde{m}_{LS}}{v}\right)\right]_{ii} \tag{5.50}$$

$$r_{N_i} = \frac{M_i'^{+2} - M_i'^{-2}}{M_i'^{+} M_i'^{-}} \approx 4\left(\frac{v_\rho v_{\rho'}}{\Lambda^2}\frac{m_i'}{M_i}\right) ,$$

$$\tilde{m}_D = m_D U_{\rm TBM} U_{13}^T, \quad \tilde{m}_{LS} = m_{LS} U_{\rm TBM} U_{13}^T . \tag{5.51}$$

Since $r_{N_i} \ll A_{N_i^\pm}$, ${r_{N_i}}^2 + \frac{1}{64\pi^2} A_{N_i^\pm}^2 \approx \frac{1}{64\pi^2} A_{N_i^\pm}^2$, for $\tilde{m}_{LS} \ll \tilde{m}_D$

$$\epsilon_{N_i^\pm} \approx -128\pi {\rm Im}\left[\tilde{m}_{LS}^\dagger \tilde{m}_D\right]_{ii} \frac{r_{N_i} v^2}{\left(\tilde{m}_D^\dagger \tilde{m}_D\right)^2} . \tag{5.52}$$

Substituting $\tilde{m}_D^\dagger \tilde{m}_D = |y_1|^2 \left(v v_{\rho'}/\Lambda\right)^2$, $\tilde{m}_D^\dagger \tilde{m}_{LS} = y_1^* y_2 v^2 \left(v_\rho v_{\rho'}/\Lambda^2\right)$ and $r_{N_i} \approx 4\left(v_\rho v_{\rho'}/\Lambda^2\right)\left(m_i'/M_i\right)$ in the above equation, we obtain

$$\epsilon_{N_i^\pm} \approx -512\pi \left(\frac{v_\rho}{v_{\rho'}}\right)^2 \frac{{\rm Im}\left[y_1^* y_2\right]}{|y_1|^4}\frac{m_i'}{M_i} . \tag{5.53}$$

Writing $y_1^* y_2 = |y_1 y_2| e^{i\theta_\epsilon}$, one can have

$$\epsilon_{N_i^\pm} \approx -512\pi \left(\frac{v_\rho}{v_{\rho'}}\right)^2 \frac{|y_2|}{|y_1|^3}\frac{m_i'}{M_i}\sin\theta_\epsilon . \tag{5.54}$$

Here we calculate the baryon asymmetry for the case $M_3 \ll M_2 < M_1$, i.e., normal hierarchy in active neutrino sector. It is mainly the decay of $M_3^\pm$ that contributes to the final baryon asymmetry. Since the decay is in strong wash out region, final baryon asymmetry is given by [39],

$$\eta_B = -\frac{28}{79}\left(\frac{0.3\epsilon_{N_3^\pm}}{g_* K_{N_3^\pm}\left(\ln K_{N_3^\pm}\right)^{0.6}}\right) , \tag{5.55}$$

where $K_{N_i^\pm} = \frac{1}{8\pi}\left(\frac{8\pi^3 g_*}{90}\right)^{-1/2}\left(\frac{M_{Pl}}{M_{N_i^\pm}}\right) A_{N_i^\pm}$, $g_* \approx 106.75$ and $M_{\rm Pl} = 2.435 \times 10^{18}$ GeV are relativistic degrees of freedom of SM particles and Planck mass respectively. Here

$$K_{N_3^\pm} = K_{N_3} \approx 0.234\left[\frac{m_3\ (({\rm eV})}{10^{-2}}\right]\frac{v_{\rho'}}{v_\rho} \gg 1 , \tag{5.56}$$

as m_3 is of the order of 10^{-2} eV and $\frac{v_{\rho'}}{v_\rho} \gg 1$. Substituting $K_{N_3^\pm}$ and $\epsilon_{N_3^\pm}$ in Eq. (5.55) gives

$$\eta_B \approx 0.174 \left(\frac{\left(\frac{m_3(\text{eV})}{10^{-2}}\right)^2}{K_{N_3}^3 (\ln K_{N_3})^{0.6}} \right) \frac{|y_2| m_3'}{|y_1|^3 M_3} \sin\theta_\epsilon \ . \tag{5.57}$$

For $y_1 \approx y_2$ and $\frac{m_3'}{M_3} \approx 1$ the above equation gives

$$\eta_B \leq 0.174 \left(\frac{\left(\frac{m_3(\text{eV})}{10^{-2}}\right)^2}{|y_1|^2 K_{N_3}^3 (\ln K_{N_3})^{0.6}} \right) . \tag{5.58}$$

For $m_1 < 0.005$ eV, $m_3 \approx 0.05$ eV, with this value of m_3, $|y_1|^2 = 10^{-3}$ and $\eta_B = 6.9 \times 10^{-10}$ from (5.56) and (5.58) we found the minimum value of $v_\rho / v_{\rho'}$ requires to generate observed baryon asymmetry as

$$\left. \frac{v_\rho}{v_{\rho'}} \right|_{min} = 5.07 \times 10^{-5} \ . \tag{5.59}$$

Comment on Non-unitarity in leptonic sector:

In usual case, the light active Majorana neutrino mass matrix is diagonalized by the PMNS mixing matrix U_{PMNS} as $U_{\text{PMNS}}^\dagger \, m_\nu \, U_{\text{PMNS}}^* = \text{diag}\,(m_1, m_2, m_3)$ where m_1, m_2, m_3 are mass eigenvalues for light neutrinos. However, the diagonalizing mixing matrix in case of linear seesaw mechanism–where the neutral lepton sector is comprising of light active Majorana neutrinos plus additional two types of right-handed sterile neutrinos is given by

$$\mathcal{N} \simeq (1 - \eta) U_{\text{PMNS}} \, , \tag{5.60}$$

where the non-unitarity effect is parametrized as [131],

$$\eta = \frac{1}{2} m_D^* m_{RS}^{\dagger\,-1} m_{RS}^{-1} m_D^T \ . \tag{5.61}$$

In the linear seesaw framework under consideration, the $N - S$ mixing matrix m_{RS} is symmetric and with $y_1 \approx y_2$, the $\nu - S$ mass term can be expressed as $m_{LS}^\dagger m_{LS} = \frac{1}{2} m_l M_0 (v_\rho / v_{\rho'})$ where m_0 and M_0 are the masses of heaviest active and lightest heavy neutrinos respectively. Thus, the above relation for η can be written in terms of light neutrino mass matrix and other input model parameters as

$$\eta = \frac{m_\nu^* m_\nu^T}{4 m_0 M_0 \frac{v_\rho}{v_{\rho'}}} \ . \tag{5.62}$$

The maximum value of η for inverted mass hierarchy with lightest neutrino mass $m_l \simeq 0.005$ eV while considering the constrained value of the ratio of VEV $(v_\rho / v_{\rho'}) = 5.07 \times 10^{-5}$ as derived from the discussion of leptogenesis and using $M_0 = 5$ TeV can be obtained as

follows

$$|\eta| \approx \frac{1}{2}\begin{bmatrix} 4\times10^{-12} & 10^{-11} & 10^{-11} \\ 10^{-11} & 5\times10^{-11} & 5\times10^{-11} \\ 10^{-11} & 5\times10^{-11} & 5\times10^{-11} \end{bmatrix}. \tag{5.63}$$

Using the representative set of model parameters m_0 and M_0, the mass matrices m_D and m_{LS} are expressed as follows

$$m_D = \sqrt{\frac{M_0 m_0}{v_\rho / v_{\rho'}}}, \quad m_{LS} = \sqrt{\frac{v_\rho}{v_{\rho'}} M_0 m_0}\,. \tag{5.64}$$

Using the constrained value of these model parameters m_0 and M_0, the Dirac neutrino mass connecting $\nu - N$ is found to be $m_D \approx 70$ MeV and the other mass term connecting $\nu - S$ is $m_{LS} \approx 3.5$ keV.

5.7 Summary and Conclusions

Linear seesaw is a fruitful mechanism that generates tiny neutrino mass with prediction of new particles which are light enough to be observed in future experiments. Realization of linear seesaw requires to turn off some of the interactions which are allowed by SM symmetry hence, SM symmetry has to be extended. Considering the success of A_4 symmetry to explain the observed lepton mixing, in this chapter we have considered A_4 realization of linear seesaw to explain the tiny mass of active neutrino as well as the lepton mixing.

The SM symmetry is extended with $A_4 \times Z_4 \times Z_3$ and a global symmetry $U(1)_X$ which is broken explicitly in Higgs potential. In addition to SM fermions, the model has six heavy fermions, three right-handed neutrinos (N_i) and three sterile neutrinos (S_i). We found that each mass state of heavy neutrino is nearly doubly degenerate with a small mass splitting, which can be neglected for the calculation of active neutrino mass and mixing parameters. The mass of active neutrinos are found to be inversely proportional to that of heavy neutrinos. The model predicts lepton mixing matrix i.e., the PMNS as $U_{TBM} \cdot U_{13} \cdot P$, where U_{13} is the rotation in 13 plane and hence, explains well the results on mixing angles and δ_{CP} from oscillation experiments. We obtained the parametric space and correlation plots between various observables by fixing θ_{13} at its best-fit value and the ratio mass squared differences, $\Delta m^2_{21}/\left|\Delta m^2_{13}\right|$ at 0.03 and varying δ_{CP} in its 3σ range.

We have demonstrated that pairs of nearly degenerate Majorana neutrinos in the model opens up the scope to resonant leptogenesis to account for the baryon asymmetry of the universe. We calculated the minimum value of $v_\rho/v_{\rho'}$ to generate observed baryon asymmetry by fixing the mass of lightest heavy neutrino in TeV for the case where heavy neutrino mass are highly

hierarchical so that the only contribution to baryon asymmetry is from the decay of two lightest heavy neutrinos, the parameter space which satisfies this condition predicts normal hierarchy in active neutrino sector with lightest one less than 0.005 eV. In this case the maximum non-unitarity value, the model can accommodate in leptonic sector is very small and is of the order of 10^{-11} and the mass parameters are found to be $m_D \approx 70$ MeV and $m_{LS} \approx 3.5$ keV.

Chapter 6

Summary and Conclusions

On account of many neutrino oscillation experiments, now we have clear idea about most of the oscillation parameters and the future experiments may fix all unknowns. Hence, the structure of neutrino mass matrix can be reconstructed and the mass matrix corresponds to current oscillation parameters is nearly $\mu-\tau$ symmetric. The deviation from $\mu-\tau$ symmetry is due to nonzero θ_{13} and deviation of θ_{23} from $\pi/4$. So the mass matrix can be $\mu-\tau$ symmetric at leading order with the symmetry breaking in higher order corrections to the mass matrix. It is also possible that at high energy there exists a bigger symmetry which breaks to $\mu-\tau$ symmetry at lower energy. Hence, the observed form of lepton mixing matrix can be due to the symmetry between the generations of fermions known as flavor symmetry that exists at high energies. This thesis explores the scope of flavor symmetries to interpret the recent results on neutrino mass and mixing.

The first chapter of this thesis discussed basic properties of neutrinos, standard model of particle physics and neutrino oscillation. The discussions on Higgs mechanism and Weinberg-Salam model explains why neutrino is massless in SM. The current best-fit values and 3σ ranges of oscillation parameters are given in this chapter which show that atleast two of the three active neutrinos are massive hence, hint towards physics beyond SM. An overview of the thesis is given at the end of this chapter.

The second chapter presents various seesaw mechanisms which give the origin of tiny neutrino mass in beyond SM framework. The seesaw mechanisms include Type-I, Type-II, Type-III, linear and inverse seesaw mechanisms. A brief discussion of neutrinoless double beta decay which is a prediction of all the above mentioned seesaw mechanisms, is included in this chapter. The chapter ends with a discussion about some symmetry forms of neutrino mixing patterns such as Tribimaximal mixing (TBM) , Bimaximal mixing (BM), Hexagonal Mixing (HG), Golden ratio A (GRA), and Golden ratio B (GRB) etc, and corresponding mixing matrices.

Possible forms of perturbations to above mentioned standard forms of neutrino mixing patterns and their phenomenological implications are discussed in third chapter. All these forms correspond to $\mu - \tau$ symmetric neutrino mass matrix in charged lepton mass diagonal basis hence, predict vanishing reactor mixing angle ($\theta_{13} = 0$) and maximal atmospheric mixing angle ($\theta_{23} = \frac{\pi}{4}$). But the recent experiments, Daya-Bay, RENO and T2K measured θ_{13} as nonzero. Moreover data from MINOS experiment hints towards deviation of θ_{23} from $\pi/4$. Hence, for being compatible with the experimental observations all these standard forms of neutrino mixing matrices have to be modified by including appropriate perturbations.

The lepton mixing matrix can be represented as $U_{PMNS} = U_l^\dagger U_\nu$, where U_l and U_ν are matrices that diagonalize charged lepton and neutrino mass matrices. Therefore, the deviations in lepton mixing matrix can be initiated from both charged lepton and neutrino sectors. In this chapter, U_l is considered as identity and U_ν as above mentioned symmetry forms at leading order along with perturbations either to U_l or U_ν. The forms of perturbations are taken as rotations in various planes since, such forms have minimum number of independent parameters, one rotation angle and one phase.

In charged lepton sector perturbations are taken as rotation in (12) and (13) planes and similar results are obtained in both cases. The mixing angles obtained for all symmetry forms of U_ν are found to be in good agreement with the experimental results. In these cases limits on Dirac δ_{CP} and Jarlskog invariant J_{CP} are obtained and upper limit J_{CP} is found to be of the order of 10^{-2}.

In neutrino sector perturbations in the form of rotation in (13) and (23) planes are considered. For the case of deviation due to (13) rotation, the mixing angles obtained with TBM, GRA, and GRB forms for U_ν are found to be in good agreement with the experimental results. While in the case of (23) rotation, predictions of TBM and GRB for U_ν are in-line with the experimental results. It is found that in both cases J_{CP} of the order of 10^{-2} is possible.

Whether these findings can be tested in the currently running $NO\nu A$ experiment with 3 years of data taking in neutrino mode followed by 3 years with anti-neutrino mode is inspected in this chapter and predicted value of δ_{CP} is expected to be supported by the data from the experiment.

Chapter 4 of the thesis discusses a model based on A_4 symmetry that gives Co-bimaximal form for lepton mixing matrix at leading order. Co-bimaximal mixing is a modified form of TBM and is given by TBM followed by a rotations in (23) plane. In this model SM symmetry is accompanied by A_4 and a global $U(1)_X$ symmetry. The $U(1)_X$ global symmetry is broken explicitly in Higgs potential which avoids the Goldstone boson that would arise if the symmetry broke spontaneously. Corrections to leading order mixing matrix due to

effective five-dimensional operator in neutrino sector is considered and found that mixing angles obtained are well within the experimental bound.

The model employs Type-I seesaw mechanism to generate tiny neutrino mass thus, one expects neutrino to be of Majorana type. Majorana type neutrinos can mediate neutrino-less double beta decay ($0\nu\beta\beta$), a process where two neutrons inside a nucleus convert into two protons without emitting neutrinos, i.e., $(A, Z) \to (A, Z+2)+2e$. And the half-life of $0\nu\beta\beta$ is proportional to square of $(1, 1)$ element of neutrino mass matrix in flavor basis, i.e., $(|M_{ee}|^2)$. Hence, an upper bound on M_{ee} is obtained from several experiments like KamLAND-Ze, EXO, and GERDA which are searching for $0\nu\beta\beta$ decay. In this regard, the variation of $|M_{ee}|$ with lightest neutrino mass m_1 (m_3) for normal (inverted) hierarchy is studied and found that $|M_{ee}|$ is below the experimental upper limit for all allowed values of lightest neutrino mass.

There are two types of Higgs doublets in the model, one is a singlet under A_4 and gives mass to neutrinos whereas the other one is a triplet under A_4 and gives mass to charged leptons. Hence, there are four Higgs doublets in this model and one of the four linear combinations of Higgs doublets should behave as SM Higgs doublet. The mixing of A_4 singlet Higgs with triplet is found to be negligible. Therefore, the singlet Higgs is in definite mass state while three linear combinations of Higgs triplet form three mass eigenstates. Out of the three mass eigenstates of Higgs triplets one behaves as SM Higgs while the other two contributes to the lepton flavor violating decay $\mu \to e\gamma$. Hence, the branching ratio of $\mu \to e\gamma$ is obtained in the context of the model and found that it is within the limit of the present experimental bound [114].

Chapter 5 talks about A_4 realization of linear seesaw. Linear seesaw mechanism generates tiny neutrino mass without involving very heavy particles. The mass of new particles involved can be of the order of TeV. Realization of linear seesaw requires inclusion of singlet fermions known as sterile neutrinos in addition to right-handed neutrinos. The sterile neutrinos are taken as right-handed hence, denoted by S_R. In this context the neutrino mass matrix in the basis $(\widehat{\nu_l}, N_R, S_R)^T$ is given by

$$M_\nu = \begin{bmatrix} 0 & m_D & m_{LS} \\ m_D^T & M_R & m_{RS} \\ m_{LS}^T & m_{RS}^T & \mu_S \end{bmatrix}.$$

The active neutrinos receive mass through linear seesaw mechanism if $m_{RS} \gg m_D, m_{LS}$ with all off-diagonal elements are vanishingly small. But SM symmetry allows all the elements other than $(1, 1)$ element of M_ν. Hence, in this chapter, extension of SM symmetry with

$A_4 \times Z_4 \times Z_3$ and a global symmetry $U(1)_X$ which is broken explicitly by Higgs potential is considered. In addition to SM Higgs doublet the scalar sector of the model includes the flavons denoted by ϕ_S, ϕ_T, ξ, ξ', ρ and ρ'. Here m_D and m_{LS} arise through effective dimension-five operators while m_{RS} arises from dimension-four terms. Therefore, m_{LS} and m_D are naturally small compared to m_{RS}.

For the chosen representations of fields under $A_4 \times Z_4 \times Z_3 \times U(1)_X$, mass of the active neutrinos are found to be inversely proportional to that of heavy neutrinos and the lepton mixing matrix i.e., U_{PMNS} is obtained as $U_{TBM} \cdot U_{13} \cdot P$, where U_{TBM} is TBM mixing matrix, U_{13} is the rotation in (13) plane and P is a diagonal phase matrix. The mixing matrix of the form $U_{TBM} \cdot U_{13} \cdot P$ is known to be in good agreement with the results of neutrino oscillation experiments. Further, the allowed parameter space and correlation plots between various observables are obtained by fixing θ_{13} at its best-fit value and the ratio of mass squared differences $\Delta m^2_{21}/|\Delta m^2_{13}|$ at 0.03 and varying δ_{CP} in its 3σ range.

In this context effective dimension-six operators generate tiny M_R and μ_s which can be neglected for the calculation of mixing angles and light neutrino masses. Due to non-zero values of diagonal elements M_R and μ_S, each mass eigenstates of heavy neutrinos are nearly doubly degenerate with a small mass split which would otherwise be doubly degenerated. Pairs of nearly degenerate Majorana neutrinos in the model opens up the scope to resonant leptogenesis to account for the baryon asymmetry of the Universe. In this context, the minimum value of ratio of vacuum expectation values of ρ and ρ' $(v_\rho/v_{\rho'})$ to generate observed baryon asymmetry is calculated by fixing the mass of lightest heavy neutrino in TeV range, for the case where heavy neutrino mass are highly hierarchical so that the only contribution to baryon asymmetry is from the decay of two lightest heavy neutrinos. The parameter space which satisfies this condition, predicts normal hierarchy in active neutrino sector with lightest one less than 0.005 eV. In this case the maximum non-unitarity value the model can accommodate in leptonic sector is very small and is of the order of 10^{-11} and the mass parameters m_D and m_{LS} are found to be of the order of 70 MeV and 3.5 KeV respectively. This model has the potential to explain baryon asymmetry of the universe as well as neutrino mass and mixing.

All these results strengthen the idea that the particular values of lepton mixing angles are the outcome of flavor symmetries rather than mere coincidence.

Bibliography

[1] F. Reines and C. L. Cowan, "Detection of the free neutrino," *Phys. Rev.* **92** (Nov, 1953) 830–831.

[2] F. Reines and C. L. Cowan, "Free antineutrino absorption cross section. i. measurement of the free antineutrino absorption cross section by protons," *Phys. Rev.* **113** (Jan, 1959) 273–279.

[3] G. Danby, J.-M. Gaillard, K. Goulianos, L. M. Lederman, N. Mistry, M. Schwartz, and J. Steinberger, "Observation of high-energy neutrino reactions and the existence of two kinds of neutrinos," *Phys. Rev. Lett.* **9** (Jul, 1962) 36–44.

[4] **DONUT** Collaboration, K. Kodama *et al.*, "Observation of tau neutrino interactions," *Phys. Lett.* **B504** (2001) 218–224, `arXiv:hep-ex/0012035 [hep-ex]`.

[5] J. Steinberger, "On the range of the electrons in meson decay," *Phys. Rev.* **75** (Apr, 1949) 1136–1143.

[6] F. Simkovic, R. Dvornicky, and A. Faessler, "Exact relativistic tritium beta-decay endpoint spectrum in a hadron model," *Phys. Rev.* **C77** (2008) 055502, `arXiv:0712.3926 [hep-ph]`.

[7] **Particle Data Group** Collaboration, C. Patrignani *et al.*, "Review of Particle Physics," *Chin. Phys.* **C40** no. 10, (2016) 100001.

[8] **KATRIN** Collaboration, A. Osipowicz *et al.*, "KATRIN: A Next generation tritium beta decay experiment with sub-eV sensitivity for the electron neutrino mass. Letter of intent," `arXiv:hep-ex/0109033 [hep-ex]`.

[9] E. Andreotti *et al.*, "MARE, Microcalorimeter Arrays for a Rhenium Experiment: A detector overview," *Nucl. Instrum. Meth.* **A572** (2007) 208–210.

[10] R. P. Feynman and M. Gell-Mann, "Theory of Fermi interaction," *Phys. Rev.* **109** (1958) 193–198.

[11] C. S. Wu, E. Ambler, R. W. Hayward, D. D. Hoppes, and R. P. Hudson, "Experimental Test of Parity Conservation in Beta Decay," *Phys. Rev.* **105** (1957) 1413–1414.

[12] **Gargamelle Neutrino** Collaboration, F. J. Hasert *et al.*, "Observation of Neutrino Like Interactions without Muon or Electron in the Gargamelle Neutrino Experiment," *Nucl. Phys.* **B73** (1974) 1–22.

[13] E. D. Bloom, D. H. Coward, H. DeStaebler, J. Drees, G. Miller, L. W. Mo, R. E. Taylor, M. Breidenbach, J. I. Friedman, G. C. Hartmann, and H. W. Kendall, "High-energy inelastic $e-p$ scattering at 6° and 10°," *Phys. Rev. Lett.* **23** (Oct, 1969) 930–934.

[14] K. Garrett and G. Duda, "Dark Matter: A Primer," *Adv. Astron.* **2011** (2011) 968283, arXiv:1006.2483 [hep-ph].

[15] **Planck** Collaboration, P. A. R. Ade *et al.*, "Planck 2013 results. XVI. Cosmological parameters," *Astron. Astrophys.* **571** (2014) A16, arXiv:1303.5076 [astro-ph.CO].

[16] L. Canetti, M. Drewes, and M. Shaposhnikov, "Matter and Antimatter in the Universe," *New J. Phys.* **14** (2012) 095012, arXiv:1204.4186 [hep-ph].

[17] M. Goldhaber, L. Grodzins, and A. W. Sunyar, "Helicity of neutrinos," *Phys. Rev.* **109** (Feb, 1958) 1015–1017.

[18] **The Super-Kamiokande Collaboration** Collaboration, R. W. et al., "Atmospheric neutrino oscillation analysis with subleading effects in super-kamiokande i, ii, and iii," *Phys. Rev. D* **81** (May, 2010) 092004.

[19] **SNO** Collaboration, B. Aharmim *et al.*, "Combined Analysis of all Three Phases of Solar Neutrino Data from the Sudbury Neutrino Observatory," *Phys. Rev.* **C88** (2013) 025501, arXiv:1109.0763 [nucl-ex].

[20] **KamLAND** Collaboration, A. Gando *et al.*, "Constraints on θ_{13} from A Three-Flavor Oscillation Analysis of Reactor Antineutrinos at KamLAND," *Phys. Rev.* **D83** (2011) 052002, arXiv:1009.4771 [hep-ex].

[21] **GNO** Collaboration, M. Altmann *et al.*, "Complete results for five years of GNO solar neutrino observations," *Phys. Lett.* **B616** (2005) 174–190, arXiv:hep-ex/0504037 [hep-ex].

[22] B. Pontecorvo, "Neutrino Experiments and the Problem of Conservation of Leptonic Charge," *Sov. Phys. JETP* **26** (1968) 984–988. [Zh. Eksp. Teor. Fiz.53,1717(1967)].

[23] S. M. Bilenky and B. Pontecorvo, "Quark-lepton analogy and neutrino oscillations," *Physics Letters B* **61** no. 3, (1976) 248 – 250.

[24] V. N. Gribov and B. Pontecorvo, "Neutrino astronomy and lepton charge," *Physics Letters B* **28** no. 7, (1969) 493 – 496.

[25] H. Fritzsch and P. Minkowski, "Vectorlike weak currents, massive neutrinos, and neutrino beam oscillations," *Physics Letters B* **62** no. 1, (1976) 72 – 76.

[26] S. M. Bilenky and B. Pontecorvo, "Lepton mixing and neutrino oscillations," *Physics Reports* **41** no. 4, (1978) 225 – 261.

[27] E. J. Konopinski, "Beta-decay," *Rev. Mod. Phys.* **15** (Oct, 1943) 209–245.

[28] M. Goeppert-Mayer, "Double beta-disintegration," *Phys. Rev.* **48** (Sep, 1935) 512–516.

[29] A. D. Sakharov, "Violation of CP Invariance, c Asymmetry, and Baryon Asymmetry of the Universe," *Pisma Zh. Eksp. Teor. Fiz.* **5** (1967) 32–35. [Usp. Fiz. Nauk161,61(1991)].

[30] A. Ibarra, "Neutrinos and dark matter," *AIP Conf. Proc.* **1666** (2015) 140004.

[31] J. Alcaide, D. Das, and A. Santamaria, "A model of neutrino mass and dark matter with large neutrinoless double beta decay," *JHEP* **04** (2017) 049, `arXiv:1701.01402 [hep-ph]`.

[32] M. Fabbrichesi and S. T. Petcov, "Low-scale neutrino seesaw mechanism and scalar dark matter," *Eur. Phys. J.* **C74** (2014) 2774, `arXiv:1304.4001 [hep-ph]`.

[33] A. Dasgupta and D. Borah, "Scalar Dark Matter with Type II Seesaw," *Nucl. Phys.* **B889** (2014) 637–649, `arXiv:1404.5261 [hep-ph]`.

[34] E. J. Chun, "Minimal dark matter in type III seesaw," *JHEP* **12** (2009) 055, `arXiv:0909.3408 [hep-ph]`.

[35] V. De Romeri, "Right Handed Sneutrino Dark Matter in Inverse and Linear seesaw scenarios," in *Proceedings, 18th International Symposium on Particles, Strings and Cosmology (PASCOS 2012): Merida, Yucatan, Mexico, June 3-8, 2012*.

[36] A. Abada, G. Arcadi, and M. Lucente, "Dark Matter in the minimal Inverse Seesaw mechanism," *JCAP* **1410** (2014) 001, arXiv:1406.6556 [hep-ph].

[37] D. Borah and M. K. Das, "Neutrino Masses and Leptogenesis in Type I and Type II Seesaw Models," *Phys. Rev.* **D90** no. 1, (2014) 015006, arXiv:1303.1758 [hep-ph].

[38] C. H. Albright and S. M. Barr, "Leptogenesis in the type III seesaw mechanism," *Phys. Rev.* **D69** (2004) 073010, arXiv:hep-ph/0312224 [hep-ph].

[39] P.-H. Gu and U. Sarkar, "Leptogenesis with Linear, Inverse or Double Seesaw," *Phys. Lett.* **B694** (2011) 226–232, arXiv:1007.2323 [hep-ph].

[40] S. Weinberg, "The Making of the standard model," *Eur. Phys. J.* **C34** (2004) 5–13, arXiv:hep-ph/0401010 [hep-ph].

[41] Y. Ne'eman, "Derivation of strong interactions from a gauge invariance," *Nucl. Phys.* **26** (1961) 222–229.

[42] S. Weinberg, "A Model of Leptons," *Phys. Rev. Lett.* **19** (1967) 1264–1266.

[43] A. Salam and J. C. Ward, "Electromagnetic and weak interactions," *Phys. Lett.* **13** (1964) 168–171.

[44] E. C. G. Sudarshan and R. e. Marshak, "Chirality invariance and the universal Fermi interaction," *Phys. Rev.* **109** (1958) 1860–1860.

[45] J. Goldstone, "Field Theories with Superconductor Solutions," *Nuovo Cim.* **19** (1961) 154–164.

[46] P. W. Higgs, "Broken symmetries, massless particles and gauge fields," *Phys. Lett.* **12** (1964) 132–133.

[47] P. W. Higgs, "Spontaneous Symmetry Breakdown without Massless Bosons," *Phys. Rev.* **145** (1966) 1156–1163.

[48] Z. Maki, M. Nakagawa, and S. Sakata, "Remarks on the unified model of elementary particles," *Prog. Theor. Phys.* **28** (1962) 870–880.

[49] S. M. Bilenky and B. Pontecorvo, "Lepton Mixing and the Solar Neutrino Puzzle," *Comments Nucl. Part. Phys.* **7** no. 5, (1977) 149–152.

[50] B. Pontecorvo, "Mesonium and anti-mesonium," *Sov. Phys. JETP* **6** (1957) 429. [Zh. Eksp. Teor. Fiz.33,549(1957)].

[51] D. V. Forero, M. Tortola, and J. W. F. Valle, "Neutrino oscillations refitted," *Phys. Rev.* **D90** no. 9, (2014) 093006, arXiv:1405.7540 [hep-ph].

[52] P. Minkowski, "$\mu \to e\gamma$ at a Rate of One Out of 10^9 Muon Decays?," *Phys. Lett.* **67B** (1977) 421–428.

[53] R. N. Mohapatra and G. Senjanovic, "Neutrino Mass and Spontaneous Parity Violation," *Phys. Rev. Lett.* **44** (1980) 912.

[54] M. Magg and C. Wetterich, "Neutrino Mass Problem and Gauge Hierarchy," *Phys. Lett.* **94B** (1980) 61–64.

[55] G. Lazarides, Q. Shafi, and C. Wetterich, "Proton Lifetime and Fermion Masses in an SO(10) Model," *Nucl. Phys.* **B181** (1981) 287–300.

[56] R. Foot, H. Lew, X. G. He, and G. C. Joshi, "Seesaw Neutrino Masses Induced by a Triplet of Leptons," *Z. Phys.* **C44** (1989) 441.

[57] M. Malinsky, J. C. Romao, and J. W. F. Valle, "Novel supersymmetric SO(10) seesaw mechanism," *Phys. Rev. Lett.* **95** (2005) 161801, arXiv:hep-ph/0506296 [hep-ph].

[58] R. N. Mohapatra and J. W. F. Valle, "Neutrino mass and baryon-number nonconservation in superstring models," *Phys. Rev. D* **34** (Sep, 1986) 1642–1645.

[59] M. C. Gonzalez-Garcia and J. W. F. Valle, "Fast Decaying Neutrinos and Observable Flavor Violation in a New Class of Majoron Models," *Phys. Lett.* **B216** (1989) 360–366.

[60] A. Melfo, M. Nemevšek, F. Nesti, G. Senjanović, and Y. Zhang, "Type ii neutrino seesaw mechanism at the lhc: The roadmap," *Phys. Rev. D* **85** (Mar, 2012) 055018.

[61] W. H. Furry, "On transition probabilities in double beta-disintegration," *Phys. Rev.* **56** (Dec, 1939) 1184–1193.

[62] W. Rodejohann, "Neutrino-less Double Beta Decay and Particle Physics," *Int. J. Mod. Phys.* **E20** (2011) 1833–1930, arXiv:1106.1334 [hep-ph].

[63] L. Wolfenstein, "Oscillations Among Three Neutrino Types and CP Violation," *Phys. Rev.* **D18** (1978) 958–960.

[64] P. F. Harrison, D. H. Perkins, and W. G. Scott, "A Redetermination of the neutrino mass squared difference in tri - maximal mixing with terrestrial matter effects," *Phys. Lett.* **B458** (1999) 79–92, arXiv:hep-ph/9904297 [hep-ph].

[65] Y. Yamanaka, H. Sugawara, and S. Pakvasa, "Permutation Symmetries and the Fermion Mass Matrix," *Phys. Rev.* **D25** (1982) 1895. [Erratum: Phys. Rev.D29,2135(1984)].

[66] F. Vissani, "A Study of the scenario with nearly degenerate Majorana neutrinos," arXiv:hep-ph/9708483 [hep-ph].

[67] V. D. Barger, S. Pakvasa, T. J. Weiler, and K. Whisnant, "Bimaximal mixing of three neutrinos," *Phys. Lett.* **B437** (1998) 107–116, arXiv:hep-ph/9806387 [hep-ph].

[68] C. H. Albright, A. Dueck, and W. Rodejohann, "Possible Alternatives to Tri-bimaximal Mixing," *Eur. Phys. J.* **C70** (2010) 1099–1110, arXiv:1004.2798 [hep-ph].

[69] Y. Kajiyama, M. Raidal, and A. Strumia, "The Golden ratio prediction for the solar neutrino mixing," *Phys. Rev.* **D76** (2007) 117301, arXiv:0705.4559 [hep-ph].

[70] L. L. Everett and A. J. Stuart, "Icosahedral (A(5)) Family Symmetry and the Golden Ratio Prediction for Solar Neutrino Mixing," *Phys. Rev.* **D79** (2009) 085005, arXiv:0812.1057 [hep-ph].

[71] W. Rodejohann, "Unified Parametrization for Quark and Lepton Mixing Angles," *Phys. Lett.* **B671** (2009) 267–271, arXiv:0810.5239 [hep-ph].

[72] S. T. Petcov, "Predicting the values of the leptonic CP violation phases in theories with discrete flavour symmetries," *Nucl. Phys.* **B892** (2015) 400–428, arXiv:1405.6006 [hep-ph].

[73] **Double Chooz Collaboration** Collaboration, Y. t. Abe, "Indication of reactor $\overline{\nu}_e$ disappearance in the double chooz experiment," *Phys. Rev. Lett.* **108** (Mar, 2012) 131801.

[74] **Daya Bay** Collaboration, F. P. An *et al.*, "Observation of electron-antineutrino disappearance at Daya Bay," *Phys. Rev. Lett.* **108** (2012) 171803, arXiv:1203.1669 [hep-ex].

[75] **Daya Bay** Collaboration, F. P. An *et al.*, "Improved Measurement of Electron Antineutrino Disappearance at Daya Bay," *Chin. Phys.* **C37** (2013) 011001, arXiv:1210.6327 [hep-ex].

[76] **RENO** Collaboration, J. K. Ahn *et al.*, "Observation of Reactor Electron Antineutrino Disappearance in the RENO Experiment," *Phys. Rev. Lett.* **108** (2012) 191802, arXiv:1204.0626 [hep-ex].

[77] **T2K** Collaboration, K. Abe *et al.*, "Evidence of Electron Neutrino Appearance in a Muon Neutrino Beam," *Phys. Rev.* **D88** no. 3, (2013) 032002, arXiv:1304.0841 [hep-ex].

[78] **T2K** Collaboration, K. Abe *et al.*, "Observation of Electron Neutrino Appearance in a Muon Neutrino Beam," *Phys. Rev. Lett.* **112** (2014) 061802, arXiv:1311.4750 [hep-ex].

[79] D. V. Forero, M. Tórtola, and J. W. F. Valle, "Global status of neutrino oscillation parameters after neutrino-2012," *Phys. Rev. D* **86** (Oct, 2012) 073012.

[80] G. L. Fogli, E. Lisi, A. Marrone, D. Montanino, A. Palazzo, and A. M. Rotunno, "Global analysis of neutrino masses, mixings, and phases: Entering the era of leptonic *cp* violation searches," *Phys. Rev. D* **86** (Jul, 2012) 013012.

[81] M. C. Gonzalez-Garcia, M. Maltoni, J. Salvado, and T. Schwetz, "Global fit to three neutrino mixing: critical look at present precision," *JHEP* **12** (2012) 123, arXiv:1209.3023 [hep-ph].

[82] F. Capozzi, G. L. Fogli, E. Lisi, A. Marrone, D. Montanino, and A. Palazzo, "Status of three-neutrino oscillation parameters, circa 2013," *Phys. Rev. D* **89** (May, 2014) 093018.

[83] D. V. Forero, M. Tórtola, and J. W. F. Valle, "Neutrino oscillations refitted," *Phys. Rev. D* **90** (Nov, 2014) 093006.

[84] P. F. Harrison, D. H. Perkins, and W. G. Scott, "Tri-bimaximal mixing and the neutrino oscillation data," *Phys. Lett.* **B530** (2002) 167, arXiv:hep-ph/0202074 [hep-ph].

[85] A. J. Baltz, A. S. Goldhaber, and M. Goldhaber, "The Solar neutrino puzzle: An Oscillation solution with maximal neutrino mixing," *Phys. Rev. Lett.* **81** (1998) 5730–5733, arXiv:hep-ph/9806540 [hep-ph].

[86] H. Georgi and S. L. Glashow, "Neutrinos on earth and in the heavens," *Phys. Rev.* **D61** (2000) 097301, arXiv:hep-ph/9808293 [hep-ph].

[87] G. Altarelli and F. Feruglio, "Discrete flavor symmetries and models of neutrino mixing," *Rev. Mod. Phys.* **82** (Sep, 2010) 2701–2729.

[88] G. Altarelli, F. Feruglio, L. Merlo, and E. Stamou, "Discrete Flavour Groups, $theta_{13}$ and Lepton Flavour Violation," *JHEP* **08** (2012) 021, arXiv:1205.4670 [hep-ph].

[89] S. F. King and C. Luhn, "Neutrino mass and mixing with discrete symmetry," *Reports on Progress in Physics* **76** no. 5, 056201.

[90] S. T. Petcov, "Predicting the values of the leptonic CP violation phases in theories with discrete flavour symmetries," *Nucl. Phys.* **B892** (2015) 400–428, arXiv:1405.6006 [hep-ph].

[91] W. Chao and Y.-j. Zheng, "Relatively Large Theta13 from Modification to the Tri-bimaximal, Bimaximal and Democratic Neutrino Mixing Matrices," *JHEP* **02** (2013) 044, arXiv:1107.0738 [hep-ph].

[92] X.-G. He and A. Zee, "Minimal Modification to Tri-bimaximal Mixing," *Phys. Rev.* **D84** (2011) 053004, arXiv:1106.4359 [hep-ph].

[93] T. Araki, "Getting at large θ_{13} with almost maximal θ_{23} from tri-bimaximal mixing," *Phys. Rev.* **D84** (2011) 037301, arXiv:1106.5211 [hep-ph].

[94] K. N. Deepthi, S. Gollu, and R. Mohanta, "Neutrino mixing matrices with relatively large θ_{13} and with texture one-zero," *Eur. Phys. J.* **C72** (2012) 1888, arXiv:1111.2781 [hep-ph].

[95] P. S. Bhupal Dev, B. Dutta, R. N. Mohapatra, and M. Severson, "θ_{13} and Proton Decay in a Minimal $SO(10) \times S_4$ model of Flavor," *Phys. Rev.* **D86** (2012) 035002, arXiv:1202.4012 [hep-ph].

[96] P. Huber, M. Lindner, and W. Winter, "Simulation of long-baseline neutrino oscillation experiments with GLoBES (General Long Baseline Experiment Simulator)," *Comput. Phys. Commun.* **167** (2005) 195, arXiv:hep-ph/0407333 [hep-ph].

[97] P. Huber, J. Kopp, M. Lindner, M. Rolinec, and W. Winter, "New features in the simulation of neutrino oscillation experiments with GLoBES 3.0: General Long Baseline Experiment Simulator," *Comput. Phys. Commun.* **177** (2007) 432–438, arXiv:hep-ph/0701187 [hep-ph].

[98] **NOvA** Collaboration, R. B. Patterson, "The NOvA Experiment: Status and Outlook," arXiv:1209.0716 [hep-ex]. [Nucl. Phys. Proc. Suppl.235-236,151(2013)].

[99] **NuMI, NOvA, LBNE** Collaboration, S. Childress and J. Strait, "Long baseline neutrino beams at Fermilab," *J. Phys. Conf. Ser.* **408** (2013) 012007, arXiv:1304.4899 [physics.acc-ph].

[100] S. K. Agarwalla, S. Prakash, S. K. Raut, and S. U. Sankar, "Potential of optimized NOvA for large $\theta_(13)$ & combined performance with a LArTPC & T2K," *JHEP* **12** (2012) 075, arXiv:1208.3644 [hep-ph].

[101] S. C, K. N. Deepthi, and R. Mohanta, "A comprehensive study of the discovery potential of NOvA, T2K and T2HK experiments," *Adv. High Energy Phys.* **2016** (2016) 9139402, arXiv:1408.6071 [hep-ph].

[102] S. K. Raut, "Effect of non-zero theta(13) on the measurement of theta(23)," *Mod. Phys. Lett.* **A28** (2013) 1350093, arXiv:1209.5658 [hep-ph].

[103] K. N. Deepthi, S. C, and R. Mohanta, "Revisiting the sensitivity studies for leptonic CP-violation and mass hierarchy with T2K, NOnuA and LBNE experiments," *New J. Phys.* **17** no. 2, (2015) 023035, arXiv:1409.2343 [hep-ph].

[104] D. Marzocca, S. T. Petcov, A. Romanino, and M. C. Sevilla, "Nonzero $|U_e 3|$ from Charged Lepton Corrections and the Atmospheric Neutrino Mixing Angle," *JHEP* **05** (2013) 073, arXiv:1302.0423 [hep-ph].

[105] P. H. Frampton, S. T. Petcov, and W. Rodejohann, "On deviations from bimaximal neutrino mixing," *Nucl. Phys.* **B687** (2004) 31–54, arXiv:hep-ph/0401206 [hep-ph].

[106] X.-G. He, Y.-Y. Keum, and R. R. Volkas, "A(4) flavor symmetry breaking scheme for understanding quark and neutrino mixing angles," *JHEP* **04** (2006) 039, arXiv:hep-ph/0601001 [hep-ph].

[107] E. Ma and G. Rajasekaran, "Softly broken A(4) symmetry for nearly degenerate neutrino masses," *Phys. Rev.* **D64** (2001) 113012, arXiv:hep-ph/0106291 [hep-ph].

[108] G.-J. Ding, S. F. King, and A. J. Stuart, "Generalised CP and A_4 Family Symmetry," *JHEP* **12** (2013) 006, arXiv:1307.4212 [hep-ph].

[109] C.-C. Li and G.-J. Ding, "Generalised CP and trimaximal TM_1 lepton mixing in S_4 family symmetry," *Nucl. Phys.* **B881** (2014) 206–232, arXiv:1312.4401 [hep-ph].

[110] S. Morisi, D. V. Forero, J. C. Romão, and J. W. F. Valle, "Neutrino mixing with revamped A_4 flavor symmetry," *Phys. Rev.* **D88** no. 1, (2013) 016003, arXiv:1305.6774 [hep-ph].

[111] E. Ma and D. Wegman, "Nonzero theta(13) for neutrino mixing in the context of A(4) symmetry," *Phys. Rev. Lett.* **107** (2011) 061803, arXiv:1106.4269 [hep-ph].

[112] W. Grimus, "Theory of Neutrino Masses and Mixing," *Phys. Part. Nucl.* **42** (2011) 566–576, arXiv:1101.0137 [hep-ph].

[113] E. Ma, "A(4) symmetry and neutrinos with very different masses," *Phys. Rev.* **D70** (2004) 031901, arXiv:hep-ph/0404199 [hep-ph].

[114] **MEG** Collaboration, A. M. Baldini *et al.*, "Search for the lepton flavour violating decay $\mu^+ \to e^+\gamma$ with the full dataset of the MEG experiment," *Eur. Phys. J.* **C76** no. 8, (2016) 434, arXiv:1605.05081 [hep-ex].

[115] S. Weinberg, "Varieties of Baryon and Lepton Nonconservation," *Phys. Rev.* **D22** (1980) 1694.

[116] P. Minkowski, "$\mu \to e\gamma$ at a rate of one out of 109 muon decays?," *Physics Letters B* **67** no. 4, (1977) 421 – 428.

[117] S. F. King, "Atmospheric and solar neutrinos with a heavy singlet," *Phys. Lett.* **B439** (1998) 350–356, arXiv:hep-ph/9806440 [hep-ph].

[118] K. S. Babu and R. N. Mohapatra, "Predictive neutrino spectrum in minimal SO(10) grand unification," in *The Fermilab Meeting DPF 92. Proceedings, 7th Meeting of the American Physical Society, Division of Particles and Fields, Batavia, USA, November 10-14, 1992. Vol. 1, 2*, pp. 1314–1316. 1992.

[119] R. N. Mohapatra and J. W. F. Valle, "Neutrino Mass and Baryon Number Nonconservation in Superstring Models," *Phys. Rev.* **D34** (1986) 1642.

[120] M. C. Gonzalez-Garcia and J. W. F. Valle, "Fast Decaying Neutrinos and Observable Flavor Violation in a New Class of Majoron Models," *Phys. Lett.* **B216** (1989) 360–366.

[121] B. Karmakar and A. Sil, "An A_4 realization of inverse seesaw: neutrino masses, θ_{13} and leptonic non-unitarity," *Phys. Rev.* **D96** no. 1, (2017) 015007, arXiv:1610.01909 [hep-ph].

[122] A. Pilaftsis, "CP violation and baryogenesis due to heavy Majorana neutrinos," *Phys. Rev.* **D56** (1997) 5431–5451, arXiv:hep-ph/9707235 [hep-ph].

[123] B. Pontecorvo, "Inverse beta processes and nonconservation of lepton charge," *Sov. Phys. JETP* **7** (1958) 172–173. [Zh. Eksp. Teor. Fiz.34,247(1957)].

[124] M. Sruthilaya, C. Soumya, K. N. Deepthi, and R. Mohanta, "Predicting Leptonic CP phase by considering deviations in charged lepton and neutrino sectors," *New J. Phys.* **17** no. 8, (2015) 083028, arXiv:1408.4392 [hep-ph].

[125] F. Capozzi, E. Di Valentino, E. Lisi, A. Marrone, A. Melchiorri, and A. Palazzo, "Global constraints on absolute neutrino masses and their ordering," *Phys. Rev.* **D95** no. 9, (2017) 096014, arXiv:1703.04471 [hep-ph].

[126] **GERDA** Collaboration, M. Agostini *et al.*, "Results on Neutrinoless Double-β Decay of ^{76}Ge from Phase I of the GERDA Experiment," *Phys. Rev. Lett.* **111** no. 12, (2013) 122503, arXiv:1307.4720 [nucl-ex].

[127] **KamLAND-Zen** Collaboration, A. Gando *et al.*, "Search for Majorana Neutrinos near the Inverted Mass Hierarchy Region with KamLAND-Zen," *Phys. Rev. Lett.* **117** no. 8, (2016) 082503, arXiv:1605.02889 [hep-ex]. [Addendum: Phys. Rev. Lett.117,no.10,109903(2016)].

[128] S. Dell'Oro, S. Marcocci, M. Viel, and F. Vissani, "Neutrinoless double beta decay: 2015 review," *Adv. High Energy Phys.* **2016** (2016) 2162659, arXiv:1601.07512 [hep-ph].

[129] J. Albert, "Status and Results from the EXO Collaboration," *EPJ Web Conf.* **66** (2014) 08001.

[130] **Planck** Collaboration, P. A. R. Ade *et al.*, "Planck 2015 results. XIII. Cosmological parameters," *Astron. Astrophys.* **594** (2016) A13, arXiv:1502.01589 [astro-ph.CO].

[131] D. V. Forero, S. Morisi, M. Tortola, and J. W. F. Valle, "Lepton flavor violation and non-unitary lepton mixing in low-scale type-I seesaw," *JHEP* **09** (2011) 142, arXiv:1107.6009 [hep-ph].

List of Publications

Thesis Publications

1 **Sruthilaya M.**, Soumya C., K. N. Deepthi and R. Mohanta, *"Predicting Leptonic CP phase by considering deviations in charged lepton and neutrino sectors"*, New J. Phys. **17** 083028 (2015), [arXiv:1408.4392(hep-ph)].

2 **Sruthilaya M.** and R. Mohanta, *"Non-zero θ_{13} and leptonic CP phase with A_4 Symmetry"*, Eur. Phys. C **77**: 140 (2017), [arXiv:1605.06029(hep-ph)].

3 **Sruthilaya M.**, Rukmani Mohanta, and Sudhanwa Patra, *"A_4 realization of Linear Seesaw and Neutrino Phenomenology"*, [arXiv:1709.01737(hep-ph)].

Other Publications

1 **Sruthilaya M.** and Srinu Gollu, *"Perturbation to TBM mixing and its phenomenological implications"*, Mod. Phys. Lett. A Vol 31, No. 38 (2016) 1650207, [arXiv:1609.09609(hep-ph)].

2 **Sruthilaya M.**, Rukmani Mohanta, and Sudhanwa Patra, *"Neutrino Mass and Neutrinoless double beta decay in SO(10) GUT with Pati-Salam symmetry"*, [arXiv:1705.04125(hep-ph)].

Conference Proceedings

- **Sruthilaya M.**,Soumya C., K. N. Deepthi and R. Mohanta, *"Predicting Leptonic CP phase by considering deviations in charged lepton and neutrino sectors"*, XXI DAE-BRNS High Energy Physics Symposium, Springer proceedings in Physics **174** (page 401-406).

Implications of discrete flavor symmetries on neutrino mixing

by Sruthilaya M

Submission date: 15-Mar-2018 04:45PM (UTC+0530)
Submission ID: 930755698
File name: Sruthi.pdf (6.19M)
Word count: 26382
Character count: 117696

Implications of discrete flavor symmetries on neutrino mixing

ORIGINALITY REPORT

34%	13%	33%	2%
SIMILARITY INDEX	INTERNET SOURCES	PUBLICATIONS	STUDENT PAPERS

PRIMARY SOURCES

1	Sruthilaya, M, C Soumya, K N Deepthi, and R Mohanta. "Predicting leptonic CP phase by considering deviations in charged lepton and neutrino sectors", New Journal of Physics, 2015. Publication	13%
2	link.springer.com Internet Source	7%
3	arxiv.org Internet Source	1%
4	Submitted to University of Hyderabad, Hyderabad Student Paper	1%
5	Klapdor-Kleingrothaus, . "Original Articles", Sixty Years of Double Beta Decay From Nuclear Physics to Beyond Standard Model Particle Physics, 2001. Publication	<1%
6	Antonio Enrique Carcamo Hernandez, Long Ngoc Hoang. "A highly predictive A_4 flavour 3-	<1%

	3-1 model with radiative inverse seesaw mechanism", Journal of Physics G: Nuclear and Particle Physics, 2018 Publication	
7	M Sruthilaya, C Soumya, K N Deepthi, R Mohanta. "Predicting leptonic CP phase by considering deviations in charged lepton and neutrino sectors", New Journal of Physics, 2015 Publication	<1%
8	Springer Proceedings in Physics, 2016. Publication	<1%
9	Ge, Shao-Feng, Manfred Lindner, and Sudhanwa Patra. "New physics effects on neutrinoless double beta decay from right-handed current", Journal of High Energy Physics, 2015. Publication	<1%
10	Guido Altarelli. "Discrete flavor symmetries and models of neutrino mixing", Reviews of Modern Physics, 09/2010 Publication	<1%
11	Olive, K.A.. "Review of Particle Physics", Chinese Physics C, 2014. Publication	<1%
12	tel.archives-ouvertes.fr Internet Source	<1%

This is to certify that the thesis titled "Implications of discrete flavor symmetries on neutrino mixing", submitted by Ms. Sruthilaya M (12PHPH28) is based on her research work done under my guidance. This thesis has been screened by Turnitin software at Indira Gandhi Memorial Library, University of Hyderabad and shows a similarity index of 34%. Of this, about 20% are from published papers where Sruthilaya M is the lead author. A thorough look at the report shows that this as well as the remaining similarity index is mainly due to the standard technical terms used in the published works in this area of research. Use of such technical and scientific terms are unavoidable.

Rukmani Mohanta
(Thesis Supervisor)